The Manufacture, Characterization and Aging of Novel High Temperature Carbon Fibre Composites.

Bronwyn Louise Fox

A thesis submitted for the degree of Doctor of Philosophy of
The Australian National University.

February 2001

To Dr. David Brian Fox

Statement of Originality

The PhD research program has been conducted under the principal supervision of Dr. Adrian Lowe (ANU, Department of Engineering) and Dr. Jonathan Hodgkin (CSIRO, Division of Molecular Science).

I declare that the work presented in this thesis is to my belief original, except as acknowledged in the text, and that the material has not been submitted either in whole or in part, for a degree at this or any other university.

Bronwyn Louise Fox

February 2001

ACKNOWLEDGEMENTS

First of all, I would like to thank *Adrian Lowe* and *Jonathan Hodgkin*, I couldn't have wished for two better supervisors. I would like to thank both of them for taking me on as an apprentice and for being such a pleasure to work with. Thanks to *Adrian* for all of his advice, support and for encouraging me to have a go at lecturing his Materials Science unit. Thanks also to *Marta* and *Daniel* for putting up with my frequent visits with various drafts. Thanks to *Jonathan* for his guidance over the years and for allowing me access to the wealth of experience he has in high temperature composites.

I would like to acknowledge funding from the Australian Research Council (ARC), the CSIRO Division of Molecular Science and the Australian Federal Government under the Targeted Institutional Links Scheme (TIL) administered by the Department of Employment, Education, Training and Youth Affairs (DEETYA).

I would also like to specially thank *Trevor Morton*, for his excellent advice during this project and *Buu Dao*. Both were an enormous help in setting up this study, providing materials and in training me in the black art of composite fabrication. Thanks also to *Russell Varley* for his assistance with the Dynamic Mechanical Thermal Analysis.

Thanks also to *Vincent Otieno-Alego* for being a huge help with the work using the Raman microscope and for giving me the patience to deal with highly fluorescent materials. Thanks to *Dudley Creagh* for enabling the Raman work to be completed.

Thanks to the staff and students of the Engineering Department for their help, support and friendship, particularly *Josephine Farmer, Pam Roberts, Sue Cameron, Shankar Kalyanasundaram, Mick Cardew-Hall, Rob Gresham, Bob Williamson*, *Michael Green, Andrew Blakers* and especially *Brenan McCarragher* for giving me the opportunity to teach "Systems Engineering Design".

I would like to *Darius Krivanek* for coming to my rescue on a number of technical matters, particularly those involving the prepregger and the autoclave.

Thanks to *James Mardel, David Attwood* and *Paul Compston* for helpful discussions.

I would like to acknowledge my appreciation of the very helpful staff of the Electron Microscopy Unit at the ANU, particularly *Roger Heady, Frank Brink* and *Sally Stowe*.

I would like to thank *Graeme Heath* from the Research School of Chemistry for assistance with the synthetic work. I would also like to thank *Horst Neumann, Stephen Lee* and *Nicholas Perkins* also from the RSC, for their help.

Thanks to *Ben Jar* and *Zbigniew Stachurski* for assisting in the first stage of this project.

Thank you to *Lucé Andrews* for his invaluable assistance with the writing up process.

A special thank you to *Margaret Fox* for being a fantastic role model and for encouraging me to pursue science. Thanks also to *David Fox* and *Paige Squires* for their frequent and amusing visits to Canberra.

Thank you to *Christine, Noel* and *Bryant Cobcroft* for their support and encouragement and for being my surrogate family in Canberra.

I owe an enormous debt to *Karen* and *James Mardel*, for their support and counselling, not to mention the culinary delights that awaited me on my frequent visits to CSIRO in Melbourne. Thanks also to *Tracey Bray* and *Heather St John* for being ever ready to join me in having Phở.

I would like to thank *Heidi Pritchard* for her boundless support, for keeping me sane (vaguely) through this whole process and for making Canberra such a fun place to live.

Finally, a very special thank you to *Tyrone Cobcroft* for accompanying me into the lab in the wee hours of the morning, providing support and for inventing spectacular ways of injuring himself just to take my mind away from it all. I couldn't have survived this far without you.

ABSTRACT

High temperature composite materials used in aerospace applications are exposed to extremely harsh conditions and must be able to withstand moisture and extremes of temperature. For example, the surface of an aircraft flying at Mach 2.4 has been estimated to reach around 177°C as a result of aerodynamic heating. This thesis has examined the effect of isothermal aging on two high temperature composite materials, a novel CSIRO composite and a commercial composite, both based on bismaleimides. Changes in mechanical properties and resin chemistry at two different temperatures were measured in order to assess the validity of accelerated aging tests.

Delamination is a major cause of failure in materials, therefore, the Mode I interlaminar fracture toughness (G_{IC}) of both materials was measured using the double cantilever beam (DCB) test. After aging at 250°C, the CSIRO CBR 320/328 composites exhibited better retention of G_{IC} than the CIBA GEIGY Matrimid® 5292 composites. After 6 weeks of aging at this temperature, the CBR 320/328 material retained 100% of its initial interlaminar fracture toughness, however the Matrimid® 5292 material retained only 64% of its initial G_{IC}. This trend was reversed at the lower aging temperature, when after 30 weeks of aging at 204°C, G_{IC} was measured at 13% of its original value for the CSIRO composites, whereas it was measured at 64% in the case of the Matrimid® composites. When the fracture surfaces of these specimens were examined using scanning electron microscopy (SEM), the commercial material was observed to show an increasing degree of porosity with aging at 204°C. It was concluded that the good property retention at the temperature, despite this observed porosity, was a result of the excellent fibre/matrix adhesion exhibited by this material.

Chemical degradation of the matrix of the composites was monitored by Fourier Transform Infrared (FTIR) and Raman Spectroscopy. Chemical changes at the core of both of these materials were found to occur concurrently with the observed changes in interlaminar fracture toughness. FTIR analysis of both matrix materials revealed the predominant degradation mechanism to be oxidation, specifically the oxidation of the methylene group bridging two aromatic rings common to the structure of both resins, was substantiated by the ingrowth of a broad peak centred at 1600cm^{-1}. In addition to this, the pyromellitic anhydride unit present only in the CBR 320/328 composites was found to be highly resistant to the effects of aging, whereas the saturated imide, common to the cured structures of both materials, was observed to degrade.

Raman spectroscopy showed an increase in the intensity of a peak at 1646 cm^{-1} in the Matrimid® 5292 composites aged at 250°C towards the centre of the sample as a result of increased reaction of the allylic carbon-carbon double bond. At 204°C, the degree of reaction increased towards the surface of the material, possibly as a result of a reverse Diels-Alder reaction. The glass transition temperatures of both materials were found to decrease with aging, with the exception of the CSR 320/328 composites aged at 204°C, which initially increased due to continued crosslinking of the resin.

It is concluded that the degradation mechanisms at the two aging temperatures are very different. The reliability of results from accelerated (elevated temperature) aging tests has been drawn into doubt.

CONTENTS

Chapter 1 – Introduction

Materials used in high-speed aerospace applications are required to withstand harsh environments. Composites used at the surface of aircraft may be exposed to moisture and temperatures of up to 177°C as well as sudden extremes in temperatures, as experienced when a fighter aircraft completes a supersonic dash. In a supersonic dash the aircraft dives from a high altitude (surface temperature of –20 to –55°C) into a low altitude supersonic run where the surface temperature increases to between 100°C and 150°C as a result of heating due to friction in air [1]. In a military jet such as the Eurofighter-Typhoon, up to 70% of the surface of the aircraft may be made up of carbon fibre composite. High temperature carbon fibre composites based on polyimides are able to withstand these conditions and offer strength and a high stiffness-to-weight ratio.

Polyimide composites are frequently utilised in applications that require materials with high temperature capabilities due to their excellent thermal stability. Of all polyimides, bismaleimides are the easiest to fabricate and can be processed using similar conditions to epoxy resins [2]. The main competition to bismaleimides, thermoplastic polyimides are tougher and resistant to even higher temperatures, however they are very difficult and expensive to process as they require long cure cycles at high temperatures and thermoplastic prepregs have very little tack or drape. Ultimately it is the ease of manufacture combined with the low cost of raw materials that make bismaleimide composites the more affordable high performance materials.

The CBR 320/328 resin system investigated in this study is one of several resin systems based on bismaleimides developed by CSIRO to meet the strict requirements of aerospace applications described above. Since the commencement of the present study, CSIRO have published results based on new resin systems utilising 2-naphthol derivatives as Diels-Alder based co-reactants for bismaleimides which have higher glass transition temperatures, tensile strength and modulus than the system investigated here [3]. However, at the time of the inception of this study, the CBR 320/328 system was the most promising matrix material that CSIRO had disclosed in the literature. The Matrimid® 5292 resin system was selected for comparative purposes due to its very

similar cure chemistry and the quantity of data published on this system in the literature.

The largest potential for composites containing bismaleimides resins is in aerospace applications, particularly at the surface of high speed aircraft. Figure 1.1 has been reproduced from the official Eurofighter-Typhoon web page [4] and shows that this aircraft utilises carbon fibre composites for over 70% of its surface. Other applications for bismaleimides composites aside from military aircraft include aerospace engines, printed circuit boards (glass fibre composites) and tooling. Tooling involves the use of high temperature resistant composites in the production of moulds for composites that have a lower temperature curing schedule.

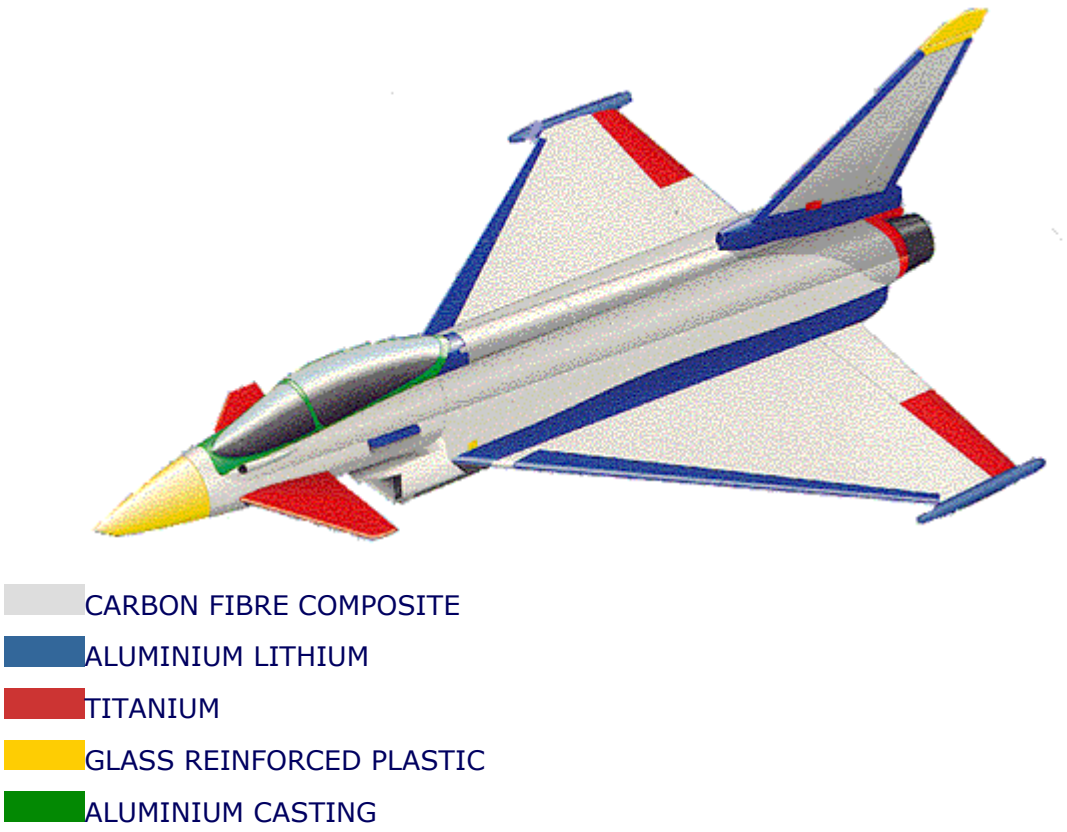

Figure 1.1: Schematic of the Eurofighter-Typhoon showing the components making up the surface area of the jet.

Until funding cuts in 1999, bismaleimide composites were also being considered for a new high-speed civil transport (HSCT) aircraft. These planes were planned to cruise at Mach 2.4 and effectively halve existing flight times for very little extra cost to the consumer due to their potential to carry large numbers of passengers. With the recent controversy over "economy class syndrome", technically known as deep veined thrombosis, the motivation towards developing civil aircraft capable of supersonic speeds may be reignited.

In all aerospace materials applications, be they military or civil, the main challenges that remain to be met are hot/wet performance and the ability to withstand sudden changes in temperature (thermal spikes). Of these, the effect of heating due to friction in air during flight (aerodynamic heating) at the surface of aircraft was selected due to its deleterious effect on composite mechanical properties and also because investigating the effect of isothermal treatments provides an excellent foundation to studying these other more complex issues.

Any aging study, by definition, takes a great deal of time. In order to get new materials into service more quickly, accelerated aging tests can be performed in order to predict the behaviour of composites at the surface of aircraft after several thousand hours of flight. These accelerated aging tests exposed composites to elevated temperatures for shorter periods of time and extrapolation of these data can be used to predict material properties after exposure to lower temperatures for shorter periods. Part of the motivation for the current study was to assess the validity of these accelerated aging tests. For this reason, a preliminary study at 250°C was performed. This temperature approaches the glass transition temperature of the materials studied and is well above the predicted temperature of 177°C, the result of the aerodynamic heating of an aircraft cruising at Mach 2.4. A second study at 204°C was performed for comparative purposes. This temperature was selected as it approached the aforementioned predicted temperature of aircraft and for ease of comparison with the data available from aging studies conducted at 400°F.

Therefore the four broad aims of the present study were as follows:

1. To assess the validity of accelerated aging tests.

2. To assess the use of chemical techniques to analyse aged composites in order to predict part lifetime.

3. To compare and contrast the thermo-oxidative stability of CBR 320/328 composites with a commercial product.

4. To compare and contrast the thermo-oxidative stability of both composites at two different temperatures.

Chapter two reviews the literature in this field. Details of the materials, the synthetic route to the CBR 320/328 resin, composite manufacture and standard test procedures are set out in Chapter three. Chapters four and five present results from the aging of composites at 250 and 204°C respectively. These results are discussed in detail in Chapter six where the aging mechanisms at the two different temperatures are compared. Finally, Chapter seven summarises the conclusions from this work and contemplates future directions.

Chapter 2 - Literature Review

2.1 High Temperature Carbon Fibre Composites

Carbon fibre reinforced composites are preferred in a number of advanced material applications as they have high specific strength and stiffness and yet they are also lightweight. High temperature composite materials that use carbon fibre reinforcement are composites where the polymer matrix has been chemically engineered to resist extreme temperatures. These advanced materials were primarily developed for aerospace applications such as the High Speed Civil Transport (HSCT) program as well as for use in defence aircraft such as the Eurofighter-Typhoon. Military jets are capable of speeds of over Mach 2.0. At this speed, the calculated surface temperature of the aircraft is 110°C and this rises to 177°C in other craft capable of flight at Mach 2.4 [5]. In addition to this, such an aircraft may also be exposed to temperatures as low as -54°C when in flight at high altitudes for long periods of time [1]. Thus the material must retain its integrity not only under extremes of temperature but also when exposed to stress and humidity as well as fuels and fluids.

Although high temperature composite materials were originally designed primarily for aerospace service, they have proved to be useful in a range of other applications. They are often used in laminated printed circuit boards, due to their resistance to damage from molten solder. They also have great potential for use in tooling, the process of making moulds for composite components that have lower temperature cure cycles as a result of their thermo-oxidative stability and comparative ease of mould production and low thermal expansion when compared to current alternatives such as aluminium.

2.2 Polyimides

Polyimides are widely used as matrix materials for carbon fibre composites due to their ability to withstand temperatures in excess of 250°C. The general polyimide structure as seen in Figure 2.1 is characterised by imide moieties along the backbone of the polymer. There are three main categories of polyimide resins used in composites: thermoplastic, condensation and addition polyimides. True thermoplastic polyimide

resins are fully polymerised prior to composite fabrication and laminates are formed when the resin from adjacent prepregs melds together. An example of a true thermosetting polyimide is ULTEM, a polyetherimide with a glass transition temperature (Tg) of 216°C. There are also pseudo-thermoplastics [6] where most of the polymerisation chemistry has been completed before composite manufacture. When the laminate is cured, the polymerisation chemistry is completed via a further reaction, which is often a condensation reaction. This has the disadvantage of releasing volatiles such as water and ethanol. These volatiles can produce voids in the laminate, which create stress concentration sites that result in a weaker final product [7]. Commercial products of this nature include AVIMID K-III, LARC-TPI (both polyimide structures) and TORLON (based on a polyamide-imide structure). Thermoplastics have excellent high temperature stabilities, however, the high glass transition temperatures of these materials result in high melt viscosities, which means that they are difficult and expensive to process.

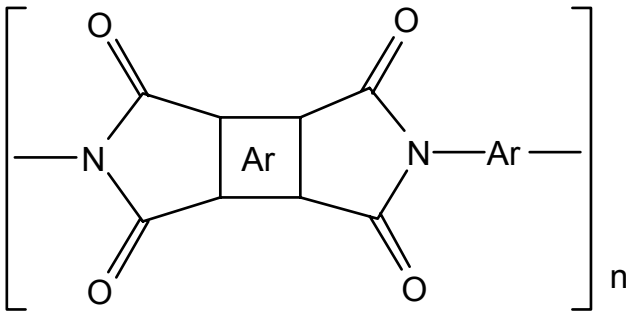

Figure 2.1: General structure of a polyimide, featuring the imide moiety along the polymer backbone.

Condensation polyimides utilize the polycondensation of a dianhydride and a diamine to form a poly (amic acid) precursor, which then undergoes thermal cyclization. Some of the pseudo-thermoplastics listed above also fall into this category. The main problem with condensation polyimides is the evolution of volatiles as mentioned above.

Addition or thermosetting polyimides consist of imidized oligomers, which polymerise via reactive end groups. Thermosetting polyimides have relatively high crosslink densities and are brittle in some cases, however there is very little evolution of volatiles during composite fabrication. Bismaleimides belong to this category and will be discussed further in the next section. An example of another type of thermosetting

polyimide is the PMR-15 (*in-situ* polymerisation of monomeric reactants) resin developed by NASA. PMR-15 composites are of very high quality and can be produced with very low void content (less than 1%) [2]. Figure 2.2 shows the cure chemistry of PMR-15. It is included here to highlight the similarities in the final cure structure with the Matrimid® 5292 and CBR 320/328 resin systems investigated (refer to Figure 2.5). Common to the structure of all three resin systems is a para-substituted aromatic structure with a methylene bridge; therefore literature based on the study of PMR-15 was a significant assistance in the present study.

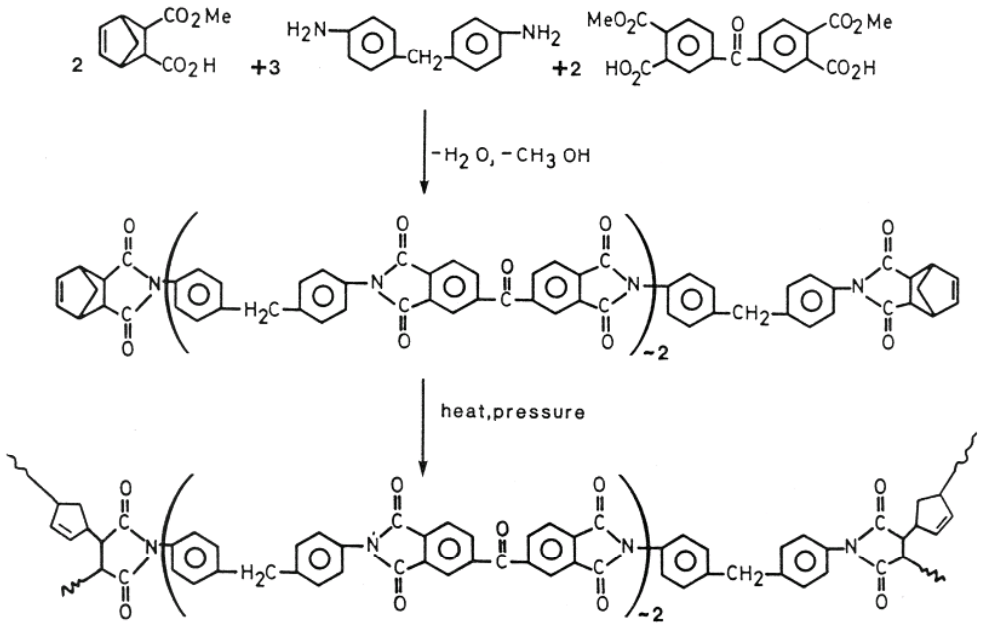

Figure 2.2: Cure of PMR-15. Note the para substituted, methylene bridged aromatic structure present [2].

Polyimides are generally formed from amines and anhydrides via a two-step synthetic route. The first step involves the formation of an intermediate amic acid (uncyclized amide acid), which is followed by dehydration and cyclization, resulting in the imidized product (Figure 2.3). The second step is much slower than the first and thus determines the rate of the reaction. This synthesis has conventionally been performed in aprotic solvents (i.e. a solvent that neither accepts nor donates protons) such as DMF (dimethylformamide) which complex with the product and must be removed later at high temperatures and under a reasonably strong vacuum. If this process (known as

degassing) is not performed adequately, then the final composite will contain an unacceptable amount of voids, which will significantly affect the mechanical properties of the material and potentially result in delamination [8]. The intermediate amic acids are often not completely converted to the imide and as a result form a major contaminant in the final product, which then must be purified. Recently, an alternative synthetic route has been reported [9] where the synthesis of polyimides have been performed in water using amine/acid salt intermediates. Not only does this synthesis avoid the use of aprotic solvents, thus eliminating the degassing step, but any amic acids formed are highly soluble in water and therefore do not contaminate the product to the same extent as in previous synthetic methods.

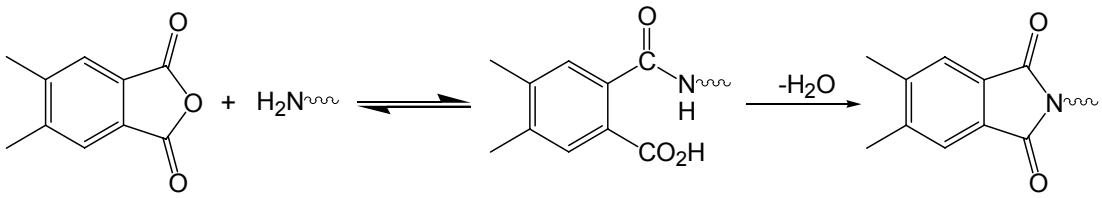

Figure 2.3: Imidized product of the reaction between an amine and an anhydride showing the poly (amic acid) intermediate.

2.3 Bismaleimides

Of the thermosetting polyimides, bismaleimides are widely used because they are cheap and can be processed and cured using techniques and conditions very similar to that of high performance epoxy resins. The polymerisation of bismaleimides was first described in the literature over 30 years ago [10]. The bismaleimides prepolymer structure is characterised by imide end groups as shown in Figure 2.4. The main problems associated with the first generation of bismaleimides are brittleness and microcracking and both can be attributed to the high crosslink density of these materials [11]. This can be largely overcome by chemical modification of the resins, [3, 12] the result being relatively low cost matrix materials, which can be cured at moderate temperatures.

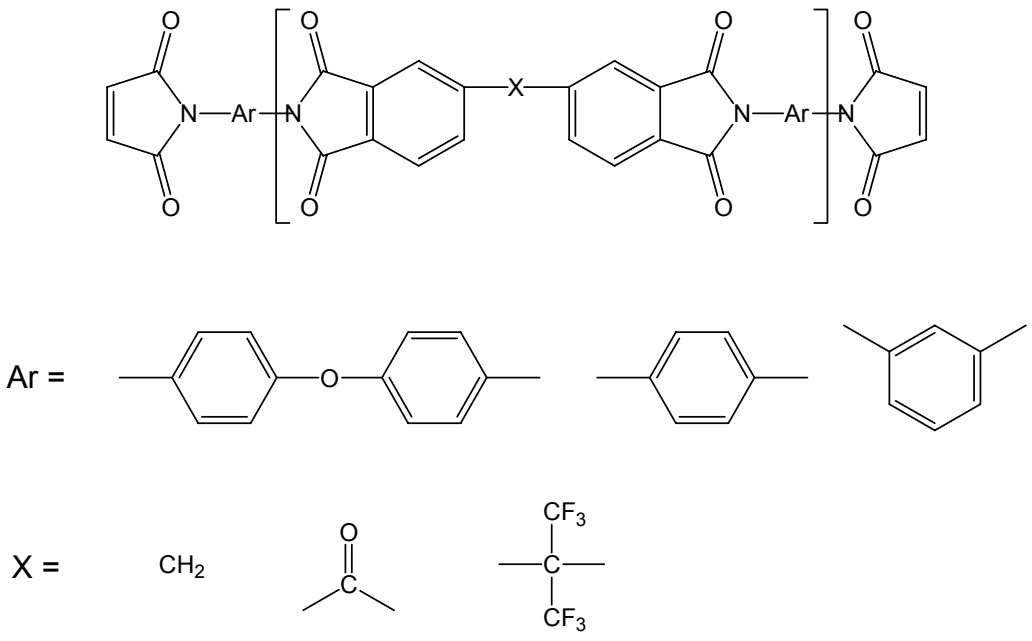

Figure 2.4: General structure of a bismaleimides indicating some of the types of bismaleimide building blocks (reproduced from [13]).

It is generally accepted that current bismaleimides are cured via an ene reaction with diallyl addition followed by a Diels Alder reaction [13]. A general reaction scheme for a bismaleimide cure is shown in Figure 2.5. The cure specifically of the Matrimid® 5292 system, used in this study, has been characterized by FT-IR spectroscopy by Morgan et al. [14] and by Near-Infrared (NIR) spectroscopy by Mijovic and Andelić [15]. The cure of a bismaleimide consisting of Matrimid® A and 4,4'-diaminodiphenylmethane was also recently analysed using FT-NIR to measure the concentration of various functional groups *in-situ* by Hopewell *et al* [16]. The authors used this technique to measure the kinetics and mechanism of this reaction in a companion paper [17]. Morgan *et al.* [18] [14] specify that the ene reaction in the Matrimid® 5292 system occurs in the 100-200°C temperature range with the principal cure reaction occurring in the 200-300°C range as well as a number of side reactions that include maleimide homopolymerisation and etherification. This is also consistent with the findings of Barton *et al.* [19] who studied the reaction of Matrimid® 5292 A with Matrimid® 5292 B and other alkenyl functionalized aromatic comonomers. Cunningham *et al*. have

studied the ene reaction between maleimides and allyl substituted aromatics in detail [20]. The reaction products were fully characterised and an evaluation of the ene and enophile reactivities made.

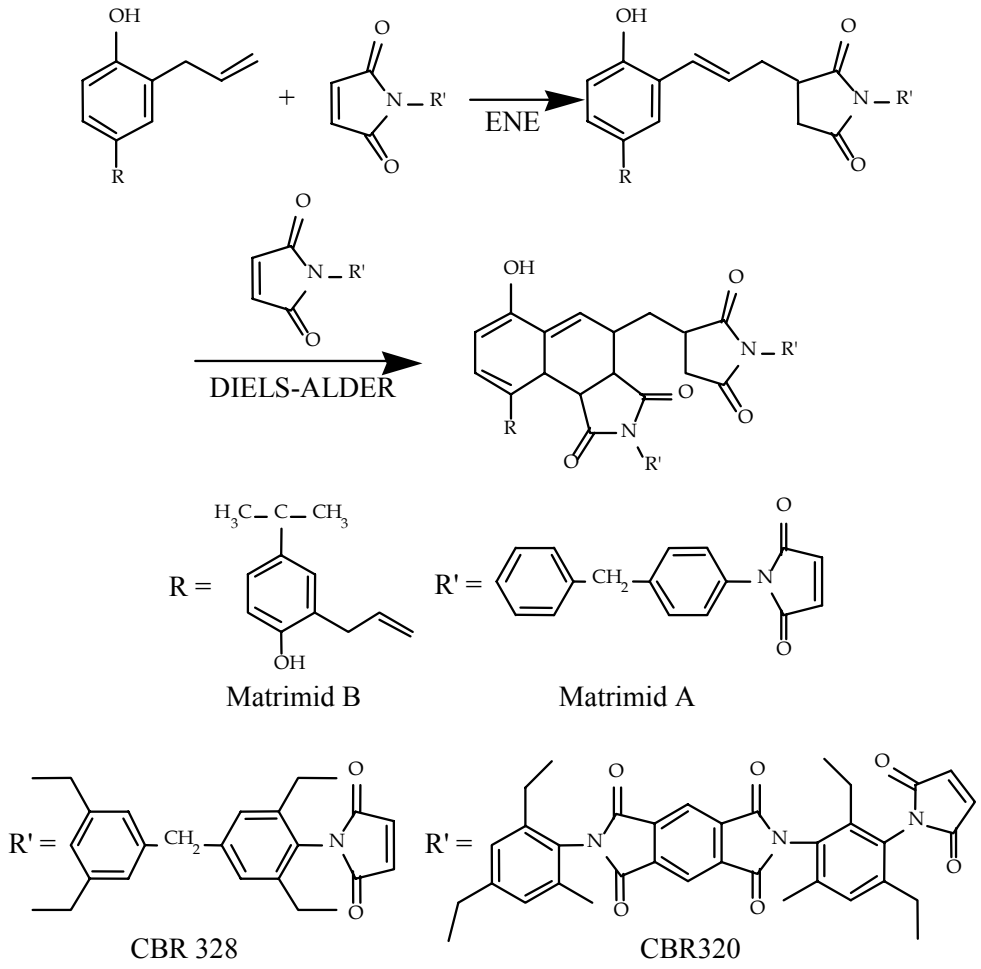

Figure 2.5: The essential curing characteristics of both the Matrimid® 5292 and CSIRO CBR 320/328 resins, showing the generic proposed reaction scheme and specific chemical structures.

Stenzenberger [10] completed a comprehensive review of bismaleimide resins in 1989. This review stated that most of the research on bismaleimides to that time has focussed on improving the handling of prepregs, toughness and processability. Any improvement that had been made in toughness had been at the expense of Tg and thermo-oxidative stability and the author identified this as the main challenge for the future. Since then, advances have been made in this area, however the balance between improving toughness and maintaining high temperature properties remains difficult. Olesen *et al*. [21] compared the toughness of three generations of bismaleimide resins

and showed that by altering the chemistry of the monomers; the toughness was improved at only a slight cost to glass transition temperature (260°C compared with 275°C). Fry and Lind [22] attempted to toughen a bismaleimide resin by chain extending the monomers prior to crosslinking. Extending the backbone of the monomers grants the polymer chains more flexibility and therefore should increase toughness. Successful chain extension was confirmed by solid-state ^{13}CNMR spectroscopy, however the authors did not offer any data to support an increase in toughness of the resin. Morgan *et al*. successfully toughened Matrimid® 5292 composites by optimising the cure cycle and then fabricating composites with polyetherimide (PEI) particulates and interleaves. The interlaminar fracture toughness of these materials was increased by 30% when particulates were added and 20% when PEI interleaves were used. However, the particulates created problems with porosity and surface undulations and adding interleaves sacrificed high temperature, wet and open hole properties.

Another strategy of toughening bismaleimides employed recently is to blend the resin with a cyanate ester. The term blend is used deliberately in this context as recent characterisation of the resulting matrix indicated that in some cases, the two polymers do not co-react, but instead form an interpenetrating network [23]. In a related study, the interlaminar fracture toughness of similar materials showed enormous (nearly 150%) improvements over the individual resins [24], while still retaining a high Tg.

2.4 Aging of High Temperature Composites.

The main motivation for studying the aging behaviour of high temperature composites is the desire to predict the lifetime of composites used in aerospace applications. Results from such studies also assist in the design of new molecules that are more resistant to aging. The ability to predict the duration of use of aerospace parts assists in the prevention of part failure in service, by quantitatively evaluating the number of cycles before the part must be replaced. The degradation of composite materials when in service is obviously not just an issue for use in the aerospace field, but is critical to all applications of these materials.

There are two mechanisms by which aging occurs, these being physical and chemical aging. The main difference between the two processes is that physical aging is thermo-reversible, however chemical aging involves a permanent chemical change in the material. These two mechanisms will now be discussed in further detail.

2.4.1 Physical aging

Physical aging can be explained in terms of free volume [25-27]. The concept of free volume was devised to assist in the understanding of viscosity and volume in polymer melts. Free volume can be defined as the difference between the specific volume of the polymer at a given temperature (V) and the equilibrium volume at absolute zero (V_0) [28].

$$V_F = V - V_0 \qquad \text{(Equation 2.1)}$$

As a polymer is cooled from a melt, there is a decrease in free volume (V_F). At the Tg, the polymer chains are frozen into a non-equilibrium glassy state and V_F is also frozen. As further cooling occurs, the free volume can no longer change at the same rate as the relatively sudden changes in temperature. If the polymer is then annealed at a temperature close to (within 50°C below Tg, according to Bigg [26]) and lower than the Tg, a decrease in free volume will occur as the polymer gradually approaches equilibrium properties. This process is physical aging. With the relaxation of free volume that occurs with physical aging, changes in the properties of the polymer also occur, depending on time and the annealing temperature. The density of the polymer may increase, along with the Tg, yield strength and modulus whilst the fracture toughness generally decreases. Thus, physical aging may be monitored through the measurement of these properties, or more accurately through the direct measurement of free volume by using Positron Annihilation Lifetime Spectroscopy (PALS). PALS works by measuring the time it takes for a positron (positively charged electron) to annihilate with an electron after being emitted into a solid or liquid sample. The lifetime of orthoPositronium (a sample of positronium in which the spins of the positron and the electron are parallel) when emitted into the spaces between molecules can be used to measure the sizes of those spaces and therefore the free volume.

The difficulty with studying the physical aging of thermosetting polymers is ensuring

that it is actually physical aging that is being examined and that chemical aging is not also occurring; it is not a trivial matter to separate the two effects. Most of the research performed on the physical aging of composite materials has focussed on composites with epoxy matrices. Kong [29] performed a comprehensive study of the physical aging of a Fiberite 934 epoxy (TGDDM/ DGOP/ DDS) composite material, which had a Tg of 236°C after postcuring. The material was quenched and then annealed at sub-Tg temperatures of 80, 110 and 140°C for up to 10 weeks in darkness to eliminate the effect of UV radiation, and no change was found in weight loss yet many changes in properties were observed. The following properties were found to increase with physical aging in this study; density, dynamic modulus, hardness, moisture/epoxy swelling and both rubbery and glassy state expansivity. Damping, ultimate mechanical properties, stress relaxation, moisture sorption and moisture diffusivity were all found to decrease and the free volume concept was used to explain these results. This paper also demonstrates that physical aging is thermoreversible. More recently, Montserrat [30] studied the physical aging of an epoxy resin based on diglycidyl ether of bisphenol-A. The fully cured neat resin had a Tg of 98.9°C and was aged at temperatures between 50 and 100°C. It was found that the rate of relaxation of the system increased with the aging temperature and decreased as the system approached structural equilibrium.

Papers referring to the physical aging of high temperature composite materials are relatively rare. A review of the application of PALS to probe free-volume effects in high temperature polymers and composites focussed mostly on high temperature epoxy systems [25]. Papers referring to the physical aging of polyimides are particularly scarce, however, a few have recently started to appear in the literature [31, 32]. Most of the research in this area has concentrated on polyetherimide (PEI) and many papers have concentrated on measuring the enthalpy recovery via differential scanning calorimetry (DSC) as a means to assessing enthalpy relaxation rates. The effect of physical aging on the viscoelastic behaviour of thermoplastic polyimide IM7/K3B carbon fibre composites was examined by Veazie and Gates [33]. The physical aging of this material was also investigated and later modelled by Bradshaw *et al.* [34]. Both the model and the experimental results found a difference in the aging behaviour of each lamina in the shear and transverse directions. Additional work on this composite was performed by Rodeffer *et al.* [35] who investigated the effects of aging on the transverse

tensile creep response and after finding that the effects were completely reversible, concluded that the aging mechanism was predominantly physical with very little if any chemical aging occurring.

2.4.2 Chemical aging of polyimide composites.

Chemical aging can be defined as an irreversible change in the chemical structure of a material caused by degradation processes. There are four main processes that result in chemical aging, these being hydrolysis (hydrolytically induced chain scission), oxidation (reaction with O_2), radiation induced damage (reactions initiated by UV radiation and gamma rays from space) and thermal decomposition (thermally induced bond dissociation). The most important issues in the chemical aging of composites are the reaction of the matrix with oxygen or moisture. It is often difficult to determine whether chemical aging at the core of a material has been caused by an anaerobic reaction or by oxygen diffusion to the core, assisted by the formation of microcracks at the surface. The final result of chemically aging a material at a given temperature is the formation of a char, consisting essentially of carbon. Chan *et al.* [36] produced a TTT diagram that clearly displays gelation, vitrification, devitrification and char formation for a high Tg epoxy resin system. Chemical changes in the matrix will often result in the loss of low molecular weight degradation products. The amount of matrix lost can be monitored by weight loss experiments.

Early studies of the degradation of polyimides were conducted at very high temperatures. Dine-hart *et al.* [37] studied the degradation of a polyimide film based on the thermally stable pyromellitic dianhydride structure. The film was exposed to temperatures of up to 400°C. A few years later, Stenzenberger and co-workers [38] published a study of the thermal degradation of a bismaleimides using pyrolysis. The authors concluded that aliphatic bridges are less stable than succinimide rings and also that the bond between the nitrogen atom and the aromatic carbon is cleaved during pyrolysis, leading to the abstraction of succinimide.

Of the relatively small amount of work published on the chemistry of degradation of polyimides, a few studies also correlate these chemical changes with changes in mechanical properties. This is particularly the case in the large body of work published by Morgan and co-workers who stress the importance of the knowledge of structure-

property relationships in predicting composite lifetime [1, 39, 40]. Much of the work on the durability of polyimides published by Morgan *et al.* has focussed specifically on the CIBA GEIGY Matrimid® 5292 resin system also under investigation in the present study. The hygrothermal degradation of these composites was characterized by the disappearance of imide carbonyl peaks in the FTIR spectra of degraded material along with the eventual disappearance of a Tg as measured by differential scanning calorimetry (DSC). The authors attributed both of these observations to depolymerisation to polyamic acid and then to the monomers [41].

The chemical degradation of PMR-15 type nadic end-capped polymers has been studied by Meador *et al*. who looked at the effect of aging at high temperatures (>300°C). FTIR analysis of the degraded polymer revealed oxidation of an aromatic methylene bridge to form a ketone [42]. The same authors also used ^{13}CNMR labelling experiments and model compounds to identify several of the products due to the degradation of the nadic end-caps [43, 44].

2.4.3 Mechanical Property Changes in Aged Polyimide Composites.

The changes in mechanical properties that occur with aging may occur due to either chemical or physical aging or a combination of the two processes. It is often difficult to distinguish between the two mechanisms; hence the topic of mechanical property changes is discussed separately. Much of the work on the aging of composite materials has investigated a change in one or more of the properties of the materials and in this review; this has also been extended to include weight loss and changes in the thermal properties of the composite. There are some excellent reviews on the aging of polymer matrix composites by Hancox on thermal cycling [45] and thermal degradation [46] and also by Liao [47], who focuses on glass fibre reinforced composites.

Bowles and co-workers at NASA have performed extensive studies of the degradation of PMR-15 composites and reported on weight loss, compression properties, Tg and microstructural changes. Aging studies have been performed at temperatures between 204 and 343°C. Oxidation was found to occur at the surface of these materials, with the development of a degraded region with a high density of microcracks. This region grows with increased aging time and penetrates further into the specimen [48, 49]. The oxidised layer was found to penetrate further into the sample at cut edges than at

moulded surfaces as a result of the development of a network of microcracks having the ability to grow parallel to and along the plies of carbon fibre cloth from the cut edges [50, 51]. The same authors also compared the thermal stability of the neat resin with unidirectional composites made from fibres with different sizing [52]. This study found a dependence of weight loss on specimen dimensions, when the ratio of cut surface area to total surface area was great, the thermal oxidative stability of the material was poor.

Other work on the aging of PMR-15 type composites includes a study by Hinkley and Nelson [53] who measured the weight loss and interlaminar shear strength (ILSS) of composites aged between 204-288°C for up to 25,000 hours and used an Arrhenius relationship to extrapolate the life time of this material to 60,000 hours at 160-180°C. Marceau and Hillaire [54] also performed weight loss studies of PMR-15 neat resin and composites and concluded that the presence of fibres had no effect on the degradation kinetics of the material. Janchud *et al.* [55] aged PMR-15 composites at 316°C and found that the fibre/matrix adhesion was greatly increased by dipole-dipole interactions at the interface, which also had the effect of slowing down the loss of ILSS with aging.

Shin *et al.* have performed extensive studies of the hygrothermal degradation of Matrimid® 5292 bismaleimide composites. [1, 56, 57]. The authors identified the critical aging mechanisms as being 1) further cure of the BMI composite matrix with associated Tg increase, mechanical property decreases and microcrack development and 2) thermal and mechanical property decreases resulting from physical and chemical changes from hygrothermal aging. Li [58] performed an isothermal aging study of a related bismaleimide composite and a compared this with a poly (ether ether ketone) (PEEK) composite. The author monitored microcrack resistance, impact and interlaminar shear strength and concluded that unidirectional composites showed better property retention than multidirectional composites, and also that the PEEK composite had better fibre/matrix adhesion and microcrack resistance than the bismaleimide.

Chapter 3 - Materials and Methods

3.1 Resin Synthesis

Matrimid® 5292 A and B (4,4'-bismaleimidophenylmethane and 3,3'-diallylbisphenol A respectively) were obtained from CIBA GEIGY. CBR320 (2,6-bis(3-amino(methyldiethyl)phenyl)-benzo{1,2-c:4,5-c'}dipyrrole-1,3,5,7(2H,6H)-tetrone) and CBR328 (4,4'-bis[2,5-dihydro-2,5-dioxo-1H-pyrrol-1-yl]-3,3',5,5'diethyldiphenyl-methane) were prepared in large-scale batches via the synthetic routes described below, from the respective diamines [59, 60]. The starting materials, Ethacure 100 (3,5-Diethyltoluene-2,4-diamine) and Ethacure 208 (4,4'-Methylene-bis-(2,6-diethylaniline)) were obtained from Fidene Australia Pty Ltd. (Sydney, Australia) and kindly donated by Albemarle Corporation (Baton Rouge, USA) respectively.

3.1.1 Synthesis of CBR 320

Ethacure 100 (3.31g) and 1,4-diazabicyclo{2.2.2}octane (1.0g) were dissolved in dimethylformamide (DMF) (50ml) in a round-bottomed flask under a nitrogen atmosphere. During stirring at 130°C, pyromellitic dianhydride (PMDA**)** (2.02g) dissolved in DMF (50ml) was added slowly over 1 hour to the diamine solution via a dropping funnel. After all the PMDA had been added the solution was heated to the point where it was just boiling. The solution became very dark, almost black, after heating due to the formation of the product, and was left to gently reflux under an air condenser overnight (about 16 hours). The solution was then concentrated and added to a 50/50-methanol/water solution to form a precipitate. The precipitate was filtered off and dried under vacuum over P_2O_5 at room temperature; the yield of crude product is quite high, typically being 82%. This diaminobisimide was endcapped by reaction with maleic anhydride according to the method reported [59] to give CBR 320.

It is necessary to purify the crude product in order to remove any reaction by-products. To purify, the crude bismaleimide (180g) was stirred in ethanol (500ml) for a few minutes and then filtered and the solid was allowed to dry under the vacuum. The solid was then dissolved in dichloromethane (1.25l) and light petroleum (boiling range 80-

100°C) (1.25l) was added and the mixture stirred for a few minutes. The insoluble material (a brown oily solid) was filtered off through celite and the filtrate was evaporated to dryness to give CBR 320 as a yellow powder that had a melting point of 304°C as measured by DSC. The yield obtained was typically 68g (37%); this was quite low as the crude material contained some residual moisture from the previous step. Major FTIR bands at 2973, 1729, 1712, 1373, 1356, 1112 and 733 cm^{-1}.

3.1.2 Synthesis of CBR 328

A solution of Ethacure 208 (150g) in dry DMF (300ml) was cooled to ≤ 15°C and stirred in a 1L round-bottomed flask. A solution of maleic anhydride (104.3g) in dry DMF (115ml) was added dropwise to this amine solution. When addition was complete (after approximately one hour) the reaction mixture was stirred at room temperature for two hours. Anhydrous sodium acetate (36.7g) was added followed by acetic anhydride (90ml). The reaction flask was heated to 55°C and held there for one hour.

The reaction mixture was then poured into a mixture of 750mL of methanol and 750mL of water and stirred for a few minutes before being decanted. Water (1.5l) was added to the product and again decanted. At this stage the product was an oily yellow solid. The solid was washed with 1L of a 5% $NaHCO_3$ solution. The product solidified and could be broken up. It was filtered and washed twice in water before being suspended in ethanol, filtered and dried in a vacuum oven overnight at 45°C. The yield of product obtained was 115.6g (51%). Major FTIR bands at 2969, 1712, 1393, 1376, 1154, 831 and 692 cm^{-1}.

3.2 Resin Degassing

The components of each resin system were combined and heated to 200°C under vacuum to remove any residual solvents from their synthesis. Failure to do this adequately can lead to voids in the cured laminate. The resin was formulated and degassed according to CIBA GEIGY recommendations [61]. The ratio of the components used was Matrimid® A: Matrimid® B, 1.15: 1 (w/w) (using an excess of the maleimide). The two components were placed in a pre-weighed round bottom flask in an oil bath heated to 120°C and the mixture was stirred until homogenous. The resin was then placed under a vacuum of -90 kPa at 130°C for 30 minutes until the resin

mixture was no longer rapidly expelling solvent. The resin was allowed to cool in the flask and was later made up into a 20% solution in dichloromethane for prepregging.

The formulation recommended by CSIRO for the experimental resin was CBR 320: CBR 328: Matrimid® B, 1: 1.5: 1.2 (w/w). The CBR 328 was placed in a round bottom flask in an oil bath heated to 150°C and placed under a vacuum of -90 kPa for 30 minutes. The CBR 320 was degassed in a separate flask at 200°C for 30 minutes. The Matrimid® B was added to the flask containing the CBR 328 and the mixture was placed under vacuum for 20 minutes at 200°C. The CBR 320 was added to the mixture and stirred until homogenous, the resin was then degassed for 30 minutes at 200°C, until the bubbling had subsided. The resin was immediately poured into a mortar and allowed to cool for several hours. Once the resin had cooled and solidified, it was ground into a powder using the mortar and pestle so that a solution of known concentration could be prepared for prepregging.

3.3 Prepregging

Prepregging, the process by which the resin is applied to the carbon fibre cloth, was performed using solution casting. Unidirectional carbon fibre cloth with E glass weft, which acted as reinforcement for the unidirectional carbon fibre tows (reference number: FC150U100), with a density of 150 gm/m^2 was obtained from Advanced Composites. Unidirectional cloths must be reinforced so that they can be handled and processed without the fibres warping. Most unidirectional carbon cloths are reinforced by either polymer webbing or paper, neither of which are particularly suited to high temperatures due to the tendency to degrade or melt and blend with the composite matrix during cure, both of which can affect the final properties of the composite. Initially this glass fibre reinforced cloth was selected as a result of the ability of glass to withstand the 250°C cure temperature. The glass fibre tows were spaced at 2mm intervals and this cloth was used only in the initial experiments until a more suitable unidirectional carbon fibre cloth was obtained. However, in the preliminary work, the glass fibre tows (perpendicular to the carbon fibre tows) were removed to create unidirectional carbon fibres in the region of crack propagation in the mode I tests. A few of the glass fibre tows were retained to prevent the carbon fibre tows from warping during prepregging. The time consuming removal of these tows helped to ensure stable

crack growth during testing (stable crack growth was observed), rather then the stick/slip behaviour observed when testing woven roving fabrics [62]. Double cantiliver beam (DCB) tests of specimens produced from these different fabrics yielded identical results. This cloth was superseded when a unidirectional fabric reinforced by a high temperature resistant polymer was obtained. This fabric was also obtained through Advanced Composites and had a density of 200gm/m^2 (reference number: FFC200U0500BS). Use of this fabric was found not to affect Mode I Interlaminar Fracture Toughness tests when results were compared to those obtained previously.

A mould for prepregging was built from a plate of aluminium with four strips of glass affixed to each edge to create a well of dimensions 340 × 190 mm^2 and approximately 6 mm in depth. TEFLON® coated glass was used to line the base of the mould as a release film. The cloth was cut to size and placed in the mould on top of the release film, whilst ensuring that the fibres remained parallel to each other. The resin loading was 1.09 grams per gram of cloth and the appropriate quantity of resin was dissolved in dichloromethane (10% w/w) and the solution was carefully poured over the unidirectional cloth in a manner that did not warp the fibres. If warpage occurs during prepregging, the stray fibres may influence the local geometry of the interlaminar matrix layer and hence deflect the propagating crack from the centre plies and invalidate the test [63, 64]. The resin was applied whilst the mould was placed on a level surface in a fume cupboard to ensure even coating of the cloth. The solvent was allowed to evaporate for 1-2 hours before the prepreg was removed and B-staged in an oven preheated to 100°C for 1 minute to remove any residual dichloromethane. As the boiling point of dichloromethane is 40°C, this temperature was sufficient to remove it.

3.4 Composite Lay-up and Cure

Prepregs were then aligned and stacked to create a 28-ply laminate to achieve a composite with the thickness for testing (approximately 4mm) recommended by the test protocol [65]. A piece of aluminium foil 15 μm thick and 70 mm long was treated with a high temperature release agent (Frekote 44NC Releasing Interface) and carefully placed in the mid-thickness of the specimen to act as the crack starter in the mode I DCB tests. A stainless steel frame, just slightly larger than the dimensions of the prepregs and 4 mm in thickness was used to prevent the unidirectional carbon tows

moving or warping during the cure. The CBR320/328 prepregs were vacuum bagged inside the frame as shown in Figure 3.1 and cured in an autoclave (American Autoclave "Mini Bonder", model number MB-2036-415-315-800) using the cure-cycle shown in Figure 3.2. An identical lay-up was used for the Matrimid® 5292 prepregs and they were cured using a similar cure-cycle according to CIBA GEIGY recommendations [61], shown in Figure 3.3.

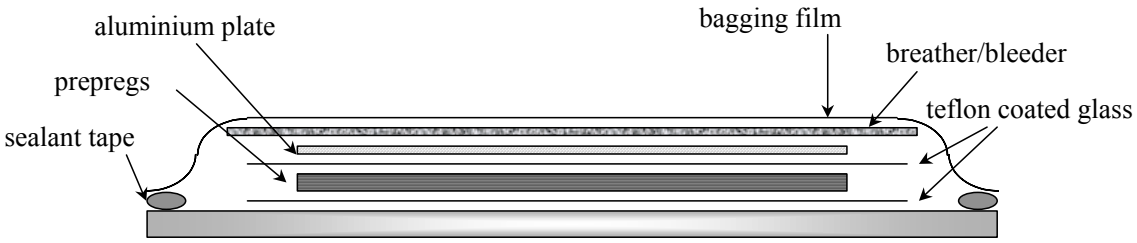

Figure 3.1: Lay-up used for fabrication of both composite materials, not shown is the aluminium frame that surrounds prepregs during cure, ensuring parallel fibre alignment.

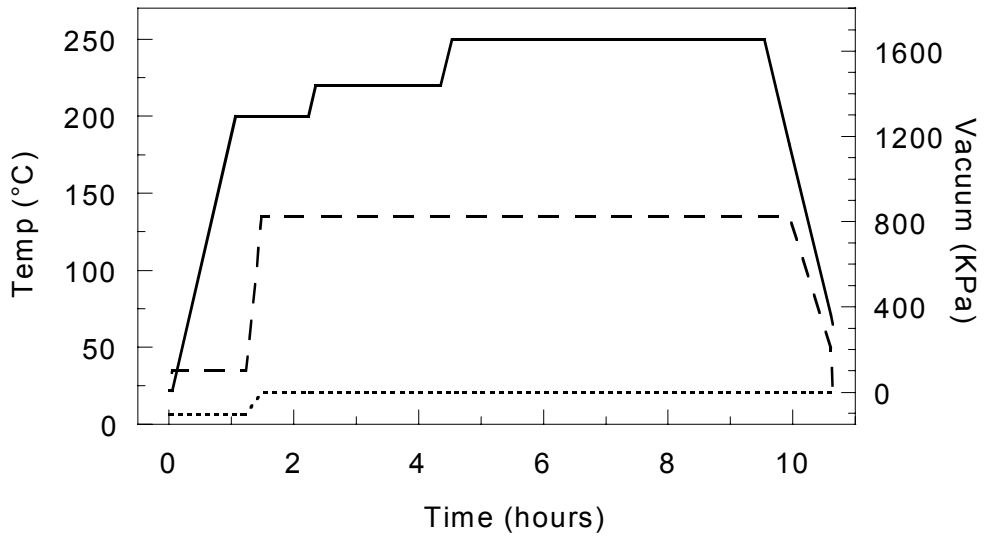

Figure 3.2: Optimal autoclave cure cycle for CBR320/328 composites where —— temperature (°C), ---- pressure (KPa) and ……vacuum (KPa).

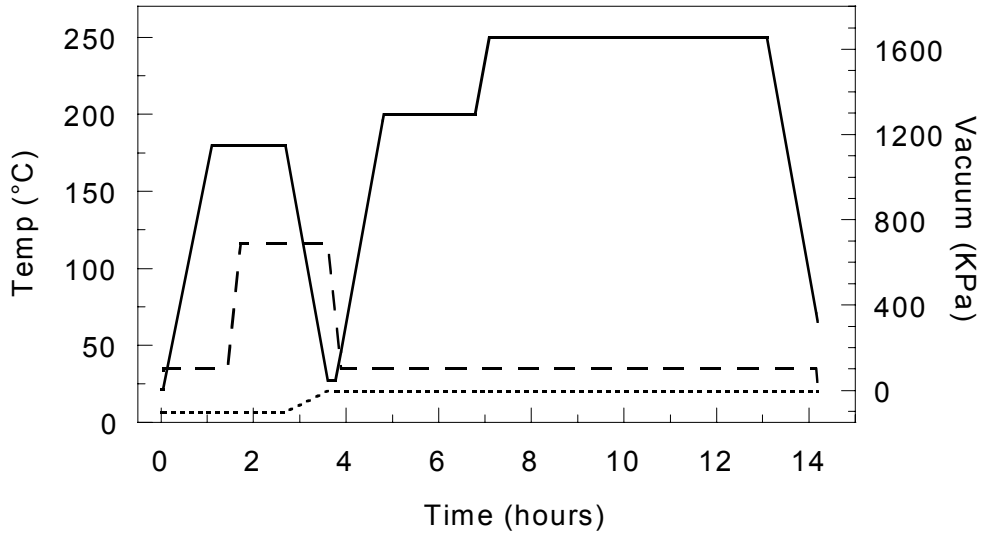

Figure 3.3: Recommended autoclave cure cycle for Matrimid® 5292 composites where —— temperature (°C), ---- pressure (KPa) and ……vacuum (KPa). CIBA GEIGY recommended a 3hour cure followed by a freestanding post cure, however for convenience, this was all carried out in the autoclave.

3.5 Composite Aging

Prior to aging in air in a preheated furnace, the specimens were preconditioned at 120°C for 24 hours to drive out any moisture the samples might have absorbed. Bismaleimide resins have a tendency to absorb a similar amount of moisture as epoxy resins (4-5% by weight), however saturation occurs more quickly than in epoxies [66]. Samples were also wrapped in glass fibre cloth before aging to protect them from contamination from any other substances in the furnace. Samples were aged in a calibrated furnace at 204 and 250°C for varying periods of time.

3.6 Mode I Interlaminar Fracture Toughness Tests

The percent fibre volume of each laminate was determined by image analysis of at least 5 representative SEM photographs of a cross section of the sample. The percentage fibre volume fraction (V_f%) calculated was in the average range of 49-55% for the CBR320/328 composites and in the average range of 68-73% for the Matrimid® 5292 composites. Although the resin loading on the prepregs was the same for both resin

systems, composites fabricated from the Matrimid® resin system had a higher V_f% due to a lower melt viscosity, which lead to greater resin run-out during cure. It was not possible to decrease the V_f% of the Matrimid® 5292 composites due to the tendency of the resin to run-out during cure. Nor was it possible to increase the V_f% of the CSIRO composites due to the tendency to form voids as a result of resin starvation. Thus the CSIRO composites had a slightly lower V_f% when compared with the composites fabricated with the commercial resin system. This initially caused some concern, however, as recently shown by Compston *et al*. [67], this should not affect the Mode I interlaminar fracture toughness test results as long as the calculated V_f% for the intralaminar regions adjacent to the crack plane does not vary. This intrinsic difference in V_f% also provides a true reflection of the V_f% of the composites when manufactured for service. SEM was also used to inspect the fibre distribution in the transverse composite sections. The fibres were homogenously distributed in all the specimens that were examined.

Double Cantilever Beam tests were performed in accordance with the protocol of the European Structural Integrity Society [65]. Specimens were cut to size using a diamond saw and were 20 mm in width, 4 mm in thickness and 160 mm in length with a 70 mm long crack starter film. The specimen geometry that was used is shown in Figure 3.4.

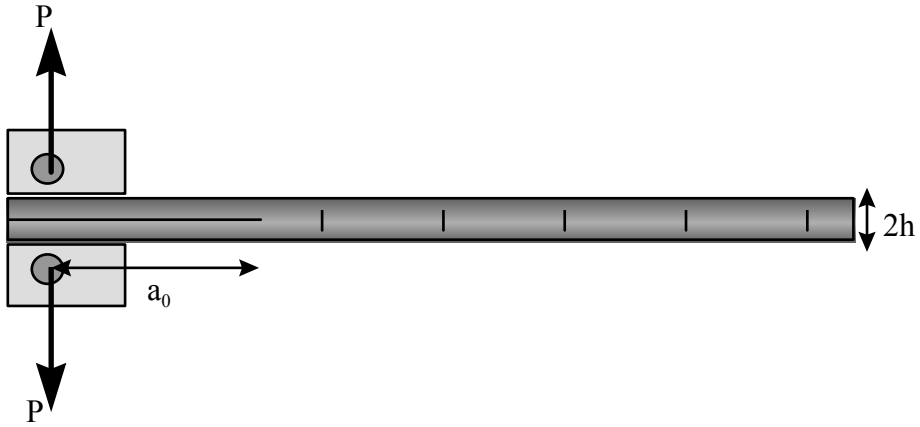

Figure 3.4: The geometry of a composite Mode I interlaminar fracture toughness test specimen (P = applied load, 2h = specimen thickness, a_0 = initial crack length).

To load the sample, aluminium tabs were adhered to the end of the specimen that contained the insert film and one side of the specimen was coated with white correction fluid to assist in monitoring the crack length. An Instron 4505 Universal Testing Machine was used to perform the tests using a crosshead speed of 1 mm/min and a load/displacement curve was produced for each test. From these data, the mode I critical strain energy release rate (G_{IC}) was calculated using corrected beam theory according to Eqn 3.1.

$$G_{IC} = \frac{3P\delta}{2B(a + |\Delta|)} \tag{3.1}$$

Where P = load, δ = displacement, B = specimen width, a = crack length and |Δ| = the crack length correction factor which is determined to be the x-axis intercept of the plot of the cube root of the compliance (C = δ/P) vs the crack length (a). Values of G_{IC} were plotted as a function of crack length (a) to produce a resistance (R) curve (see Figure 3.5). G_{IC}-*init* is defined as the first deviation from linearity on the load/displacement curve (or equivalently, the first point of the resistance curve). G_{IC}-*prop* is defined as the value of G_{IC} during steady state crack propagation, which corresponds to a plateau in the resistance curve. The fracture surfaces of the specimens were examined using Scanning Electron Microscopy to confirm that pure mode I failure had occurred and to check for any abnormalities. Any mode II (shear) behaviour is easily detected by the distinctive, deep hackles that it creates along the fracture surface of the specimen. Mode II behaviour arises when shear forces are introduced as the laminate is tested. These shear forces may arise from the unidirectional fibres not being parallel or from uneven thicknesses of the two arms of the specimen to which the tensile force is applied.

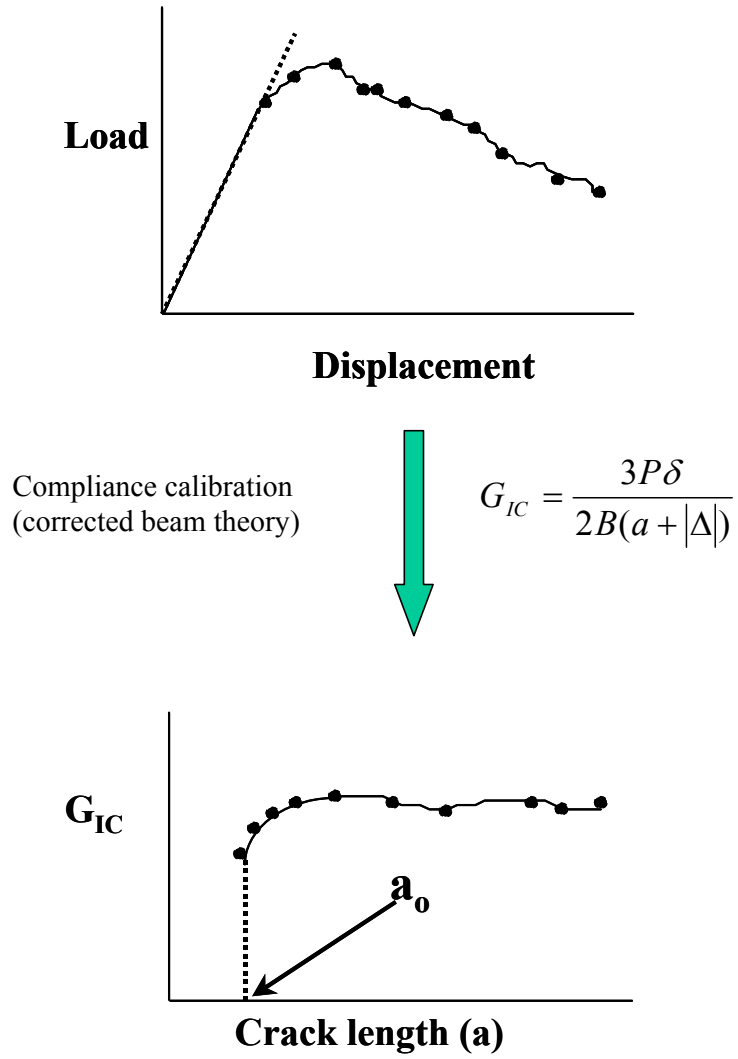

Figure 3.5: The construction of a resistance curve from a load/displacement curve. G_{IC}-init is defined as the first point of the resistance curve and G_{IC}-prop is defined as the plateau value in the resistance curve.

3.7 Fourier Transform Infrared Spectroscopy

Analysis of the resulting FTIR spectrum gives information as to the type of functional groups present in a molecule. The intensity of each peak arising from a particular functional group can be used to determine the concentration of that particular molecule in the sample. In Infrared Spectroscopy, a sample is irradiated by a source (typically by a Nernst source - a heated ceramic filament containing rare earth oxides) that emits radiation of wavelength 2.5 – 25 μm. When the sample is irradiated, some wavelengths will be absorbed by the sample whereas others will pass through the sample. In Infrared

Spectroscopy, those wavelengths absorbed by the sample correspond to molecular vibrations that involve a change in the dipole moment of the molecule being irradiated. Thus each molecule within the sample possesses a characteristic Infrared Spectrum consisting of a series of peaks that represent absorptions at different wavelengths.

Conventionally a typical infrared spectrum is a plot of the absorbance (or conversely transmission) against the wavenumber (cm^{-1}) where one wavenumber = $10^4/\mu m$. A typical IR spectrum will scan the region from 400 to 4000 cm^{-1}. Until the advent of Fourier Transform Infrared Spectroscopy (FTIR), the sample was irradiated one frequency at a time and the absorbance measured to generate an entire spectrum. FTIR has the advantage that it measures the entire spectrum simultaneously and to analyse the individual frequencies in the composite signal, a Michelson Interferometer is used, much like a chord played on a piano can be separated into individual notes.

Fourier Transform Infrared Spectroscopy (FTIR) was performed using potassium bromide (KBr) discs containing finely ground composite samples on a Perkin Elmer "Spectrum One" Fourier Transform Infrared Spectrometer. Samples were prepared in this way to take advantage of the infrared transparency of KBr and because it is highly suitable technique for composites samples which require a great deal of grinding, due to the presence of fibre fragments. The aged composite samples were split in half so that the exposed surface and the interior of the sample could both be examined. Samples were prepared by scraping a small amount of material (taking care not to include too much carbon fibre) from the composite and grinding this in a mortar and pestle under a heat lamp to exclude as much moisture as possible. A KBr disc of this material was then prepared and examined. A small amount of fibre present will broaden the baseline of the spectrum slightly, however the features of the spectrum can still be observed.

3.8 Raman Spectroscopy

Raman Spectroscopy detects molecular vibrations where a change in the polarizability of the molecule occurs, whereas FTIR Spectroscopy, discussed in the previous section, detects a change in the dipole moment of a molecule. As a result of this, Raman and FTIR are sensitive to different functional groups present on molecules and as a consequence, bands that may be weak in the Raman spectra are often strong in the FTIR

spectra and vice versa. Sample preparation is much more convenient with Raman Spectroscopy as a result of it being a scattering technique. Powders, fibres and composites can be analysed with only minimal sample modification and with small amounts of material. With the advent of the Raman Microscope, regions of a sample as small as 2μm in diameter can be analysed. When several of these regions are examined across a transverse section of a composite panel, chemical changes through the thickness of the sample can be examined.

While FTIR spectroscopy is particularly effective in detecting C=O moieties, Raman Spectroscopy is highly sensitive to C=C bonds, therefore the two techniques provide complementary information. In Raman Spectroscopy, a sample is irradiated by a laser source. When a photon of energy $h\nu_0$ collides with a molecule this results in the scattering of light. The light may be scattered either elastically or inelastically. When an elastic collision occurs, neither the photon nor the molecule changes in energy, resulting in Rayleigh scattering. In Rayleigh scattering, the scattered light has the same frequency as the incident light. Raman scattering arises from an inelastic collision between the photon and the molecule where the photon either gains energy from or loses energy to the molecule. The energy of this scattered light is $h(\nu_0 \pm \Delta\nu)$ and this corresponds to the vibrational energy of the molecule. In Raman scattering, the scattered light has a different frequency to the incident light and this frequency difference ($\pm\Delta\nu$) can be detected and used to give information about the molecular vibrations of the molecule. Raman transitions occur according to the selection rule $\Delta\nu = \pm 1$. Lines for which $\Delta\nu = -1$ are called anti-Stokes lines where the scattered light shifts to higher frequency and these lines are generally weak as they occur when a molecule is initially in a sparsely populated excited state (the ground vibrational state has the highest population of molecules). Lines for which $\Delta\nu = +1$ (shift to low frequency), are of much higher intensity and are called Stokes lines. It is these lines that are usually made use of in Raman Spectroscopy. Figure 3.6 shows the mechanisms of various light-scattering processes including resonance fluorescence, which will be discussed later.

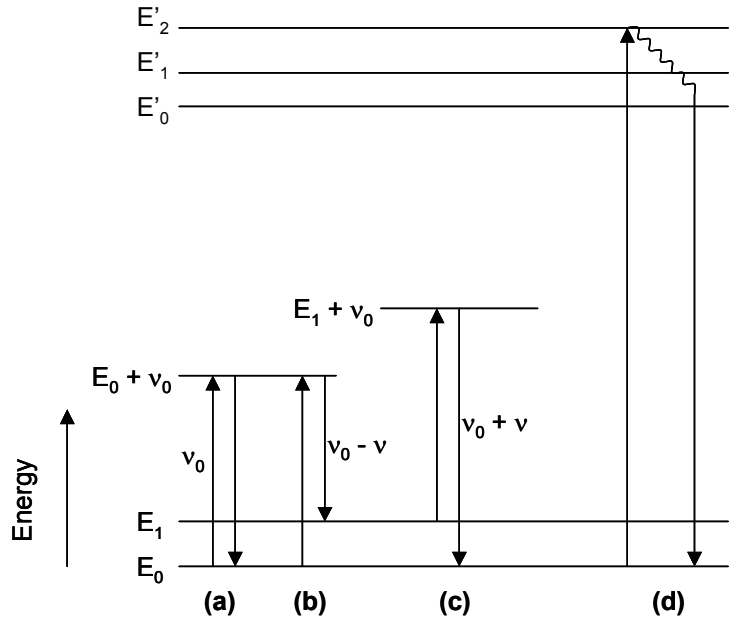

Figure 3.6: Mechanisms of various light-scattering processes. (a) Rayleigh, (b) Stokes, (c) Anti-stokes and (d) resonance fluorescence.

Fluorescence is often a problem when using Raman Spectroscopy to analyse polymers, particularly those containing chromophores in their structure, as the presence of chromophores (structural feature of a molecule responsible for its absorption of UV or visible light to give a coloured compound) tends to make the sample prone to unquenchable fluorescence [68]. In fluorescence, the system absorbs radiation and is excited to a higher electronic state before re-emitting this radiation. Raman scattering does not involve the absorption of radiation or any excited electronic states and the whole process of scattering is relatively quick (10^{-12} s) compared with fluorescence (10^{-9} s) [69]. The effect of fluorescence is to veil the Raman signal as even if it arises from a chromophoric impurity present at parts per million level with a low quantum yield, there may be 10 fluorescent photons for every Raman photon [68]. There are several methods to counteract the effect of fluorescence, including changing the laser frequency. However the most success was had in this study through the use of the well-established technique known as photo-bleaching. Photo-bleaching involves exposing the sample to the laser beam until the fluorescence decays. The laser used to photo-bleach the sample is the same as the laser used when accumulating spectra, therefore chemical modification of the polymer as a result of this process was not a concern. The aged

CBR 320/328 composites exhibited the highest degree of fluorescence due to the presence of extended aromatic chromophores in the structure and the (assumed) degradation products. In this case, samples were photo-bleached for several hours and the spectra accumulated overnight.

Raman spectra were obtained using a Renishaw Raman Imaging Microscope 2000, with a 718nm NIR laser source. Composite samples were prepared by casting the specimens in an epoxy resin to facilitate polishing. After the sample had been polished with 6 μm diamond paste, it was ultrasonically cleaned in ethanol and mounted on a microscope slide so that the surface was level. The main problem associated with preparing the specimen by polishing is that residues from the polishing process are smeared across the surface of the specimen. Both diamond paste and the epoxy mounting resin have very distinctive Raman spectra and can easily be identified as impurities.

3.9 Dynamic Mechanical Thermal Analysis

Dynamic Mechanical Thermal Analysis (DMTA) is a useful means of determining the glass transition temperature (Tg) of the polymer matrix in composite samples. The response of a polymer to an induced deformation is not perfectly elastic, there are elements of a viscous response, and hence polymers are described as exhibiting viscoelastic behaviour. In DMTA, an oscillating strain is imposed on the polymer sample, which inturn means that the stress is also oscillating. With each cycle, some of the strain energy is stored elastically and some of this energy is dissipated in a viscous manner, typically as heat. If the imposed strain is kept small enough to preserve linear viscoelasticity, where stress and strain are linearly proportional, then stress and strain may both be represented by sine waves of the same period, but with a phase lag. The ratio of the magnitude of the two sine waves is known as the dynamic modulus (E_d) and the phase lag (δ) is a measure of the ability of the polymer to dissipate the strain energy. For polymers, the phase lag is temperature dependent and lies between 0° (purely elastic) and 90° (purely viscous). It is more useful, however, to consider the complex modulus (E*), which is comprised of two components, being the storage modulus (E') and the loss modulus (E"). The ratio of the storage and loss moduli is also known as tan δ. At temperatures below their Tg, polymers, at low strain, behave almost

elastically. As the material approaches Tg, the behaviour is much more viscoelastic and the Tg is characterised by a peak in the tan δ curve and a sudden decrease in the storage modulus (E'). These methods of calculating the Tg of the polyimide matrix were both utilised in this study and are referred to as the peak and the extrapolated onset respectively.

DMTA was conducted on a Polymer Laboratories Mk2 instrument using 2 mm thick composite specimens in single cantilever mode. The imposed strain was small enough to ensure linear viscoelasticity.

3.10 Scanning Electron Microscopy

Scanning Electron Microscopy (SEM) was used in the present study to examine the fracture surfaces of the composite specimens after testing. The purpose was to ensure that put Mode I failure had occurred and to check for any abnormalities in the composite microstructure. SEM can produce a magnified image of a sample by scanning an electron beam across the surface of a sample and building up the image point by point. The probe in SEM consists of a focussed electron beam (known as the primary beam) and a detector measures the intensity of the reflected beam, the signal from the detector representing the topographic contrast of the sample is displayed on a monitor. SEM has much higher resolution than Optical Microscopy (10 nm compared with 300nm respectively) and can be used to magnify an image up to 100,000 times. Sample preparation for SEM is relatively simple and in the case of non-conductive samples such as composite materials, involves only coating the sample with a conductive coating such as gold or carbon, which is given electrical contact with the sample holder.

Three important signals arise from the contact of the coated sample from the primary beam; these are secondary electrons, backscattered electrons and X-rays. X-rays are produced in the largest volume, however they have very low resolution and will not be discussed any further. Secondary electrons are produced from the top few nanometres of the surface of the sample and are of low energy and have high resolution, hence they are the most frequently utilised signal. Backscattered electrons escape from the surface of the sample from a depth of 1μm or less. They arise when electrons from the primary

beam are elastically scattered by nuclei at the surface of the sample and are of high energy and generally travel in straight lines after leaving the sample. The fraction of backscattered electrons escaping from each nuclei is dependent on the type of atom, thus the intensity of backscattered electrons is determined by the chemical makeup of the sample and although the resolution is low, the compositional contrast is high. Backscattered electrons were used to build up the signal for the composite samples used to calculate fibre volume fraction, as these signals gave the maximum amount of contrast between the carbon fibres and the polyimide matrix.

Microscopy was performed using a Cambridge S360 scanning electron microscope. Secondary electron images from the fracture surfaces of the composites were obtained after coating the specimens with gold. Backscattered electron images used to calculate the V_f% of the samples were obtained after lightly coating the samples with carbon.

Chapter 4 - Isothermal Aging at 250°C

4.1 Introduction

Both the CSIRO and the commercial composite materials were aged isothermally at 250°C as a preliminary study so that the conditions for aging at a lower temperature, closer to the predicted in service temperature of 177°C could be estimated as described below. The experiments at 250°C were also conducted to investigate the effect of aging at a temperature just below the glass transition temperature of the material. Based on the weight loss data for similar resin systems from previous studies [12], it has been shown that one week of aging at 250°C is equivalent to approximately seven weeks of aging at 204°C. From the results of the 250°C study, it was possible to estimate the approximate length of time required before chemical changes could be observed at the lower temperature.

4.2 Mode I Interlaminar Fracture Toughness

Mode I delamination tests were completed after composite specimens of both resin systems were aged between 1 and 8 weeks at 250°C. Stable crack growth was observed for all samples tested. A small region of fibre bridging was detected just behind the crack tip during testing in both materials, an observation common in the case of unidirectional specimens [62]. This fibre-bridging zone appeared by visual inspection to increase in size as the specimens tested were aged for longer periods of time. Hutapea *et al*. [70] also observed that more extensive fibre bridging occurred in double cantilever beam specimens with increased aging time in a study of another high temperature composite material aged at similar temperatures. Further evidence of this increased fibre bridging is shown in the scanning electron micrographs in Chapter 5. One explanation for this proposed by Hutapea is that after aging the composite for long periods, most of the matrix has been oxidised and very little remains to bind the fibres together, so that delamination occurs primarily along the fibre–matrix interface. This behaviour leads to an increase in fibre bridging which then means that more energy is required to propagate the crack, leading to an increase in $G_{IC\text{-prop}}$.

4.2.1 Delamination Testing of Matrimid® 5292 Composites

Figure 4.1 shows typical R-curves for samples of the Matrimid® 5292 resin aged for 0, 1,2,4 and 6 weeks at 250°C. The first point on the curve is defined as $G_{IC\text{-init}}$ and $G_{IC\text{-prop}}$ is calculated from the plateau in the R-curve. Prior to thermal treatment $G_{IC\text{-init}}$ was measured to be 150 J/m^2 and this value is consistent with other published values for high temperature composites [71]. The general trend in these results is that $G_{IC\text{-init}}$ decreases with the amount of time the material is aged. $G_{IC\text{-prop}}$ initially increases with the amount of time aged, before decreasing dramatically. After 1 and 2 weeks of aging at 250°C, $G_{IC\text{-prop}}$ increases by 40% and 15% of the unaged value respectively. After 4 weeks, however, this value decreases dramatically to approximately 30% of the original value and remains more or less the same after 6 weeks of aging. A general decrease in toughness as the aging time is increased may be expected, however an initial increase in composite toughness is at first glance, counter-intuitive. This initial increase may partially be attributed to an increase in fibre bridging as will be explored further in Chapter 6.

4.2.2 Delamination Testing of CBR 320/328 Composites

Figure 4.2 shows the results of Mode I interlaminar fracture toughness tests for CBR 320/328 composite samples aged for 0, 2, 6 and 8 weeks at 250°C. Samples aged for 4 weeks were also tested, however, they all failed by cracking at the surface of the sample rather than by a mode I mechanism and the results had to be discarded. This occurred in all of the samples tested despite separate panels being used to produce each sample, thus eliminating the theory that this may have been caused by a manufacturing defect in a particular panel.

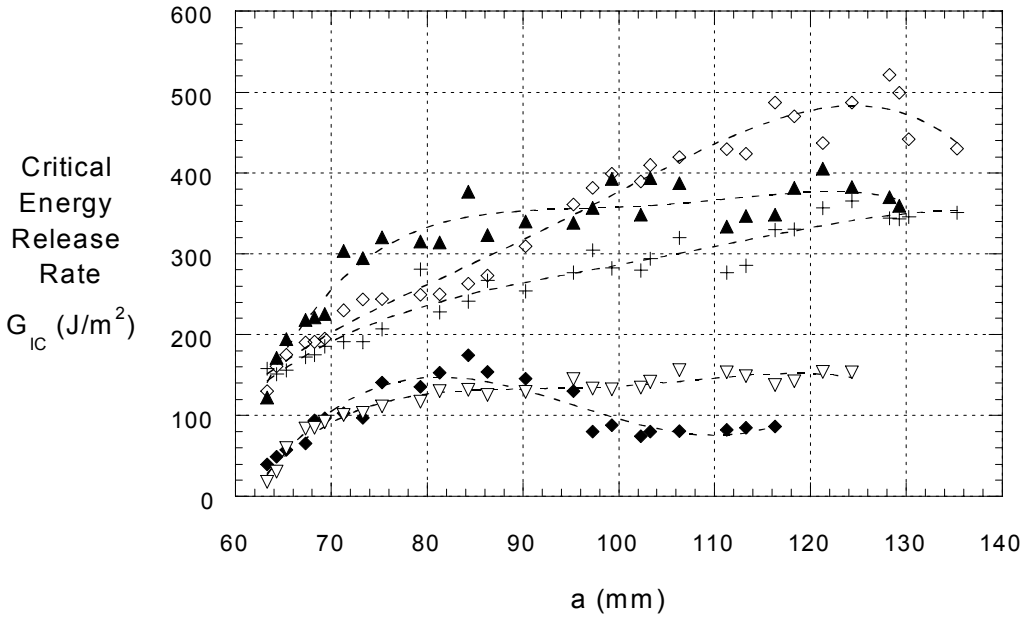

Figure 4.1: The effect of isothermal aging at 250°C on the interlaminar fracture toughness (Mode I R-curve) of a carbon fibre/Matrimid® 5292 composite. (+ 0 weeks, ◇ 1 week, ◢ 2 weeks, ◆ 4 weeks and ▽ 6 weeks of aging at 250°C.)

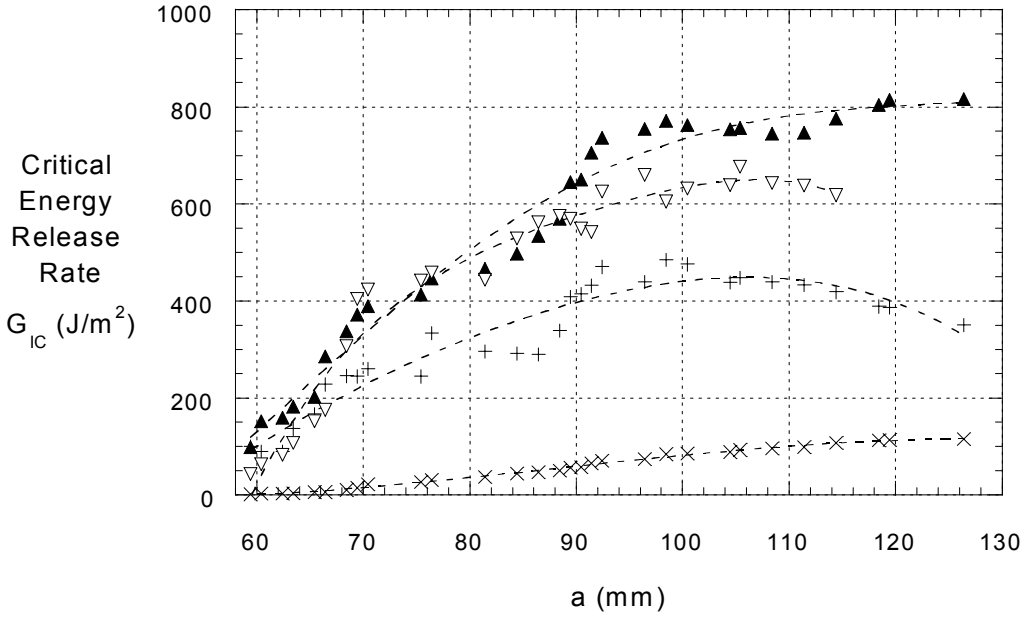

Figure 4.2: The effect of isothermal aging at 250°C on the interlaminar fracture toughness (Mode I R-curve) of a carbon fibre/CBR320/328 composite. (+ 0 weeks, ◢ 2 weeks, ▽ 6 weeks and × 8 weeks of aging at 250°C.)

The general trend in these results is quite similar to the trend observed in the case of Matrimid® 5292 composites. $G_{IC\text{-init}}$ decreases with the amount of time the material is aged, however $G_{IC\text{-prop}}$ initially increases before a substantial decrease is observed. After 2 weeks of aging the value of $G_{IC\text{-prop}}$ has increased by 80% of the original value and this decreases back to approximately the original value after 6 weeks of aging. Significant fibre bridging was observed during the testing of these samples and this may have increased this result. There was also a great deal of scatter in the four samples tested. At 4 and 6 weeks of aging, substantial degradation was evident at the surface of the sample, however the interlaminar fracture toughness did not change as dramatically, remembering that this test measures properties at the core of the sample. After 8 weeks of aging $G_{IC\text{-prop}}$ decreases significantly, to only 35% of the untreated value.

4.2.2 Comparison of the Interlaminar Fracture Toughness Results.

The variation of the critical energy release rate with time aged at 250°C for both Matrimid® 5292 and CBR 320/328 composites is plotted in Figure 4.3. Each point represents an average of four values and error bars signify ± 1 standard deviation.

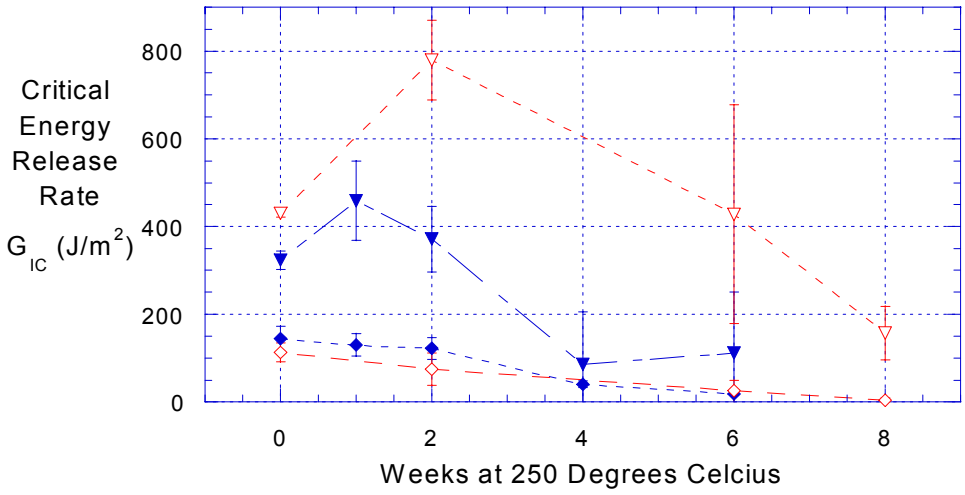

Figure 4.3: $G_{IC\text{-init}}$ (◇, ◆) and $G_{IC\text{-prop}}$ (▽, ▼) as a function of the number of weeks of isothermal aging at 250°C of composites of Matrimid® 5292 (closed symbols) and CBR320/328 (open symbols). (Error bars signify ±1 standard deviation).

$G_{IC\text{-init}}$ measurements were much more consistent than of $G_{IC\text{-prop}}$ measurements, which have a greater variation due to the variable effect of fibre bridging. Even after considering the variation in values, $G_{IC\text{-prop}}$ measurements for CBR 320/328 are consistently higher than those for Matrimid® 5292 composites, indicating that the experimental material has better delamination resistance and is able to retain this behaviour after heat treatment more effectively than the commercial material.

Inspection of Figure 4.3 indicates that the CBR 320/328 composites exhibit slightly better property retention than the Matrimid® 5292 composites as evidenced by the property retention after 6 weeks of aging. $G_{IC\text{-prop}}$ decreases to 30 % of the unaged value after 6 weeks of aging in the case of Matrimid® 5292 composites, whereas after 6 weeks $G_{IC\text{-prop}}$ measured for the CBR 320/328 composites is equivalent to the untreated value. $G_{IC\text{-prop}}$ decreases to 35% of the original value after 8 weeks of aging in the case of CBR 320/328 composites. This may be partially attributed to the higher fibre volume fraction (V_f%) of the Matrimid® 5292 composites. As discussed in chapter 3, the commercial composites produced have a V_f% of 68-73%, considerably higher then that of the CBR 320/328 composites, which have a V_f% of 49-55%. As explained in Chapter 3, the two materials could not be manufactured with identical volume fractions as the Matrimid® 5292 resin has a low melt viscosity and is prone to bleeding during cure. Thus, despite attempts to dam the Matrimid® 5292 to reduce bleeding, a V_f% of 68% was the lowest experimental limit. The volume fraction of CBR 320/328 composites could not be increased above 55% without the introduction of a significant number of voids.

This difference in V_f% helps to explain the difference observed in $G_{IC\text{-prop}}$ after aging. $G_{IC\text{-prop}}$ is measured at the core of the specimen. Composites of Matrimid® 5292 have a higher fibre volume fraction than those from CBR 320/328, therefore the matrix volume fraction is substantially lower. The matrix is oxidised during aging at this temperature, and the fibres are not greatly affected [72]. A relatively small percentage weight loss in the case of the Matrimid® composites corresponds to a large percentage loss of resin. If the weight loss of both composite materials is similar (see section 4.6), then the commercial composite materials will tend to be much more susceptible to the

deleterious effects of aging.

In addition to this, the CBR 320/328 composites appear to initiate a char protection mechanism, similar to that observed by Turi [73]. The surface of the samples undergoes severe oxidation and the matrix forms a char (carbon rich oxidation product), which then protects the remainder of the matrix from further oxidation. This theory is consistent with the observation that the surface of the CBR 320/328 composites appeared to be heavily degraded whilst the core appeared relatively intact. This is further supported by results from the Raman Spectroscopy study (section 4.5), which indicate heavily degraded regions at the surface of both composites. Bowles also made similar observations of surface degradation and photographed micro-crack formation at the surface of aged PMR-15 composite samples [52].

$G_{IC\text{-init}}$ measurements are similar for both materials as $G_{IC\text{-init}}$ is matrix dominated. The greater variation in $G_{IC\text{-prop}}$ measurements arises due to the dependence of this value on the fibre/matrix interfacial adhesion. This is discussed further in Chapter 6.

4.3 Scanning Electron Microscopy

Samples were examined by scanning electron microscopy (SEM) to ensure that pure Mode I failure had occurred. Figure 4.4 compares Scanning Electron Microscope images of the propagation regions of typical delamination specimens of Matrimid® 5292 and CBR 320/328 composites, magnified 400 times. Both images confirm pure mode I failure, with no sign of any of the distinctive, deep hackles which are typical of Mode II (shear) failure. The fibres in the CBR 320/328 composite are very clean when compared with the fibres in the commercial composites, which indicates better matrix/fibre adhesion in the latter. Good matrix/fibre adhesion generally leads to the crack growing mostly through the matrix during mode I testing. Poor adhesion as observed in Figure 4.4 (b), indicates that the crack propagates along the fibre/matrix interface during testing. This leads to an increase in fibre bridging, which increases the energy required to propagate the crack and may partially explain why the results for $G_{IC\text{-prop}}$ for the CBR 320/328 composites are considerably higher than those for the commercial composite. Very little matrix deformation is observed in either case, indicating that both types of resin undergo brittle failure.

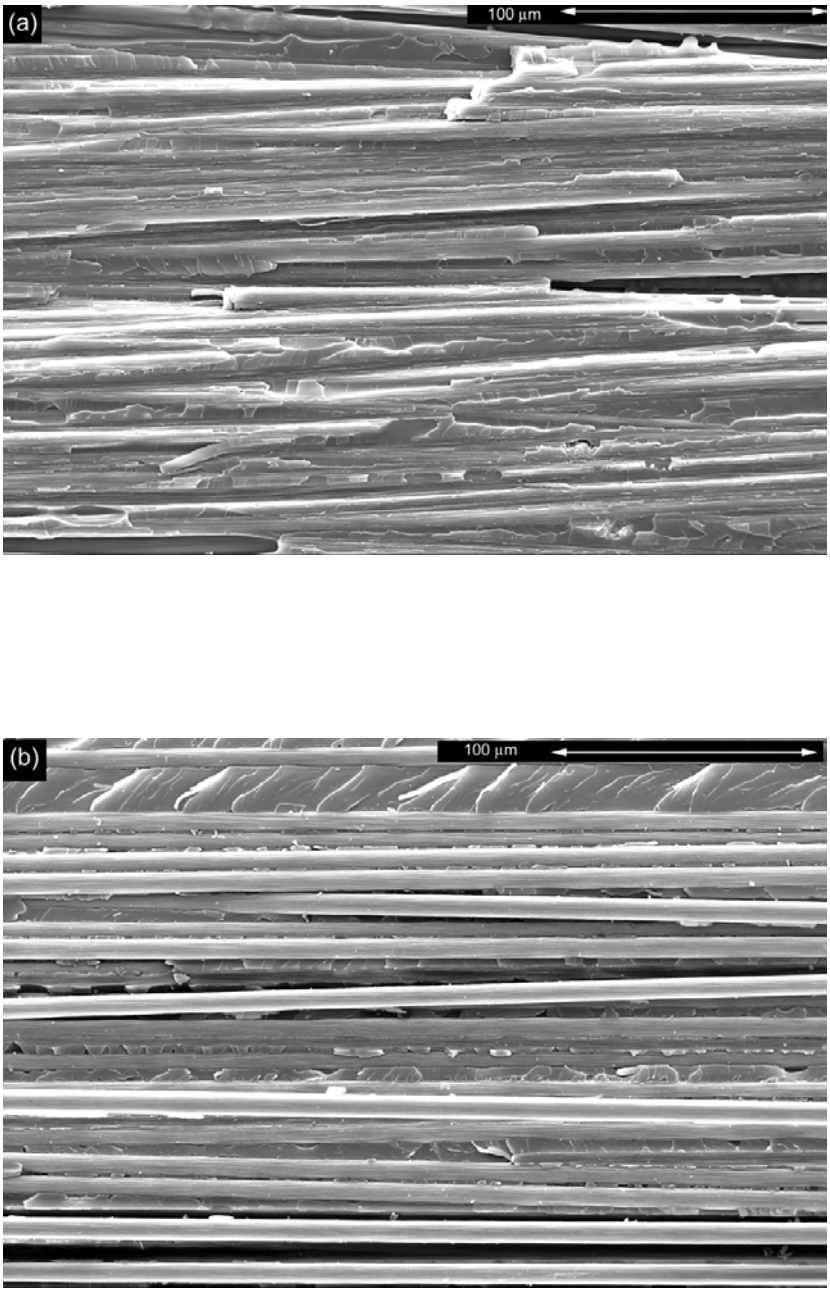

Figure 4.4: SEM of the propagation region of untreated delamination test specimens of a) Matrimid® 5292 and b) CBR 320/328 composite, confirming that pure Mode I failure has occurred during testing.

A comparison with aged materials is not shown here as this was performed as a preliminary study and the samples were consumed in the process of conducting other tests. With only a limited amount of resin available at the time of manufacture, the focus was then concentrated on the lower temperature aging study. SEM of aged materials is discussed in more detail in Chapter 5.

4.4 Fourier Transform Infrared Spectroscopy

4.4.1 FTIR Spectroscopy of the surface of composites aged at 250°C.

Changes in the infrared spectra at the surface of the composites aged at 250°C were monitored daily over a period of four weeks. KBr discs were made from small amounts of composite that were removed using a scalpel either from the surface of the specimen or from the core after the interlaminar fracture toughness had been measured. Chemical changes observed in the core of the material (discussed later) were highly relevant to the changes observed in interlaminar fracture toughness as the crack propagates through the centre region of the specimen during testing.

In both composites made with the CSIRO resin and the commercial resin, oxidation of the surface of the panels was observed during the first four days of aging. After this, no further changes were observed at the surface. The FTIR spectra showing these initial changes are shown in Figure 4.5. The spectra shown in this Figure are of CBR 328/328 composites, however similar changes were observed in composites of Matrimid® 5292 composites. The most noticeable change as aging progresses is the broadening of the spectra and the loss of the detail that can be seen in the control spectrum. Sharp, distinctive peaks at 2969, 2935, 2875 cm^{-1} that have previously [74] been assigned to asymmetric stretches of CH_3 and CH_2 groups and the symmetric stretch of a CH_3 group respectively, disappear. The imide carbonyl group at 1779 cm^{-1} appears to merge into neighbouring peaks and the ingrowth of a broad peak at 1615 cm^{-1} is observed. The peaks arising from the degradation of the matrix in this surface layer is consistent with the oxidation of the methylene moiety of Matrimid® A to a carbonyl group. This reaction was also observed at the core of the sample and will be discussed in further detail later. The changes observed in the FTIR spectra from the core of the specimen were studied in greater detail than spectra from the surface of the samples as they can be

correlated with changes noted in the interlaminar fracture toughness of the composite as mentioned above.

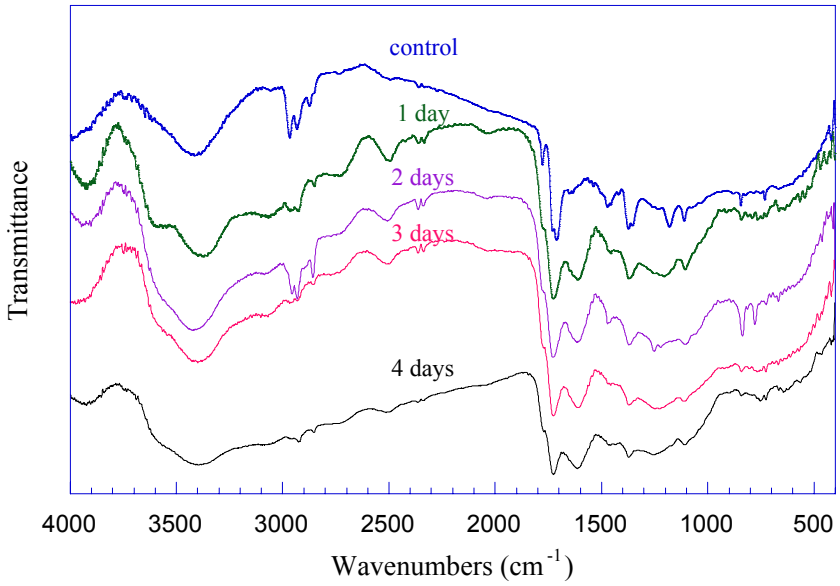

Fig. 4.5: FTIR spectra of the surface of a CBR 320/328 composite shown after 0, 1, 2, 3 and 4 days of aging at 250°C, highlighting the rapid chemical changes at the surface of the composite.

4.4.2 FTIR Spectroscopy of the core of Matrimid® 5292 composites aged at 250 °C.

Evidence of chemical changes that occur after the Matrimid® 5292 composites have been aged at 250°C is shown in Figure 4.6. After 1 and 2 weeks of aging, the most significant change that occurs is the growth of the imide peak at 1715 cm^{-1} concomitant with the diminishing of the a peaks at 1111 and 1384cm^{-1}. The peak at 1384 cm^{-1} may be assigned to the aromatic CH_3 present in the Matrimid® 5292 B structure, however the assignment of peaks in the region around 1100 cm^{-1} is quite contentious and this peak does not appear to be highly relevant to the present study as will be discussed later.

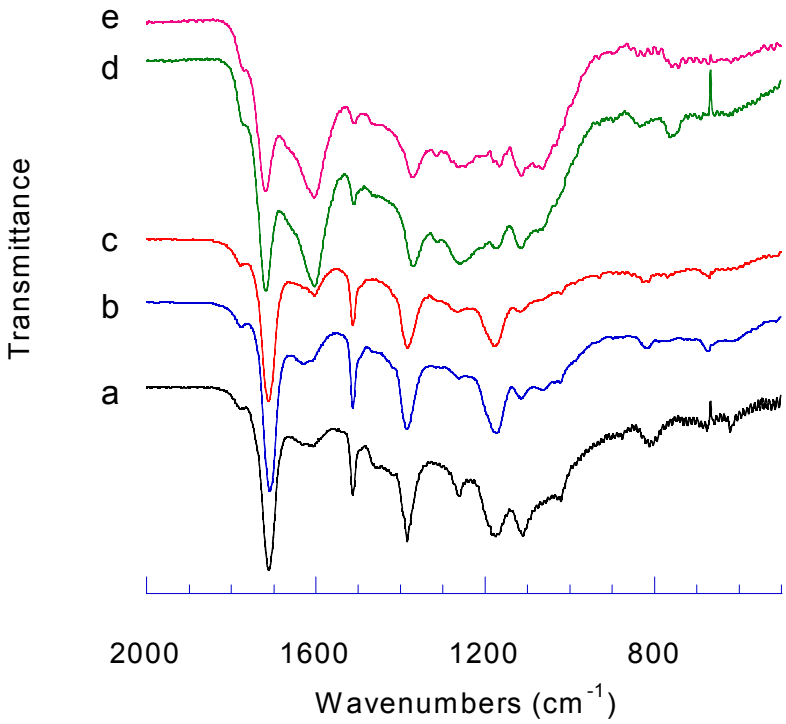

Figure 4.6: FTIR spectra of the core of Matrimid® 5292 composites aged at 250°C for (a) 0, (b) 1, (c) 2, (d) 4 and (e) 6 weeks.

It is not until after 4 weeks of aging that significant change in FTIR spectra occurs, consistent with the significant loss of interlaminar fracture toughness after 4 weeks as described previously in this chapter. The region between 1500 and 1000cm^{-1} broadens significantly and it difficult to distinguish individual peaks. The carbonyl peak has shifted slightly from 1711 to 1718 cm^{-1}, but more importantly the peak at 1512 cm^{-1} assigned to the ring breathing of the para-substituted aromatic in the methylene diamine moiety of Matrimid® 5292 A, disappears at the same time as the ingrowth of a peak due to a substituted aromatic sensitive C=O conjugation at 1604cm^{-1}. This is consistent with oxidation of this methylene group to form a carbonyl group based on the work by Jewell and Sykes on the thermoxidation of methylene bridging groups in polyimides [75]. This reaction occurs concurrently with the dramatic decrease in the critical energy release rate during steady crack propagation ($G_{IC\text{-prop}}$) reported in section 4.1. The oxidation of this methylene moiety was also observed by Meador *et al.* [42] who employed FTIR to monitor changes in PMR-15 samples aged at 318, 335 and 345°C. Methylene dianiline in PMR-15 undergoes imidization during cure to form a very

similar structure to Matrimid® 5292 A. In this study, the oxidation was observed at the surface of the sample, only in a "reaction zone" 0.1-0.2 mm in thickness. Samples were aged for only 300 hours (12 days) rather than for periods of weeks as in the present study. After weeks of aging at similar temperatures, the matrix can become quite porous and this extended period of aging explains why oxidation occurs in the core of the specimen here rather than just being confined to a reaction zone.

4.4.3FTIR Spectroscopy of the core of CBR 320/328 composites aged at 250°C.

A comparison of FTIR spectra of 320/328 composites aged at 250°C for 0, 2, 4, 6, and 8 weeks is shown in Figure 4.7. Assignment of the peaks arising from this novel resin is relatively difficult, however studies of similar compounds in the literature proved to be useful.

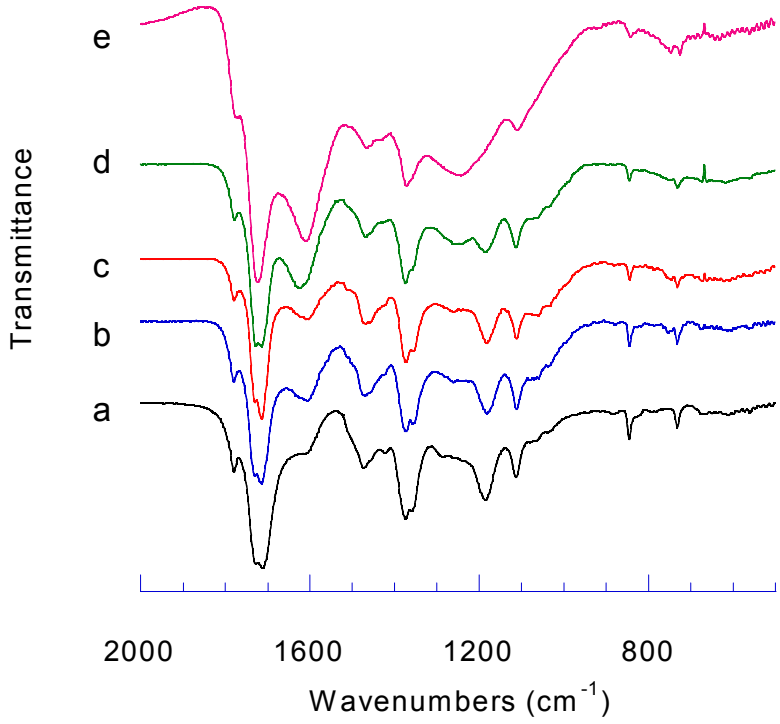

Figure 4.7: FTIR spectra of the core of Matrimid® 5292 composites aged at 250°C for (a) 0, (b) 2, (c) 4, (d) 6 and (e) 8 weeks.

It is not until 6 weeks of aging at this temperature that significant chemical changes are observed. Theses changes occur concurrently with the decrease in $G_{IC\text{-prop}}$ observed in

section 4.1, just as they did in the case of the commercial composites. At 6 weeks of aging, the two imide carbonyl peaks at 1728 and 1712 cm^{-1} become one single peak at 1723 cm^{-1}. This occurs as a result of the degradation of the saturated imide. The unsaturated imide from the PMDA building block proves to have higher thermal stability, the mechanism will be discussed further in chapter 6. The ingrowth of a broad carbonyl peak at 1609 cm^{-1} is also observed as it was in the spectra of aged Matrimid® 5292 composites. This is again consistent with the oxidation of the methylene group (also present in CBR 320/328) to a carbonyl group.

4.5 Raman Spectroscopy

As Raman spectroscopy is a light scattering technique, it is extremely versatile and is particularly useful in the analysis of composite materials due to the ability to focus on small (5μm) pockets of resin between tows in the laminate. A spectrum can be obtained from this small region that enables the mapping of chemical changes in the Raman spectrum across the width of a sample.

The Raman spectrum for the unaged Matrimid® 5292 composite is shown in Figure 4.8 (A) and compared with the spectrum of a sample aged for 1 week at 250°C (B). Assignments for the observed signal frequencies are indicated in Table 4.1 [76, 77]. CBR 320/328 composites are not examined here as they exhibited a high degree of fluorescence after aging and spectra could not be measured. This fluorescence is caused by the presence of extended aromatic chromophores. The most obvious change is seen in the intensity of the peak at 1646cm^{-1} (peak 11) relative to its neighbouring peak at 1608 cm^{-1} (peak 10). These peaks may be assigned to the C=C stretching modes of the alkene moiety (present in Matrmid B) and the aromatic rings (present in both Matrimid® 5292 A and B) respectively. The relative intensity of the alkene peak decreases as the material is aged for 1 week. This observation is consistent with the recorded increase in $G_{IC\text{-}prop}$ values and further supports the contention that continued crosslinking of the resin occurs during the first week of aging as cure involves the reaction of this allylic double bond. As crosslinking continues during aging it appears that the interaction with the maleimide end group is such that the polarizability of the C-N-C bond increased as evidenced by the relative increase in intensity for peak 9. The relative intensities of the other bands associated with the C=C stretch (alkene) are also expected to decrease.

This can also be observed in the FTIR spectra in Figure 4.6 where the intensity of peak 7 (C-H in-plane deformation, alkene) decreases with aging.

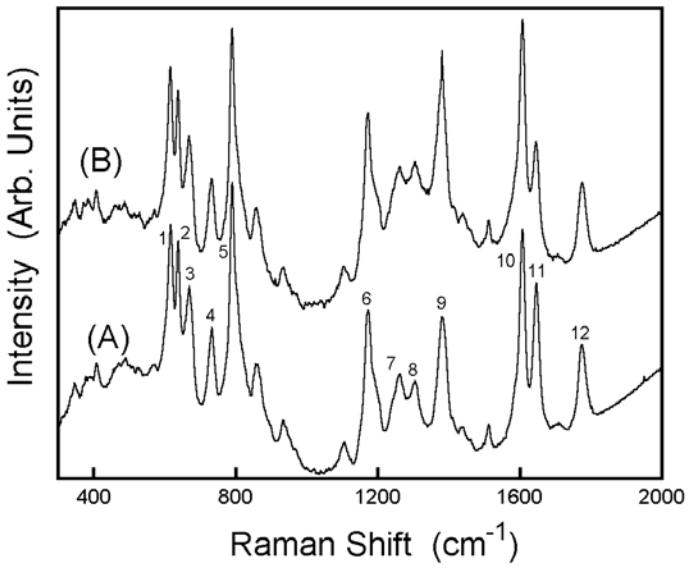

Figure 4.8: Raman spectra of the unaged Matrimid® 5292 composite material (A) and the same material after aging for 1 week at 250 ºC (B).

Peak No.	Wavelength (cm^{-1})	Assignment
1	617 s	aromatic ring def. (mono)
2	638 s	aromatic ring def. (para)
3	670 m	aromatic ring bending (tri)
4	733 m	aromatic ring vibration (para)
5	791 vs	aromatic ring stretch
6	1173 s	N-Phenyl stretch
7	1262 m	C-H in-plane def. (alkene)
8	1305 m	CH_2 bend
9	1383 s	CNC symmetric stretch
10	1608 vs	C=C stretch (aromatic)
11	1646 s	C=C stretch (alkene)
12	1775 m	C=O symmetric stretch

Key: m = medium signal, s = strong signal, vs = very strong signal; def.=deformation

Table 4.1: Assignment of peaks in the Raman spectrum of the cured Matrimid® 5292 carbon fibre composite.

The Raman samples aged for 4 and 6 weeks contained no discernable features due to a high degree of fluorescence, which occurred concurrently with the dramatic decrease in

the interlaminar fracture toughness of the material. The same highly fluorescent, highly degraded material was also located at the surfaces of the samples aged for lesser periods of time. For example, a specimen that had been aged for a period of one week was found to have a layer of degraded material that had penetrated to a depth of 50 μm from the surface. This degraded zone was detected by Raman as a region of extremely high fluorescence. This can provide a great deal of information as to the physical path of the degradation and is consistent with the work of Bowles [49] who found that in neat resin, polyimide degradation (as seen in SEM micrographs) occurred within a thin surface layer that developed and expanded during thermal aging. The fact that this material is highly fluorescent also assists in determining the chemical structure of the degraded material as it suggests a high concentration of chromophores. Further work could concentrate on the use of model compounds to elucidate the types of structures of the chromophores present.

Figure 4.9 shows the Raman Spectra collected at different depths below the surface of the composite material aged for 1 week. This depth profiling was achieved by cutting a cross section of the aged specimen and using the Raman Microscope's xyz computer controlled stage to perform line scans across the transverse section. On examination of Figure 4.9, it can be seen that the composite material exhibited a gradient in its degradation properties. For the aged specimen, the outermost region where the effect of the heat treatment was maximum (less than 50μm from the edge) was completely degraded and the material fluoresced heavily. Subtle changes were observed on the spectra collected at different depths below the surface of the aged specimen. Those spectral changes appear to be prominent in the peaks 7, 9 and 11, suggesting the occurrence of the same chemical changes observed previously between the unaged specimen and the specimen aged for 1 week (Figure 4.8). The degradation process decreased with increasing depth and the scan generated from the core of the aged specimen (spectrum C) was similar to that of the unaged material (spectrum D). Line scans on the unaged specimen did not show any variation.

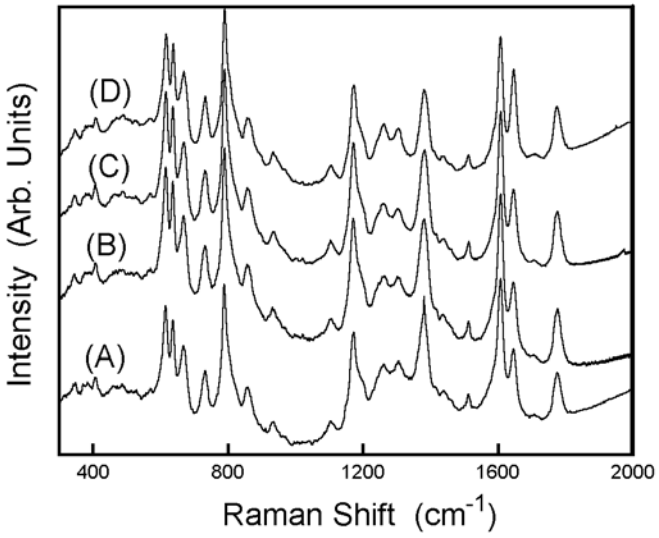

Figure 4.9: Raman Spectra taken at various intervals across a transverse section of the Matrimid® 5292 composite aged for 1 week. (A) 50 μm from the surface; (B) 600 μm from the surface; (C) the centre of the 4mm thick specimen; and (D) Unaged sample.

4.6 Dynamic Mechanical Thermal Analysis

Dynamic Mechanical Thermal Analysis (DMTA) was performed on composites of both materials that had been aged for up to six weeks. The DMTA trace of the unaged commercial material showed a rather broad Tg peak at 365°C, this indicates that the material was not completely cured (Figure 4.10). The other peak observed at 409°C is due to degradation of the matrix. This is consistent with the previous results from mode I fracture toughness tests that indicated that crosslinking of the matrix continued to occur even after two weeks of aging, causing the observed increase in the value of G_{IC}-*prop*. After two weeks of aging, this peak was no longer as broad and the Tg of the matrix had dropped to 347°C. At four and six weeks of aging at 250°C, there was no measurable Tg (a peak in this region was no longer observed), indicating that the matrix had degraded substantially. Composites made with the CSIRO resin behaved similarly and there was a slight decrease in Tg after two weeks of aging at 250°C. The unaged Tg was measured to be 302°C, after two weeks it was measured to be 273°C, this decreased further to 230°C after six weeks of aging.

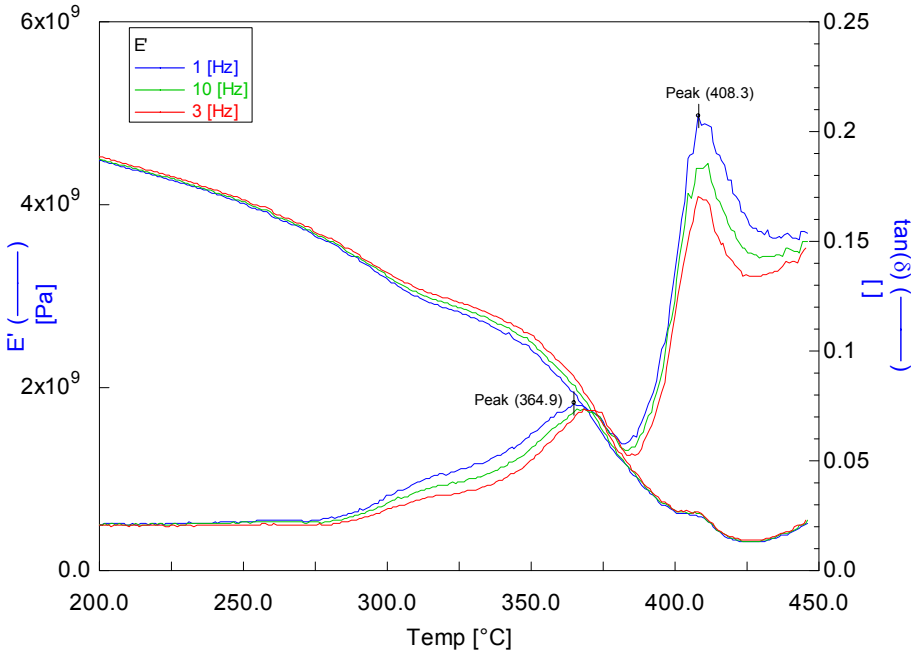

Figure 4.10: DMTA trace of the untreated Matrimid® 5292 composite sample, the shoulder to the peak at 365°C indicates that the matrix has not been fully cured.

4.7 Composite Thermal Stability

There are several methods for evaluating the thermal stability of composite materials including kinetic mapping techniques and thermal gravimetric analysis (TGA). However, one of the simplest techniques, monitoring the weight loss, remains one of the most reliable means of comparing the thermal stability of different composites [54, 78]. Figure 4.11 compares weight loss data over a period of four weeks of aging at 250°C. Both the CSIRO and commercial composites have the same specimen geometry. Despite all of the previous results that seem to indicate that the CSIRO resin system withstands aging at 250°C better than the commercial system, the thermal stability of the commercial laminates, according to the weight loss data, appears to be superior to the CSIRO laminates. One explanation for this might be that although the weight loss is slightly greater in the CSIRO system (16% compared to 12%), the chemical changes that occur create the formation of some kind of protective oxidised layer which prevents the centre of the material from deteriorating. It must be pointed out that the weight loss

results presented here are as high as 16%, which is extremely high when we consider that these composites have an approximate fibre volume fraction of 55% and the weight loss is predominantly due to degradation of the matrix as there is very little degradation of the carbon fibres. At 16% weight loss, over a third of the matrix has decomposed, thus figures of over 3% weight loss are now considered to render the composite unreliable in the eyes of the aerospace industry.

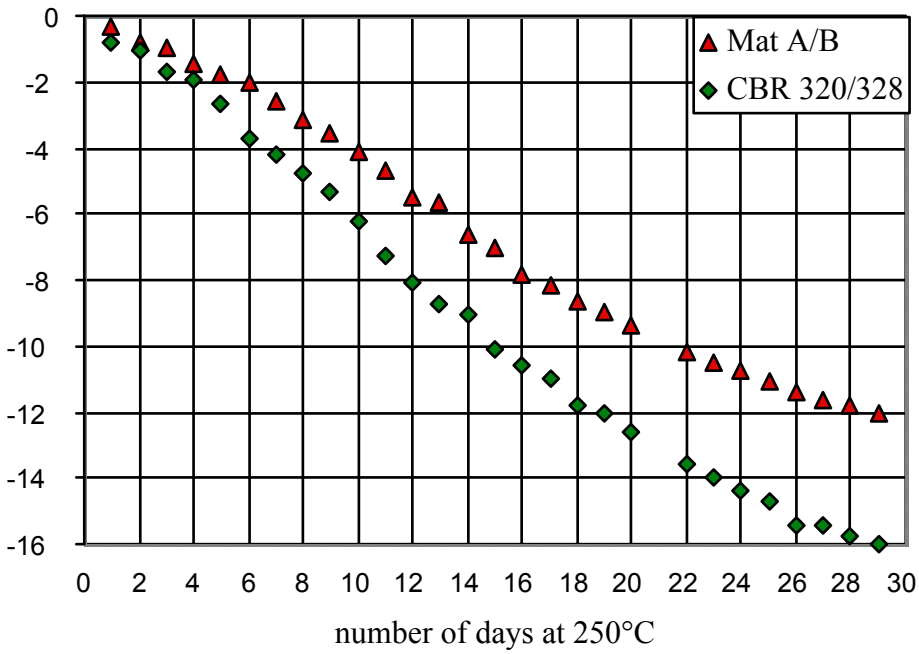

Figure 4.11: Plot of the weight losses observed over 29 days at 250°C of the two laminates (vertical scale indicates percentage weight loss).

4.8 Summary of the Results of Aging at 250°C

Table 4.4 provides a summary of the result presented in this chapter. The critical energy release rate (G_{IC}) during steady crack propagation of composites with a Matrimid® 5292 matrix was found to initially increase by 100 J/m^2 as the material continued to crosslink during the first two weeks of aging. DMTA confirmed that this was due to incomplete cure of the material, which suggests that the recommended cure cycle should be re-examined. During the following stage in the heat treatment of the material, this value decreases from 400 to 100 J/m^2 after four weeks at 250°C.

TECHNIQUE	MATRIMID® 5292	CBR 320/328
Mode I ILFT	Decreases to 30% of unaged value after 6 weeks of aging.	Properties equivalent to unaged composite after 6 weeks of aging, decreases to 35% of unaged value after 8 weeks.
FTIR Spectroscopy	Rapid chemical changes at surface of samples, slower changes at the core. Oxidation of bridging CH_2 to C=O.	Rapid chemical changes at surface of samples, slower changes at the core. Oxidation of bridging CH_2 to C=O. Degradation of saturated imide while unsaturated imide survives.
Raman Spectroscopy	Degree of reaction of allylic C=C bond is greatest at surface of composite. Degraded region penetrates 50μ from surface.	Unable to be measured due to highly fluorescent degradation products.
DMTA	Tg initially 365°C, decreased to 347°C after 2 weeks, then could not be measured.	Tg initially 302°C, decreased to 273°C after 2 weeks, then to 230°C after 6 weeks.
Weight loss	Measured to be 12% after 29 days.	Measured to be 16% after 29 days.

Table 4.4: Summary of information gathered on the thermo-oxidative stability of the two composites at 250°C using the various techniques employed.

This decrease coincided with oxidation at the centre of the specimen as detected by FTIR spectroscopy. However, this was not observed in composites of the CSIRO experimental resin. The FTIR spectra of the surface of composites of both materials showed oxidation of the exposed surface of the sample after only four days of aging. No further changes were observed at the surface after this time. A highly degraded

surface layer 50 μm in thickness was also detected by Raman spectroscopy. Similarly, a DMTA study showed a slight decrease in the glass transition temperature of the commercial composite after two weeks of aging and there was no recordable Tg after four and six weeks of aging. The Tg of the CSIRO composites decreased slightly after aging, and was measured to be 230°C after six weeks of aging. In contrast to these results in which the CSIRO resin seems to be more able to withstand high temperature treatments, the weight loss data measured over four weeks indicates that the commercial resin has slightly better thermal stability. One possible explanation for this is that the oxidised surface layer in the CSIRO resin provides a protective coating for the composite, which helps to prevent degradation of the centre of the specimen. This will be explored further in the discussion (Chapter 6).

Chapter 5 - Isothermal Aging at 204°C

5.1 Introduction

As discussed in chapter 4, samples were aged at 250°C so that the effects of aging at a temperature very close to the Tg of the composite could be observed. The estimated in-flight temperature of an aircraft at Mach 2.5 is 177°C, [5] so a second temperature was chosen closer to this for comparative purposes. There is great deal of information already published for polyimide composites aged at 204°C [12, 32, 48, 50, 79] as this temperature converts to 400°F and can easily be compared with existing data, particularly the large amount of research conducted in the USA in this field.

Chapter 4 examined the effect of aging the two composites compared in this study at a temperature just below the glass transition temperature of these materials. Although accelerated aging studies are frequently cited in the literature [34, 37, 54, 55, 80-82], it is questionable whether this information is useful in estimating the thermo-oxidative stability of composites at temperatures closer to that experienced whilst in service. Chapter 5 will examine how both materials behave after aging at 204°C.

Results from the preliminary aging study at 250°C were considered when devising the experimental program for an aging study at 204°C. Previously published weight loss data for similar materials indicated that one day of aging at 250°C is equivalent to one week of aging at 204°C [12]. The assumption that chemical changes occur at a similar rate to weight loss was made and it was therefore decided to select increments of time between 0 and 30 weeks (5040 hours) at 204°C to monitor the samples.

5.2 Mode I Interlaminar Fracture Toughness

Mode I delamination tests were conducted after 1, 5, 10, 15 and 30 weeks of aging at 204°C. Stable crack growth was observed in all of the samples tested along with a fibre-bridging zone just before the crack tip. The amount of fibre bridging was noticeably greater after the composites had been aged for longer periods of time. This

was particularly true in the case of CBR 320/328 composites. This observation was also made when testing samples that had been aged at the higher temperature, as stated in chapter 4.

5.2.1 Delamination Testing of Matrimid® 5292 Composites.

Typical resistance curves for composites of the Matrimid® 5292 resin aged for 0, 5, 10, 15 and 30 weeks at 204°C are shown in Figure 5.1. The first point on the curve is defined as $G_{IC\text{-init}}$ and $G_{IC\text{-prop}}$ is calculated from the plateau in the R-curve. $G_{IC\text{-init}}$ can be closely correlated to the matrix toughness [67] and in this case, the measured $G_{IC\text{-init}}$ corresponds to G_{IC} for the neat Matrimid® 5292 resin given in the CIBA GEIGY Material Safety Data Sheet (150 J/m^2 and 170 J/m^2 respectively) [61].

G_{IC} during steady crack propagation increases by 15% after 5 weeks of aging at 204°C and remains at this level after 10 weeks of aging. At 15 weeks, $G_{IC\text{-prop}}$ starts to decrease so that it returns to approximately the initial value measured. It is not until 30 weeks that the aging process has a deleterious effect on the Interlaminar Fracture Toughness of this material.

5.2.2 Delamination Testing of CBR320/328 Composites.

Typical R-curves for composites of the CBR 320/328 resin system aged at 204°C for 0, 5, 10, 15 and 30 weeks are plotted in figure 5.2. The average value of $G_{IC\text{-prop}}$ for the unaged material was measured to be 430 J/m^2, slightly higher than that of the Matrimid® 5292 composites. After 5 weeks at 204°C, this value increases by 50% of the initial value before dropping to just below the original value after 10 weeks of aging. By 15 weeks at 204°C, $G_{IC\text{-prop}}$ has decreased dramatically to 28% of the untreated value. The trend in the measured values for $G_{IC\text{-init}}$ was found to be completely different to this, instead a steady decrease was observed. The reason for this difference will be explored further in Chapter 6, $G_{IC\text{-init}}$ is matrix dominated, whereas $G_{IC\text{-prop}}$ is highly influenced by the strength of the fibre/matrix interface.

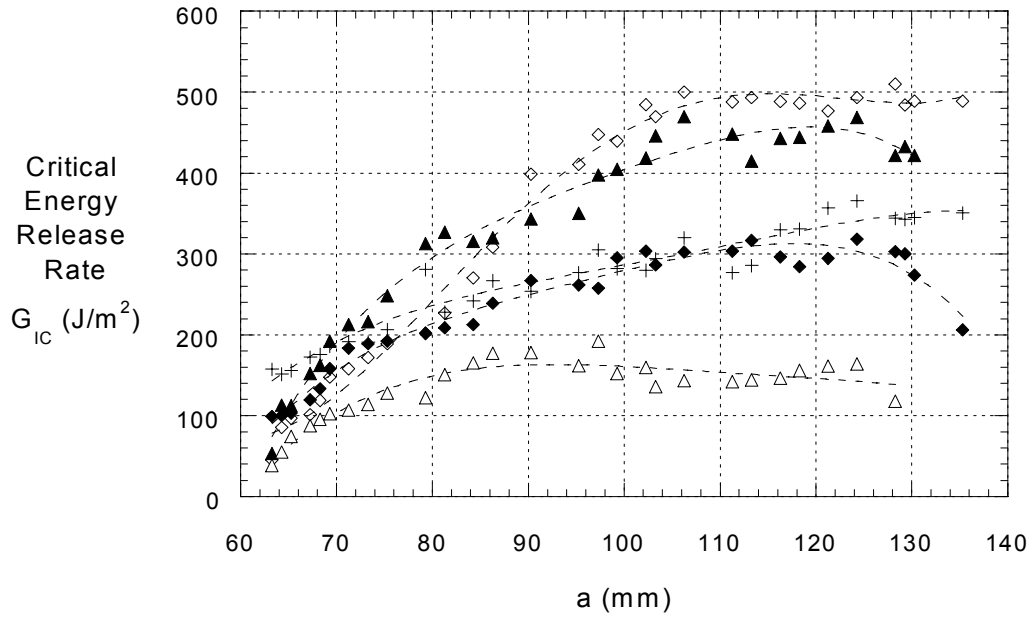

Figure 5.1: The effect of isothermal aging at 204°C on the interlaminar fracture toughness (Mode I R-curve) of a carbon fibre/Matrimid 5292 composite. (+ 0 weeks, ◇ 5 weeks, ◢ 10 weeks, ◆ 15 weeks and △ 30 weeks of aging at 204°C).

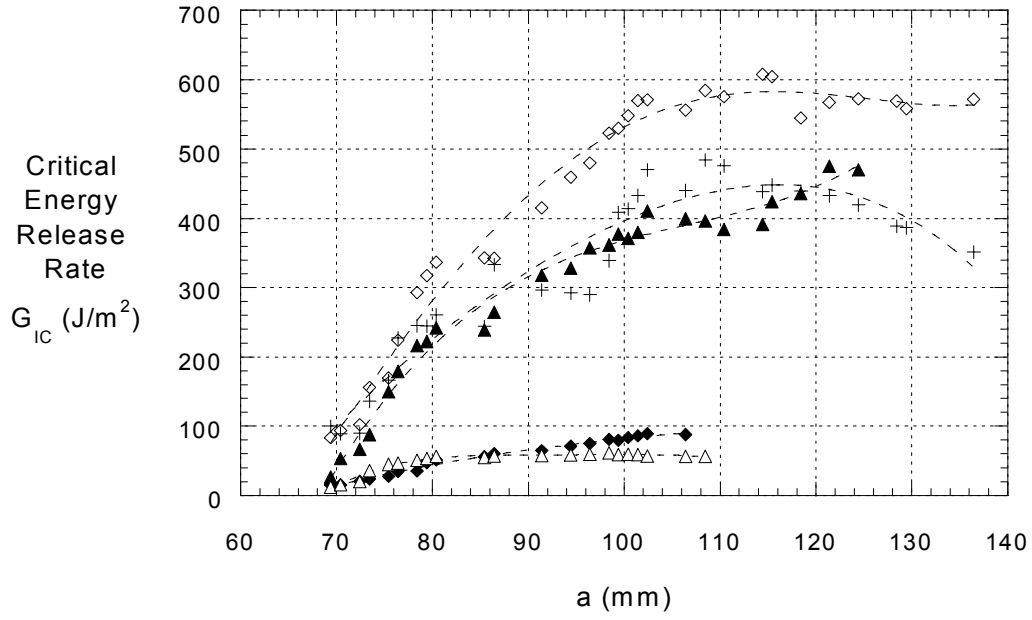

Figure 5.2: The effect of isothermal aging at 204°C on the interlaminar fracture toughness (Mode I R-curve) of a carbon fibre/CBR320/328 composite. (+ 0 weeks, ◇ 5 weeks, ◢ 10 weeks, ◆ 15 weeks and △ 30 weeks of aging at 204°C.)

5.2.3 Comparison of the Interlaminar Fracture Toughness Results

A summary of the effect of aging at 204°C on composites of both of the resin systems studied is shown in figure 5.3. Each point represents an average of four values and error bars signify ± 1 standard deviation. Average values obtained for $G_{IC\text{-init}}$ show a lot less variation than those measured for $G_{IC\text{-prop}}$ in both materials and this is due to the added influence of fibre bridging on the latter. A fibre-bridging zone was observed to increase in both materials after aging. This may have artificially increased the critical energy release rate as the presence of fibre bridging increases the energy required to grow the crack during testing. The influence of fibre bridging therefore explains the greater reproducibility in unaged samples and $G_{IC\text{-init}}$ measurements.

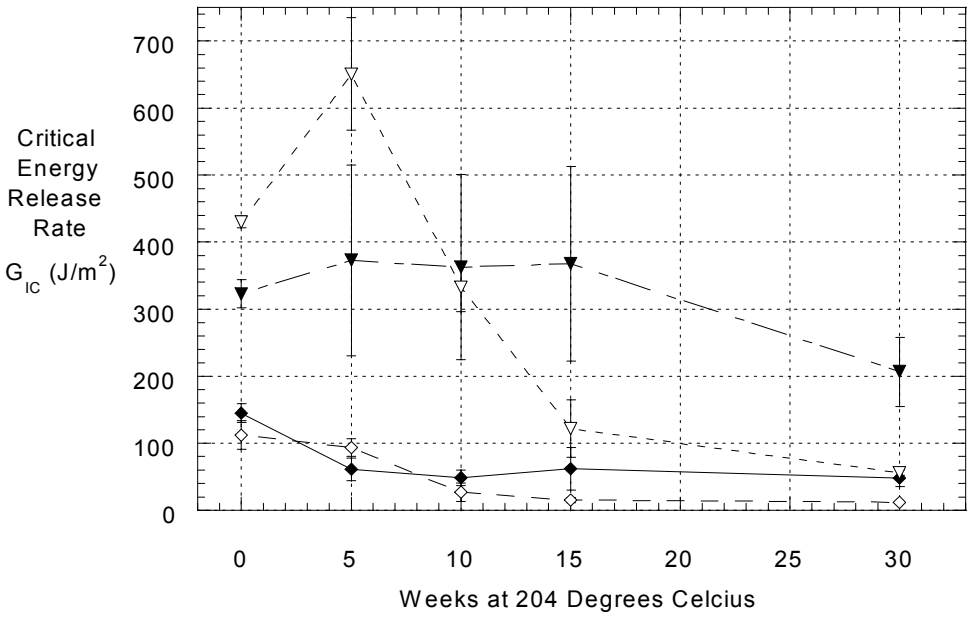

Figure 5.3: $G_{IC\text{-init}}$ (◇, ◆) and $G_{IC\text{-prop}}$ (▽, ▼) as a function of the number of weeks of isothermal aging at 204°C of composites of Matrimid® 5292 (closed symbols) and CBR320/328 (open symbols). (Error bars signify ±1 standard deviation).

The trend in $G_{IC\text{-init}}$ measurements is a constant decrease in the case of CBR 320/328 composites, whereas in Matrimid® 5292 composites, $G_{IC\text{-init}}$ reaches a stable value after an initial decrease. As $G_{IC\text{-init}}$ can be approximated to the matrix neat resin G_{IC} [67], it appears that the commercial matrix may withstand the effects aging at 204°C better than CBR 320/328. When $G_{IC\text{-prop}}$ measurements are compared, the unaged value for CBR 320/328 is slightly higher than the corresponding value for Matrimid® 5292 composites. After 5 weeks, this difference is increased greatly where the CBR 320/328 $G_{IC\text{-prop}}$ increases to 50% of the unaged value whereas the Matrimid® 5292 increases just slightly. The commercial material has a much more stable measured $G_{IC\text{-prop}}$ that only decreases to 64% of the initial value after 30 weeks (approximately 5000 hours) of aging. The $G_{IC\text{-prop}}$ measured for CBR 320/328 composites decreases steadily after 5 weeks of aging until it reaches a mere 13% of the untreated value.

Overall the Matrimid® 5292 composites appear to withstand the effects of aging at 204°C considerably better than the CBR 320/328 composites, despite the latter initially having a higher interlaminar fracture toughness. This is contradictory to the findings of the previous chapter.

5.3 Scanning Electron Microscopy

Scanning Electron Microscopy (SEM) was used to examine the fracture surfaces of double cantilever beam specimens after testing had been completed. Figures 5.4 and 5.5 show micrographs of the region of crack propagation in Matrimid® 5292 and CBR 320/328 composites respectively. These specimens were aged for 1, 5, 10 and 15 weeks, the samples aged for 30 weeks are not shown here as they were so porous that a sufficient vacuum could not be achieved to gold coat them for examination. These micrographs confirm that failure was via a mode I mechanism and show no traces of the distinctive, deep hackles associated with Mode II (shear) failure.

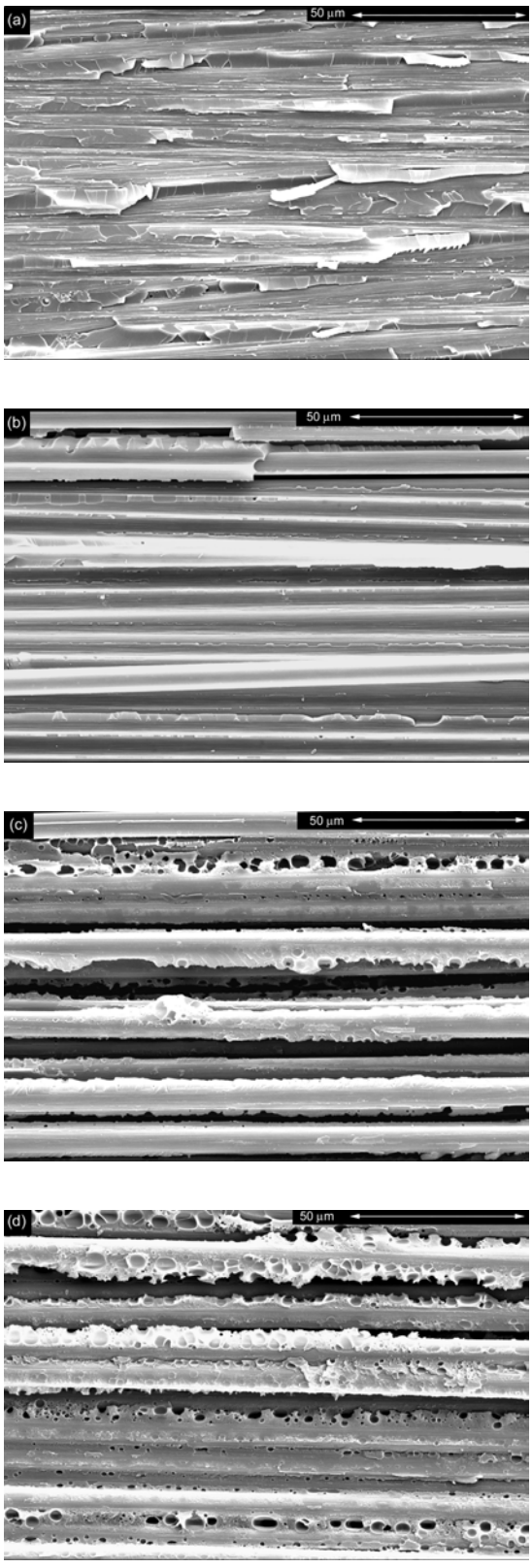

Figure 5.4: Matrimid® 5292 composites aged at 204°C for a) 0 weeks, b) 5 weeks, c) 10 weeks and d) 15 weeks, showing an increasing degree of porosity.

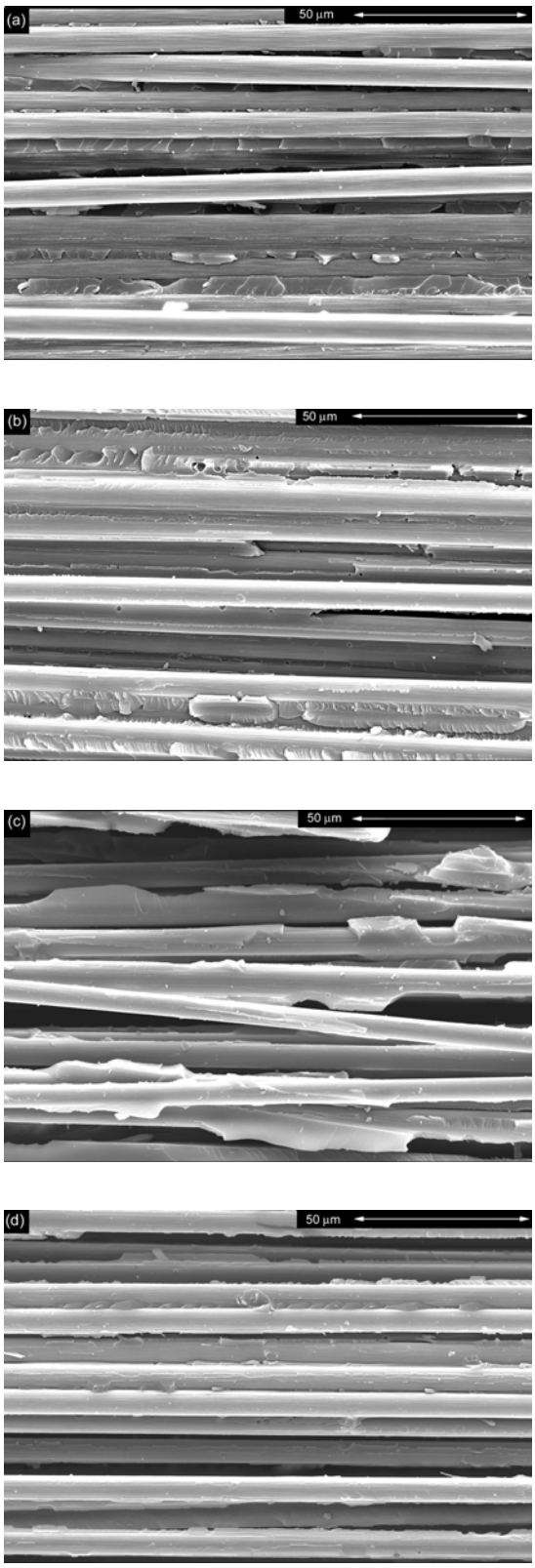

Figure 5.5: CBR 320/328 composites aged at 204°C for a) 0 weeks, b) 5 weeks, c) 10 weeks and d) 15 weeks.

As with the 250°C study, the Matrimid® 5292 composites exhibit much better fibre/matrix adhesion than the CBR 320/328 composites where bare fibres are observed. As a consequence of this poor fibre/matrix adhesion, the crack propagates along the fibre/matrix interface during delamination testing. This may increase the measurement of $G_{IC\text{-prop}}$ due to increased fibre bridging causing an increase in the energy required to propagate the crack as mentioned previously. The micrographs show that the longer the CBR 320/328 is aged, the worse the fibre/matrix adhesion becomes. After 15 weeks of aging, the fibres are quite bare and numerous stray, irregularly broken fibres were observed, a further indication that substantial fibre bridging had occurred.

Dramatic changes were observed for Matrimid® 5292 composites after aging at 204°C. The fracture surface of the unaged specimen (Figure 5.4a) is consistent with Mode I failure and provides evidence that very few voids are present in the composite prior to aging. After 5 weeks at 204°C (Figure 5.4b), a few voids are noted and by 10 weeks (Fig 5.4c) the matrix has taken on a honeycomb appearance. This porosity is further exacerbated after 15 weeks of aging (Figure 5.4d). Interestingly, in all of these micrographs, the fibre/matrix adhesion remains strong, despite the plethora of voids caused by oxidation of the matrix. No corresponding difference in interlaminar fracture toughness was observed with this change in microstructure. Despite the severe degradation of the matrix, the composites retain good properties, due to excellent fibre/matrix adhesion. In addition to this, there is very little change in the microstructure of the CBR 320/328 composites even though a dramatic decrease in interlaminar fracture toughness was observed after 10 weeks at 204°C.

5.4 Fourier Transform Infrared Spectroscopy

Chemical changes occurring in the matrix during aging of both composite materials were monitored by Fourier Transform Infrared Spectroscopy (FTIR). In chapter 4, it was established that changes at the surface of the composites occur rapidly and then appear to remain stable. This was also observed in the study at the lower temperature, therefore the focus was placed on the chemical changes that occurred at the core of the material. As mentioned previously, chemical changes at the core of the material are of

great relevance to the changes in interlaminar fracture toughness. Like the FTIR spectra, this test also examines changes in the centre of the specimen.

5.4.1 FTIR Spectroscopy of the core of Matrimid® 5292 composites aged at 250 °C.

FTIR spectra showing chemical changes at the core of Matrimid® 5292 composites aged at 204°C for 0, 5, 10, 15 and 30 weeks are shown in Figure 5.6. The most noticeable change is the ingrowth of a very broad peak centred at 1610 cm^{-1} which may be assigned to an aromatic ring with C=O conjugation, whilst at the same time the peak at 1512 cm^{-1} assigned to the aromatic ring bridged by a methylene group decreases in intensity. Those changes aside, there is significant broadening in the region from 1000 to 1300 cm^{-1}, making it difficult to determine precisely what is occurring. Assignment of peaks in this region is quite contentious and this will be discussed in more detail in Chapter 6.

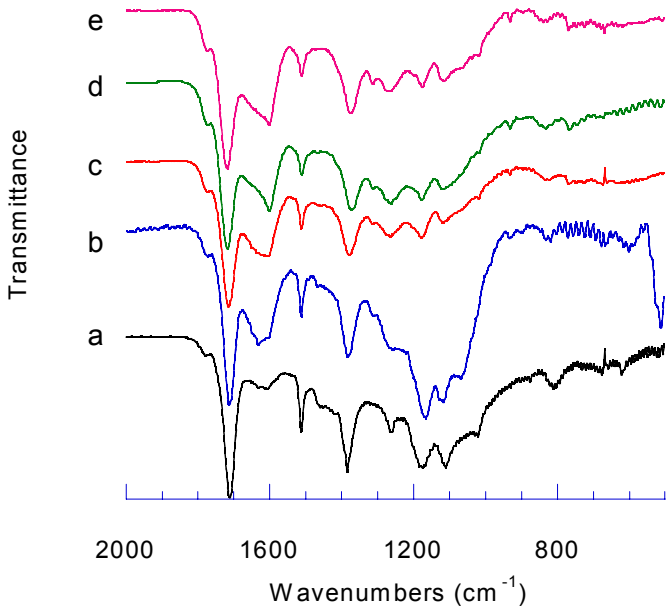

Figure 5.6: FTIR spectra of the core of Matrimid® 5292 composites aged at 204 °C for (a) 0, (b) 5, (c) 10, (d) 15 and (e) 30 weeks.

Significant changes in these spectra are observed even at 5 weeks of isothermal aging. Despite this, the interlaminar fracture toughness was measured to be quite stable even after 30 weeks of aging. The FTIR observations are consistent with the micrographs

taken of these samples, which show an increase in porosity after 5 weeks of aging, indicating degradation of the matrix. SEM also showed excellent fibre/matrix adhesion in the Matrimid® 5292 composites. The excellent property retention of this material is a result of the measurement of $G_{IC\text{-prop}}$ being determined by this interfacial strength.

5.4.2 FTIR Spectroscopy of the core of CBR 320/328 composites aged at 250°C.

FTIR spectra showing chemical changes at the core of CBR 320/328 composites aged at 204°C for 0, 5, 10, 15 and 30 weeks are shown in Figure 5.7. As in the case of the Matrimid® 5292 composites, the peak near 1500 cm^{-1} is observed to decrease in intensity at the same time as the ingrowth of a peak at 1600cm^{-1}. Peaks in the region of 1000 to 1300 cm^{-1} show significant broadening and become difficult to distinguish. The other significant difference that occurs with aging is the disappearance of imide carbonyl peaks at 1779 and 1712 cm^{-1}. These peaks are associated with the saturated imide, which is less stable than the unsaturated imide structure of pyromellitic dianhydride. By examination of these spectra, it appears that degradation initially takes

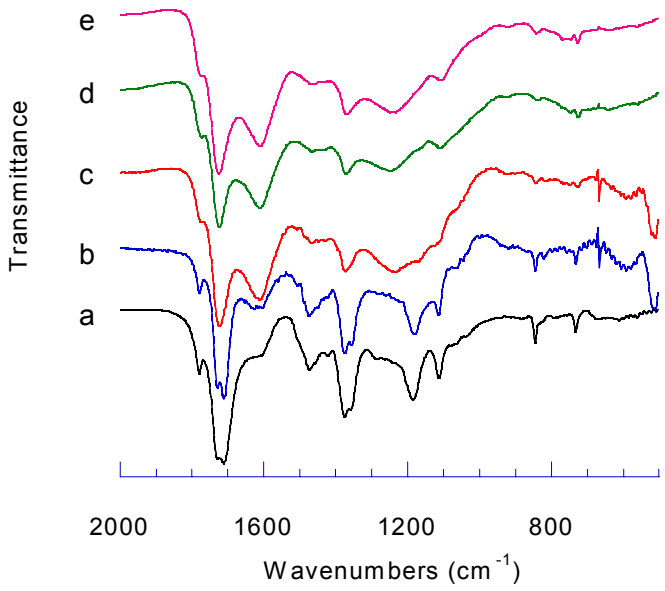

Figure 5.7: FTIR spectra of the core of CBR 320/328 composites aged at 204°C for (a) 0, (b) 5, (c) 10, (d) 15 and (e) 30 weeks.

effect between 5 and 10 weeks of aging at this temperature, at the same time as the significant decrease observed in the measurement of $G_{IC\text{-prop}}$. Therefore there is a strong correlation between the chemical changes at the core of sample and changes in

interlaminar fracture toughness, also measured at the core of the sample in this instance.

5.5 Raman Spectroscopy

5.5.1 Matrimid® 5292 composites

Matrimid® 5292 composite samples were aged for 5, 10 and 15 weeks at 204°C before being examined using the Raman Microscope technique. Assignments for the various peaks were given in Table 4.1. A transverse sample of each specimen was scanned from the surface of the specimen towards the core of the aged material, thus a profile of the changes in chemical structure with depth through the sample was accumulated by conducting line scans across a transverse section of the composite. Raman Spectra from samples aged for 5 weeks (Figure 5.8) showed very little variation through the thickness of the specimen with the exception of the surface of the material, where a degraded region approximately 50μm in thickness was detected as evidenced by a high degree of fluorescence.

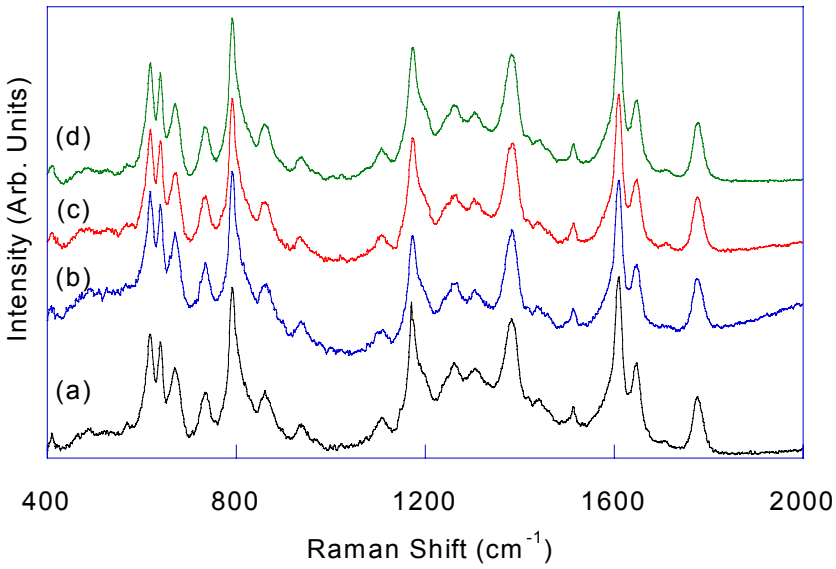

Figure 5.8: Raman Spectra taken at various intervals across a transverse section of the Matrimid® 5292 composite aged for 5 weeks at 204°C. (a) 100μm from the surface; (b) 400μm; (c) 800 μm and (d) 1600 μm from the surface.

Samples aged for 10 and 15 weeks (Figures 5.9 and 5.10) show a gradual decrease of the intensity of the peak at 1646 cm^{-1} (corresponding to the alkene double bond in Matrimid® B) as the sample is mapped from the surface to the core of the material. This

can be correlated to the further reaction of this group, indicating increased crosslinking of the material. A line scan across the sample aged for 15 weeks shows a similar trend with a high degree of reaction at the core of the sample.

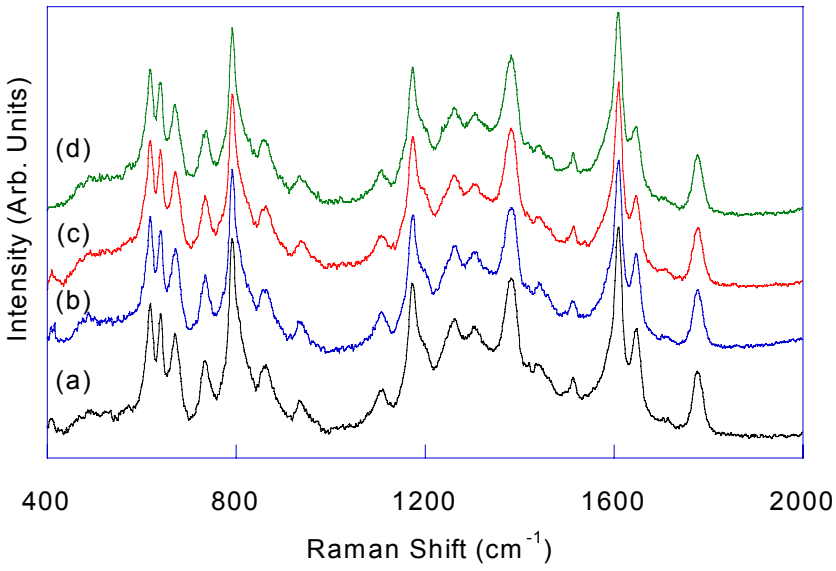

Figure 5.9: Raman Spectra taken at various intervals across a transverse section of the Matrimid® 5292 composite aged for 10 weeks at 204°C. (a) 100μm from the surface; (b) 400μm; (c) 800 μm and (d) 1600 μm from the surface.

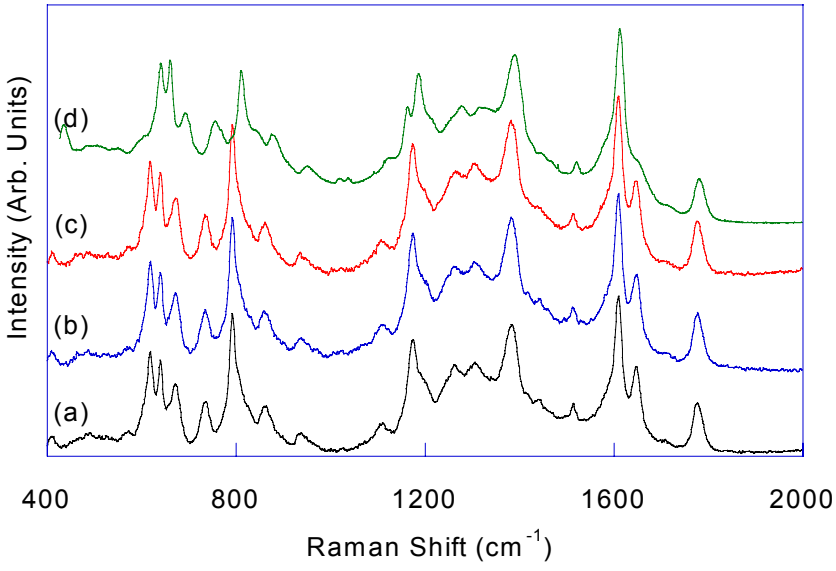

Figure 5.10: Raman Spectra taken at various intervals across a transverse section of the Matrimid® 5292 composite aged for 15 weeks at 204°C. (a) 100μm from the surface; (b) 400μm; (c) 800 μm and (d) 1600 μm from the surface.

Figure 5.11 compares spectra taken from the core of samples aged for 5, 10 and 15 weeks with an unaged sample and again confirms an increase in crosslinking with the amount of time the material is aged. This is again evidenced by the reduction in intensity of the alkene peak at 1646 cm^{-1}, together with an increase in intensity of the polarizability of the C-N-C bond, which causes an increase in the peak at 1383 cm^{-1}. A small shoulder appears on the peak at 1173 cm^{-1}, assigned to the N-phenyl stretch after 15 weeks of aging.

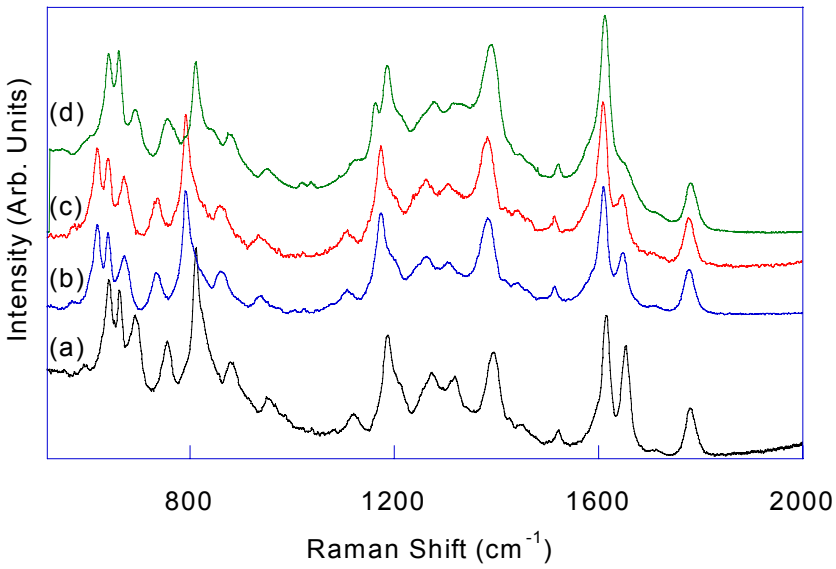

Figure 5.11: Raman Spectra taken at the centre of a transverse section of the Matrimid® 5292 composite aged at 204°C (a) unaged; (b) 5 weeks; (c) 10 weeks and (d) 15 weeks.

5.5.2 CBR320/328 composites

A Raman study of CBR 320/328 composites aged at 250°C could not be performed due to problems with a high degree of fluorescence from the material. A similar observation was made with composites aged at 204°C for 15 weeks and spectra recorded were featureless, however spectra were obtained for samples aged for 5 and 10 weeks at this temperature. Figure 5.12 represents Raman spectra recorded across a transverse section of a composite aged at 204°C for 5 weeks. Relevant peak assignments are set out in Table 5.1.

Peak No.	Wavelength (cm^{-1})	Assignment
1	540 s	aromatic ring def. (mono)
2	590 s	aromatic ring def. (para)
3	663 vs	aromatic ring bending (tri)
4	721 s	aromatic ring vibration (para)
5	804 m	aromatic ring stretch
6	867 m	
7	937 m	
8	992 m	
9	1063 m	N-Phenyl stretch
10	1262 s	C-H in-plane def. (alkene)
11	1333 m	CH_2 bend
12	1383 vs	CNC symmetric stretch
13	1425 m	
14	1450 m	
15	1604 vs	C=C stretch (aromatic)
16	1646 s	C=C stretch (alkene)
17	1791 m	C=O symmetric stretch

Key: m = medium signal, s = strong signal, vs = very strong signal; def.=deformation

Table 5.1: Tentative assignment of peaks in the Raman spectrum of the cured CBR 320/328 carbon fibre composite.

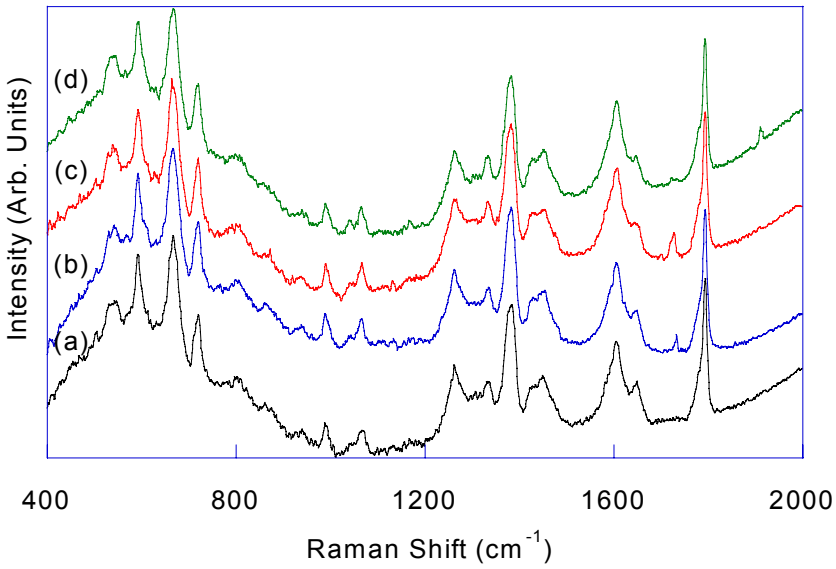

Figure 5.12: Raman Spectra taken at various intervals across a transverse section of the CBR 320/328 composite aged for 5 weeks at 204°C. (a) 100μm from the surface; (b) 400μm; (c) 800 μm and (d) 1600 μm from the surface.

The most obvious change to be noted in these spectra is the disappearance of the small peak at 1646 cm^{-1} that arises from the alkene group in the Matrimid® 5292 B coreactant.

Again this peak is observed to disappear, consistent with an increase in the degree of crosslinking. The fact that further crosslinking occurs with aging is not unexpected, however it is interesting to note that according to these Raman spectra, the degree of crosslinking is much higher in the core of the material than it is at the surface. When this is compared to Figure 5.13, which depicts Raman Spectra of a transverse section of a sample that has been aged for 10 weeks, the aforementioned peak at 1646 cm^{-1} has almost disappeared completely. Also noticeable in this diagram is the considerable broadening of the spectra and the loss of the features of many of the peaks. The intensity of the peaks at 1262 and 1333 cm^{-1} has increased with respect to the peak at 1383 cm^{-1}, also consistent with continued crosslinking of the sample as discussed in Chapter 4.

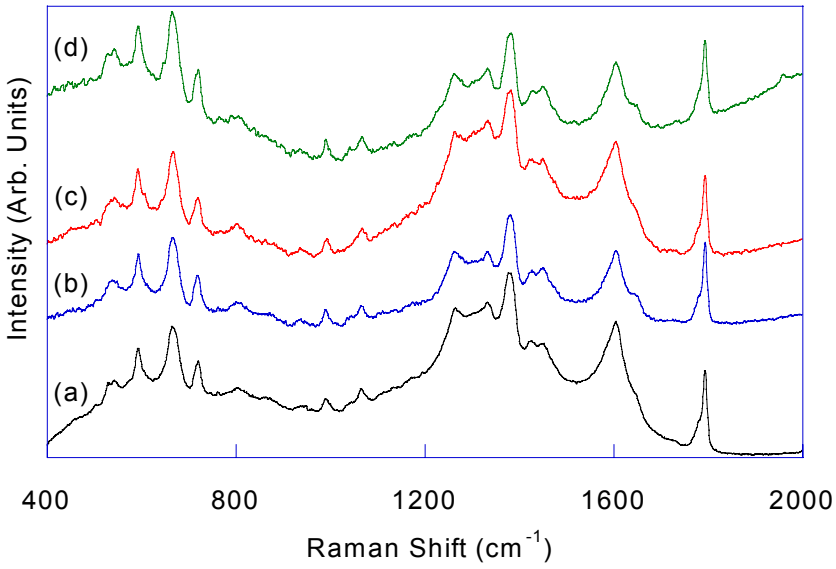

Figure 5.13: Raman Spectra taken at various intervals across a transverse section of the CBR 320/328 composite aged for 10 weeks at 204℃. (a) 200μm from the surface; (b) 400μm; (c) 800 μm and (d) 1600 μm from the surface (centre of specimen).

Finally, Figure 5.14 compares Raman spectra of the unaged material with those aged for 5 and 10 weeks. This emphasises the broadening and loss of features of the spectra observed earlier. The main changes to be noted are the disappearance of the alkene peak at 1646 cm^{-1}, the increase in intensity of peaks at 1262 and 1333 cm^{-1}, as well as

the disappearance of several small peaks at 804, 875 and 938 cm^{-1}. The changes observed through the thickness of material, which increase in severity as the centre of the specimen is approached, are very similar to the changes observed in samples aged for different periods of time, with the most severe changes occurring in the sample aged for 10 weeks.

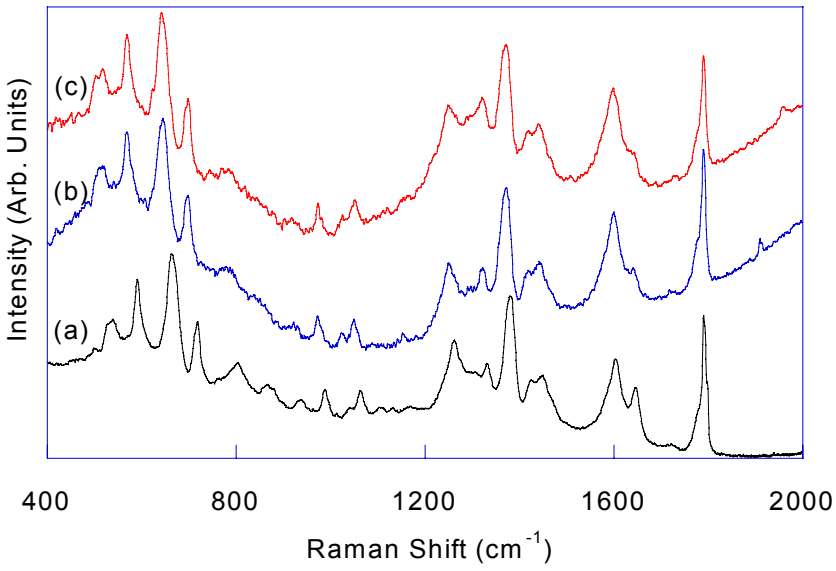

Figure 5.14: Raman Spectra taken at the centre of a transverse section of the CBR 320/328 composite aged at 204°C. (a) unaged (b) 5 weeks; and (c) 10 weeks.

5.6 Dynamic Mechanical Thermal Analysis

Dynamic Mechanical Thermal Analysis (DMTA) was performed on composites of both materials that had been aged for 5, 10 and 15 weeks at 204°C. Table 5.2 presents the results for glass transition temperatures measured as both a peak in the tan δ curve (the value of which will be cited from here onwards) and by the extrapolated onset of the storage modulus (E'). The Tg of the Matrimid® 5292 composites was initially found to be 365°C and the Tg of the CBR 320/328 composites was found to be 302°C. The Tg of the Matrimid® 5292 remains stable until 10 weeks of aging when it decreases slightly. Finally, after 15 weeks of aging, the Tg of this material has decreased by almost 20°C. The Tg of the CBR 320/328 composite increases initially and then

remains quite stable. This is consistent with work by Morgan *et al*. [39] who observed a Tg increase as the matrix continued to crosslink.

	Weeks at 204°C	0	5	10	15
Mat A/B	**Peak**	**365**	**362**	**358**	**348**
	Onset of E'	**355**	**350**	**358**	**341**
320/328	**Peak**	**302**	**330**	**324**	**329**
	Onset of E'	**256**	**303**	**301**	**301**

Table 5.2: The glass transition temperature of the aged composite materials (°C) as measured by Dynamic Mechanical Thermal Analysis.

5.8 Summary of the results of aging at 204°C

The results presented in this chapter from the isothermal aging of the two composite materials at 204°C are summarised in Table 5.3. The effect of isothermal aging on the interlaminar fracture toughness of the composites was much more severe on the CBR 320/328 composites than it was on the commercial composites. After 30 weeks of aging the value of $G_{IC\text{-prop}}$ had dropped to a mere 13% of the untreated value. The Matrimid® 5292 composite retained 64% of its original measured value after the same period of aging. On the basis of the interlaminar fracture toughness results, the commercial material appears to withstand isothermal aging better than the CSIRO composite.

Scanning electron micrographs of the fracture surfaces of these materials revealed that the CBR 320/328 composites exhibit poor fibre/matrix adhesion. The Matrimid® 5292 composites exhibited excellent fibre/matrix adhesion, however the samples became increasingly porous with aging time until after 30 weeks of aging, the matrix resembled honeycomb. The good property retention observed might be explained by the strength of the fibre/matrix interface compensating for the effect of the matrix porosity.

TECHNIQUE	MATRIMID® 5292	CBR 320/328
Mode I ILFT	Decreases to 64% of unaged value after 30 weeks of aging.	Decreases to 13% of unaged value after 30 weeks of aging.
SEM	Good fibre/matrix adhesion observed. Increase in porosity with period of time aged.	Poor fibre/matrix adhesion observed.
FTIR Spectroscopy	Oxidation of aromatic CH_2 to C=O.	Oxidation of aromatic CH_2 to C=O. Degradation of saturated imide while unsaturated imide survives.
Raman Spectroscopy	Degree of reaction of allylic C=C bond is greatest at core of composite.	Degree of reaction of allylic C=C bond is greatest at core of composite.
DMTA	Decreases from 365°C to 348°C after 15 weeks of aging.	Increases from 302°C to 329°C after 15 weeks of aging.

Table 5.3 Summary of information gathered on the thermo-oxidative stability of the two composites at 204°C, using various techniques.

FTIR changes were monitored and in the case of the CBR 320/328 composites, the chemical changes could be correlated with changes in mechanical properties. This was not the case in the Matrimid® 5292 composites, however the chemical changes were consistent with oxidation of a bridging methylene group to a bridging carbonyl group and this oxidation could be correlated with the porosity observed by SEM.

Raman spectroscopy revealed that the degree of reaction of the allylic C=C was greatest at the core of the sample, in contrast to the results from the study at the higher temperature where the degree of reaction was greatest at the surface.

Changes in the glass transition temperature of these materials were monitored by DMTA. The Tg of the CBR 320/328 composite increased initially after 5 weeks of aging and then remained stable. The Tg of the Matrimid® composites remained the

same until 10 weeks of aging when the effects of degradation became evident and the Tg began to decrease.

Chapter 6 – Discussion

6.1 Introduction

Perhaps the most reliable method of evaluating the thermo-oxidative stability of aerospace materials would be to place witness panels on aircraft for later examination. However, this process would take years to complete, hence the motivation for accelerated aging tests that could potentially make this information available faster, but still be reliable. New advanced materials could then be certified and implemented in the manufacture of aircraft more rapidly. Most of the current accelerated aging tests involve aging at higher temperatures for shorter periods of time, although (more recently) elevated oxygen pressures have been used to accelerate thermo-oxidative aging in composites [83]. In order to assess the validity of these accelerated aging tests, it is therefore necessary to compare results from studies conducted at a range of temperatures. Examination of the aging behaviour of composite materials is often conducted at temperatures well in excess of in-service requirements. Elevating the aging temperature decreases the length of time of the test and these temperatures have commonly been in the order of 300°C - 500°C [37, 54, 55, 80-82] whereas the surface of an aircraft in flight at Mach 2.5 has been predicted to reach about 177°C [2, 5, 40]. The present study has set out to answer the question of how accurately results from accelerated aging tests reflect longer-term use at much lower temperatures. In order to do this, two studies have been completed using two high temperature composite materials, a preliminary study at 250°C, a temperature approaching the glass transition temperature of the materials and a more detailed study at 204°C, a temperature well below the glass transition temperatures of both composites and closer to the predicted service temperature. The degradation mechanisms were investigated under both conditions and this chapter compares and contrast these findings.

6.2 Composite Manufacture

As explained in the previous chapters, the two resin systems selected for this study were

the commercial Matrimid® 5292 bismaleimide system and a CSIRO developed bismaleimide of structure shown in Figure 2.5. Although both are nominally bismaleimides, they have very different chemical structures, hence the difference in degradation mechanisms. The components of the CSIRO developed CBR 320/328 resin system are easy to synthesise and raw materials are available in commercial quantities. These two factors result in the resin being relatively cheap and easy to produce in large quantities using standard large-scale reaction facilities. Therefore the CBR 320/328 resin system has a great deal of potential in commercial applications. The only difficulty in the process of manufacturing this matrix is the degassing step where components are mixed at 200°C under relatively high (-90kPa) vacuum to remove any residual solvents from the synthesis. This step is not unique to the CBR 320/328 resin system and must also be performed when preparing other commercial resin systems such as the Matrimid® 5292 system. It is foreseeable that the vacuum degassing step may eventually become obsolete after the recent development of the water synthesis of polyimides [9]. When water is used as a solvent in the synthesis of these materials, it has the advantage of being removed much more easily than the current aprotic solvents in use such as Dimethyl Formamide (DMF).

Prepregging both resin systems using the small-scale solvent-based prepregging technique developed during this study proved to be facile once conditions were established. The technique enabled a precise amount of resin to be delivered to the carbon fibre fabric placed in the mould via solution. On a commercial scale, prepregging could easily be performed using melt impregnation on standard commercial equipment with high temperature capability and adequate ventilation. The prepregs produced from both resin systems did not have the excellent tack and drape of carbon/epoxy prepregs, however improving the tack and drape of polyimide prepregs, particularly tack lifetime, has been a challenge for scientists for a number of years [2], but with manufacturers able to capably process thermoplastic prepregs, the motivation for increasing the tack of bismaleimide prepregs is declining [10]. Although ensuring that no warpage was present in the unidirectional prepregs that were produced was a concern in the present study, this issue is also a common consideration in the manufacture of carbon/epoxy unidirectional laminates and standard techniques were

implemented to prevent this from occurring as described in Chapter 3.

Dynamic Mechanical Thermal Analysis was used to evaluate the cure cycles of both matrix materials. In the case of the 320/328 composites, absence of any shoulders on the tan δ peak indicated that very little unreacted material was present after cure. Analysis of the Matrimid® composites showed a shoulder to the main Tg peak in the tan δ curve (Figure 4.10), indicating the presence of a significant amount of unreacted resin. From this it can be concluded that the cure cycle recommended by CIBA GEIGY requires either a post cure or a longer period of time at the 250°C stage to approach a fully reacted state. It is not uncommon for manufacturers to recommend a bismaleimide cure profile that slightly undercures products in order to improve the composite toughness. Lincoln *et al*. [18] recently reported that increasing the cure time and temperature of the Matrimid® 5292 system lowered the resin density (by increasing the crosslink density, leading to a less well packed structure with more spaces) and increased the Tg, in a study of neat resin specimens. In the present study, a Tg increase was observed when the CBR 320/328 composites were aged at 204°C for 5 weeks. Increasing the cure time is one approach to ensuring complete cure of the matrix, however increasing the cure time also increases the cost of production due to the high costs of running autoclaves at high temperature and pressure. A better alternative to this might be to include a postcuring step after the laminate has been removed from the autoclave. Morgan *et al*. [84] attained full cure of the Matrimid® 5292 resin system after a 3 hour postcure at 300°C. The fully cured polymer was found to have a Tg of 350°C, G_{IC} was measured to be 330 J/m^2 both before and after postcuring. This value was equivalent to the measurement in the present study. The authors also found that the compression after impact strength of the material after postcuring was low (98.5 MPa when 200 MPa was considered an acceptable value) and attributed this to resin shrinkage and microcracking during postcure.

6.3 Mode I Interlaminar Fracture Toughness

Mode I Interlaminar Fracture Toughness Tests were performed on the aged samples in order to gain an impression of the effect of aging on the material at the core of the

sample and also because delamination (separation of the carbon fibre layers) is the most critical mode of failure in laminated composite materials [8]. The Mode I double cantilever beam (DCB) test is the most commonly performed delamination test and this test was selected for ease of comparison with other published data. Mode II (end notched flexure) tests and mixed mode tests would have complemented this study, however short supply of the experimental raw materials at the time of manufacture, did not enable enough panels to be fabricated to perform these tests. Mode I tests in most cases measure the interlaminar fracture toughness during steady crack propagation (particularly for brittle matrices such as bismaleimides). Mode II tests, which place the specimen under a three point bend load, mostly generate unstable crack growth and may provide additional information about the shear characteristics of the material as a result of this different testing configuration. However, in a recent study by Tsotsis, [85] a large change in Mode I interlaminar fracture toughness was observed with aging, with only a slight change in the corresponding Mode II results. A reason for this might be that Mode II delamination failure involves shearing and the formation and merging of micro-cracks in the matrix and is less affected by fibre bridging than Mode I where the crack is forcibly opened. Results from mixed mode tests most accurately represent the types of stresses experienced by the composite when in service as laminates have been shown to be subject to both normal and shear loads when in use [8], however these results can be difficult to characterise.

Mode I tests provide two useful measures of composite toughness; $G_{IC\text{-init}}$ (the first deviation from linearity on the load-displacement curve) and $G_{IC\text{-prop}}$ (the value of G_{IC} during steady crack propagation or the plateau in the resistance curve). The value of $G_{IC\text{-init}}$ is matrix dominated and is usually very similar in value to the G_{IC} of the neat resin [62]. It is therefore useful in establishing the effect of aging on the matrix. $G_{IC\text{-prop}}$ is heavily influenced by fibre bridging, and therefore better models the delamination behaviour of composites when in service as the toughness of these materials will also be affected by fibre bridging. Even though the crack opening displacement is less *in situ* than during the DCB test, this should not influence the extent of fibre bridging to a large extent as it is caused by a weakening of the fibre/matrix interface. The presence of fibre bridging will lead to an increase in toughness, as the fibre breaks away from the matrix and bridges the gap across the crack

tip. As this gap expands with increasing tensile force applied to the specimen, the fibre becomes strained and diverts some of the energy away from the crack tip. Thus the energy required to propagate the crack is consequently increased and the measured interlaminar fracture toughness is greater [63]. In addition to this, as fibres are pulled out of the matrix, new surfaces are formed, which also requires additional energy. The extent of fibre bridging has been correlated to the strength of the fibre/matrix interface with large amounts of fibre bridging indicating a weak interfacial bond where the fibres are easily removed from the matrix during testing [72].

In the present study, stable crack growth was observed in all tests, consistent with both composite matrices being relatively brittle, being bismaleimides. Tough matrices generally show unstable crack growth when tested, characterised by peaks in the load displacement curve and the crack exhibiting slip/stick behaviour during propagation. This phenomenon may be explained by the tendency of the crack to change planes in tough materials where the damage zones are larger [8]. In both of the current composite materials, the fibre-bridging zone was observed to increase with aging time. This increase was greater in the case of the CBR 320/328 composites where the fibre-bridging zone appeared to be larger than in the commercial composite material by visual inspection. It is likely that the increased fibre bridging may arise from the degradation of the fibre matrix interface. Evidence for this was found when the specimens were examined by SEM, where bare fibres and fibre breakage were observed along the fracture surface. These findings are supported by Hutapea and Yuan [70] who performed an aging study of IM7/LaRC-RP46 composites and observed an increase in fibre bridging and attributed this to the loss of adhesion between the fibres and the matrix. An increase in the fibre bridging zone and subsequent decrease in interfacial strength with aging was observed in a study of carbon/epoxy composites [72], with the Mode I interlaminar fracture toughness during steady crack propagation increasing constantly with the period of time the composite was aged as the extent of fibre bridging also increased.

The results from Interlaminar Fracture Toughness tests of aged samples from both of the composite materials under investigation were found to be very different at the two discrete aging temperatures. In summary, the effect of aging at 250°C on both materials

was much more severe than the effect of aging at 204°C, with a dramatic decrease in both $G_{IC\text{-init}}$ and $G_{IC\text{-prop}}$ over the total aging period. Although these values also decreased with the total amount of time that material was aged at 204°C, the reduction was not as severe and the data observed from the different materials contained significant differences. In both studies, previously published weight loss data were used to estimate the amount of time the materials were aged [12]. Knowledge of the time taken to observe dramatic change in weight loss were used to estimate the total required aging time before significant change in properties might be observed. Testing intervals were selected arbitrarily. Caution should be exercised when using weight loss data to predict composite property changes as a small error in weight loss measurement can cause a large error in the mechanical property calculation. In one study [86], the compression strength of a carbon/epoxy composite was found to decrease by 30% after only a 2% weight loss. One contributing factor is that almost all of this measured weight loss is due to degradation of the resin and in a composite with a fibre volume fraction of 65%, a 2% weight loss corresponds to a loss of 6% of the matrix. This is mostly a problem when weight loss data alone are used to estimate composite performance, whereas, in the current study, weight loss data is used as a basis for further investigation.

$G_{IC\text{-init}}$ was observed to decrease with increasing aging times for both materials and at both aging temperatures. As $G_{IC\text{-init}}$ can be closely correlated to matrix toughness as mentioned previously, so this trend was not unexpected. This style of trend was also observed by Hutapea [70] in the study mentioned previously where $G_{IC\text{-init}}$ decreased by 32% after 6000 hours of aging at 232°C. The authors proposed that this decrease was because oxidation had weakened both the matrix and the interfacial strength. In the present study, surface degradation and delamination were visually observed to occur in both materials, however this did not affect the calculation of $G_{IC\text{-init}}$ and $G_{IC\text{-prop}}$ as they are both measured at the core of the sample. The correlation between these results and FT-IR spectra also taken from the core of the sample will be discussed in section 6.5. Surface degradation and the possible role it plays in protecting the core of the material was examined by Raman spectroscopy and will be discussed in Section 6.6.

Mode I interlaminar fracture toughness tests for CBR 320/328 composite samples aged

for 4 weeks all failed by cracking at the surface of the sample rather than by a mode I mechanism and the results had to be discarded. It appears that after 4 weeks of aging the surface of the sample is much weaker than the core, thus causing the specimen to fail at the surface. Visual inspection of these samples revealed that although the core was almost intact, the exterior of the specimen was highly degraded, with bare fibres evident along the surface. After 6 weeks of aging, it appears that the degradation path has progressed to the core so that the sample undergoes a mode I failure with the crack growth occurring along the centre of the specimen.

In both resin systems and at both aging temperatures, the value measured for $G_{IC\text{-prop}}$ initially increased before decreasing substantially. This occurred despite the propensity of both bismaleimides to continue to crosslink with time. This increased crosslinking is due to unreacted C=C bonds (such as those present in Matrimid® 5292 B) undergoing further "ene" reactions, resulting in the increase in Tg observed by DMTA. Although an increase in the crosslink density results in embrittlement of the matrix, the value of $G_{IC\text{-prop}}$ is highly influenced by the strength of the fibre/matrix interface and the effect of the increased crosslink density on the interfacial strength is uncertain. The main factor contributing to this initial rise is the observed increase in fibre bridging. These two effects appear to be eventually superseded by the deleterious effect of the degradation of the matrix. With longer periods of aging, it seems that it is the strength of the matrix eventually becomes so poor that the strength of the fibre/matrix interface also decreases and is responsible for the decrease in $G_{IC\text{-prop}}$. This degradation was verified through SEM examination of the specimens, through the observation of bare fibres and an increase in porosity of the matrix as discussed in the Section 6.2. Although the general trend in the measurement of this value was similar for studies at both temperatures, the period of time before this decrease in properties observed differed significantly.

At 250°C, the CBR 320/328 composites demonstrated better retention of interlaminar fracture toughness with the amount of time the material was aged than the Matrimid® 5292 composites. After 6 weeks of treatment at this temperature $G_{IC\text{-prop}}$ for the CBR 320/328 composite was measured to be similar to that of the untreated composite whereas $G_{IC\text{-prop}}$ for the commercial composite was a mere 30% of the original value.

One explanation for this occurrence is that the surface of the CBR 320/328 degrades rapidly to form a protective layer that prevents the core from the effects of the thermal treatment. This phenomenon is known as char protection and is reported by Turi [73] in her book on the thermal analysis of polymers. Evidence of surface degradation occurring in both composites was found using Raman spectroscopy (section 6.6). Another factor might be that the Matrimid® 5292 composites have a higher fibre volume fraction (refer to Section 3.6) and are therefore more compacted. A higher degree of compaction means that there is less resin holding the fibres together and protecting the core of the material, therefore gaseous species (such as oxygen) are able to diffuse to the core of the composite more readily than in the CBR 320/328 composites.

At 204°C, it is the commercial material that exhibits better property retention with aging. After 15 weeks of aging at the lower temperature, $G_{IC\text{-prop}}$ for the CSIRO composite was measured to be 28% of the value for the untreated material, whereas $G_{IC\text{-prop}}$ for the Matrimid® composite was measured to be equivalent to the untreated value. After 30 weeks of aging, this value has decreased only slightly, whereas $G_{IC\text{-prop}}$ for the CSIRO composite decreased to less than 20% of the original. In the case of the CBR 320/328 composites, it appears that when aged at the lower temperature, char protection does not occur to the same extent as at the higher temperature. This phenomenon can be likened to cooking a steak at a high temperature for a very short time compared with cooking a steak for a longer time at a lower temperature. In the case of the former, a charred layer is formed on both sides of the steak when exposed to heat and the centre of the steak remains rare. If the steak was cooked at a lower temperature for a longer period of time, the heat penetrates further into the steak and the centre is medium to well done. This analogy of cooking steak can be used to explain the effect of aging on the interlaminar fracture toughness of the composites. The penetration of heat at 250°C is restricted by the formation of a protective charred surface whereas at 204°C, the damaged zone penetrates further into the composite. The excellent property retention of the Matrimid® 5292 composites is most likely due to the very good fibre/matrix adhesion as observed by SEM (section 5.3). These micrographs show that despite the increase in porosity as the material is aged, the interfacial adhesion remains quite strong as evidenced by the coating of resin on the fibres. As the interlaminar fracture toughness measurement is dominated by the interfacial

adhesion, the properties of this composite were relatively unaffected. Other mechanical property tests such as compression after impact may show a change with aging in this case. From these observations, it can be reasonably concluded that the aging mechanisms at the two temperatures are different and that results from accelerated aging tests may lead to incorrect assumptions about the behaviour of the material at lower temperatures.

The results from the accelerated aging study are considerably different to the results from isothermal aging of the composites at the lower temperature. The differences in these results are due to different aging mechanisms, the chemical nature of which were investigated by Raman and FT-IR spectroscopy and will be discussed in sections 6.5 and 6.6. The degradation of both materials was observed visually to be much worse at the surface than at the core of the specimen. It is suspected that the decomposed surface forms a protective layer that helps to prevent degradation at the core of the material and that the CBR 320/328 composite is particularly effective in doing this when aged at 250°C. Most importantly, the results from interlaminar fracture toughness tests at 250°C are very different than those obtained from the study at 204°C.

6.4 Scanning Electron Microscopy

Scanning Electron Microscopy was used to examine the fracture surfaces of the specimens after testing to ensure that pure Mode I failure had occurred and that there were no obvious effects from shear failure present. Any Mode II (or shear) failure can easily be detected upon examination of the fracture surface of the specimen due to the sharp, distinctive hackles that it creates in the matrix. The difference in Mode I and Mode II fracture surfaces is illustrated very clearly by Russell [63], who published a micrograph of the transition from a Mode I pre-crack to a Mode II fracture. While samples aged at 204°C were examined in detail, samples aged at 250°C could not be thoroughly examined due to their high degree of porosity, a direct consequence of oxidation of the matrix. Although most of the porosity appeared by visual inspection, to arise as a result of damage to the surface of the samples, it prevented adequate sample preparation for SEM, as a vacuum sufficient for gold coating the specimens could not be achieved after any period of aging at this temperature. Despite the sample surfaces containing large amounts of conductive carbon fibres, gold coating was essential to

obtaining a SEM image using the available instruments.

It was possible to perform a more thorough study of the samples aged at 204°C for periods from 0-15 weeks, however the samples aged for 30 weeks were again too porous to be successfully gold coated. CBR 320/328 samples aged at 204°C exhibited poor fibre/matrix adhesion as evidenced by the large number of clean fibres and very little matrix deformation observed in the micrographs. This poor fibre matrix adhesion appears to become progressively worse as the period of aging time was increased. As a result of this, the crack propagates mostly along the fibre/matrix interface during testing which leads to extensive fibre bridging in the composite. Evidence of this increased fibre bridging can also be observed in the micrographs, a higher degree of fibre bridging is indicated by an increase in fibre breakage and the number of detached fibres [63]. The result of all of the above will be that the apparent fracture toughness of the aged CSIRO material measured may be higher than the matrix G_{IC}, however, the increased value will provide a good reflection of how the composite may perform when in service. Similar observations were also made by Hutapea and Yuan [70] in a study of IM7/LaRC-RP46 composites aged at 232°C, 288°C and 316°C.

Micrographs of the Matrimid® 5292 composites demonstrate better fibre/matrix adhesion than the CBR 320/328 composites, however an increase in porosity of the matrix of the former can be clearly observed as the aging time is increased. Despite the obvious degradation of the matrix, these composites exhibit excellent property retention when exposed to this temperature (as discussed previously). One explanation for this is that the good fibre/matrix adhesion is able to compensate for the increase in porosity to an extent, up until 30 weeks of aging, at which point the porosity appears to reach a critical level and the fracture toughness is compromised. The cause of this porosity is most likely due to degradation of the relatively unstable saturated imide and subsequent by-products as detected by FTIR and discussed in the section to follow. The CBR 320/328 matrix contains a more stable pyromellitic dianhydride-based structure in the polymer backbone.

6.5 Fourier Transform Infrared Spectroscopy

The Matrimid® 5292 resin system has been commercially available for some time and as a result there is a significant amount of information about it published in the literature. However, there is relatively little published on the analysis of the resin chemistry using techniques such as Fourier Transform Infrared Spectroscopy (FTIR) and some of what has been published is contradictory. In particular there has been considerable variation in the assignment of various peaks as will be discussed later in this section. The assignments of peaks in the present work were based on publications by Morgan [14], Grenier-Loustalot [87], Phelan and Sung [88] and also the "Atlas of Polymer and Plastics Analysis" by Hummel [89]. Assignments for peaks arising from the CBR 320/328 resin system proved to be slightly more difficult due to the novelty of the material. Model compounds were of assistance in this case. Publications referring to PMR-15 composites are also highly relevant as one of the monomers used in these composites is methylenedianiline which undergoes imidization during cure to form a structure very similar to that of both Matrimid® A and CBR 328 (refer to Figure 2.2).

Tables 6.1 and 6.2 show the tentative peak assignments for Matrimid® 5292 and CBR 320/328 composites respectively. The two tables also compare the final spectra of the composites aged at the different temperatures, although these peaks are in similar positions, they have different relative intensities. There is some disagreement over the assignment of peaks in the region from 1000 to 1400 cm^{-1}. Both Grenier-Loustalot *et al*. [87] and Phelan and Sung [88] have assigned peaks at 1180 and 1150 cm^{-1} to succinimide and maleimide C-N-C stretches respectively. Morgan *et al*. [14] however, disagree and assign the peak at 1180 cm^{-1} to a C-O-C stretch. Both Phelan and Sung and Morgan et al. studied the cure reactions of the Matrimid®5292 resin system and while Phelan and Sung propose that the cure is predominantly via an ene followed by a Diels-Alder reaction, Morgan provides evidence of an additional reaction undertaken by Matrimid®5292 B, which undergoes etherification by dehydration of the hydroxyl groups. Morgan follows this reaction by FTIR and observes the ingrowth of the ether peak at 1182 cm^{-1}, which occurs at the same time as the hydroxyl band at 3473 cm^{-1} diminishes. Both assignments of this peak at 1180 cm^{-1} are possible and convincingly argued. Phelan and Sung and Morgan agree on the assignment of the allyl peak arising

from Matrimid®5292 B at 915 cm^{-1}. Although this peak was not observed here, probably due to the relative insensitivity of FTIR to C=C bonds, the allyl peak was observed clearly in the Raman study (presented in the next section).

Matrimid® 5292 FTIR peak positions			
Unaged	Aged at 204°C for 30 weeks	Aged at 250°C for 6 weeks	Tentative assignment
3429 (s)	3434 (s)	3439 (s)	OH stretch
2966(w)			Asymmetric CH_3 stretch
2922 (w)	2922 (w)	2922 (w)	Asymmetric CH_2 stretch
2852 (w)			Symmetric CH_3 stretch
1711 (s)	1718 (vs)	1718(vs)	Asymmetric C=O
1606 (w)	1606 (s)	1609 (vs)	Phenyl with C=O conjugation
1512 (w)	1511 (w)	1507 (vw)	Phenyl with CH_2 bridge
1384 (m)	1375 (m)	1371 (m)	Aromatic CH_3
	1313 (vw)	1313 (vw)	
1260 (vw)	1269 (w)	1263 (w)	
1175 (m)	1175 (w)	1167 (w)	C-N-C succinimide or C-O-C
1111 (w)	1114 (vw)	1114 (vw)	
1021 (vw)			
	931 (vw)		Aromatic C=O wag
811 (w)			C=C maleimide deformation
	838 (w)	839 (w)	

Key: m = medium signal, s = strong signal, vs = very strong signal, w = weak, vw = very weak

Table 6.1: Assignments of peaks in the FTIR spectra of Matrimid® 5292 composites.

CBR 320/328 FTIR peak positions			
Unaged	Aged at 204°C for 30 weeks	Aged at 250°C for 8 weeks	Tentative assignment
3441 (s)	3438 (s)	3421 (s)	OH stretch
2970 (w)			Asymmetric CH_3 stretch
2934 (w)	2926 (vw)	2925 (vw)	Asymmetric CH_2 stretch
2877 (w)			Symmetric CH_3 stretch
1779 (w)			Symmetric C=O (unsaturated)
1728 (s)	1725 (s)	1723 (s)	Asymmetric C=O (unsaturated)
1712 (w)			Asymmetric C=O (saturated)
	1610 (s)	1609 (s)	Phenyl with C=O conjugation
1473 (w)	1466 (vw)	1466 (vw)	Phenyl with CH_2 bridge
1421 (vw)			
1374 (m)	1370 (m)	1371 (m)	Aromatic CH_3
1358 (sh)			Aromatic CH_3
1284 (vw)			
1184 (m)			C-N-C succinimide or C-O-C
1112 (w)	1107 (vw)	1110 (vw)	
	921 (vw)		Aromatic C=O wag
845 (w)	841 (w)	842 (w)	C=C maleimide deformation
731 (w)		731 (vw)	Imide (unsaturated)
	725 (vw)	725 (vw)	

Key: m = medium signal, s = strong signal, vs = very strong signal, w = weak, vw = very weak

Table 6.2: Assignments of peaks in the FTIR spectra of CBR 320/328 composites.

The FTIR analysis of the aging of both materials revealed a common trait. In both resin systems and at both temperatures, the most significant change with aging was the ingrowth of a broad peak at around 1600cm^{-1}, which grows concurrently with the decrease in size of a peak at around 1500cm^{-1}. Both of these peaks arise from the vibrations involving the aromatic rings, the peak at 1500cm^{-1} from two aromatic rings bridged by a methylene group and the peak at 1600 cm^{-1} from two aromatic rings bridged by a carbonyl group (see Figure 6.2). The thermo-oxidation of methylene bridging groups to form a carbonyl group in polyimides was first reported by Jewell and Sykes [75]. The broadness of the peak at 1600 cm^{-1} is due to the overlap of peaks from other degradation products (i.e. the ethyl groups in the CSIRO material) that have similar structures. Young and Chang [90] studied the FTIR changes of PMR-15 after thermal spiking and also observed this change along with the ingrowth of peaks at 1660 and 930 cm^{-1}, both arising from the bridging carbonyl group. A scheme depicting the oxidation of the methylene to a carbonyl group is shown in Figure 6.2. In the samples aged at 204°C, the peak at 930 cm^{-1} can be observed and the peak at 1660 cm^{-1} may be obscured in a shoulder of the broad peak at 1604 cm^{-1}. Samples aged at 250°C do not show either of these peaks, this product may have undergone further degradation at this higher aging temperature.

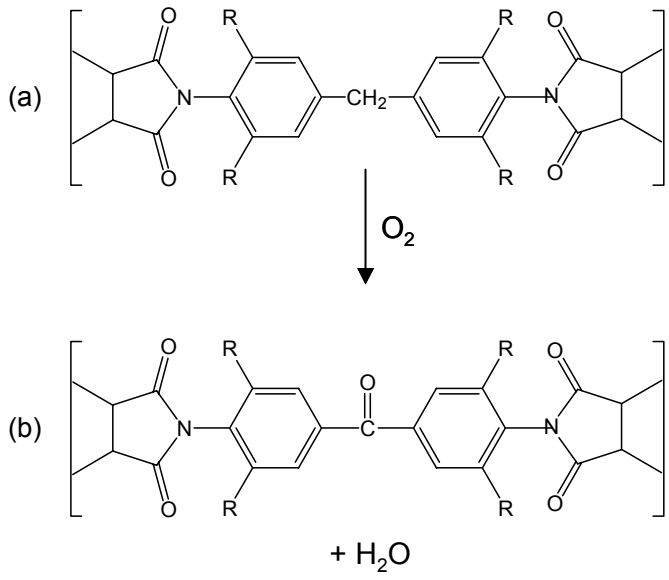

Figure 6.2: Scheme showing the oxidation of the methylene group common to both resin systems (a) to a carbonyl group (b). (R = H for Matrimid® 5292, R = CH_2CH_3 for CBR 320/328).

FTIR spectra of the aged CBR 320/328 composites show additional changes to those above as the chemical structure of the monomers is more complicated than that of the commercial resin. FTIR spectra of the unaged CBR 320/328 composites reveal three imide carbonyl peaks at 1779, 1728 and 1712 cm^{-1}. These peaks may be assigned to the symmetric and asymmetric stretches of an unsaturated imide (1779 and 1728 cm^{-1}) and the asymmetric stretch of a saturated imide (1712 cm^{-1}). Figure 6.3 shows a saturated and unsaturated imide in the final cure structure. The unsaturated structure results from the incorporation of a pyromellitic dianhydride based structure from the CBR 320. These types of structures have very high thermal stabilities. When CBR 320/328 is aged at both 204 and 250°C, the peaks arising from the saturated polyimide at 1779 and 1712 cm^{-1} disappear while the peak due to the more stable unsaturated imide remains (refer to Figure 6.2). One possible degradation mechanism might be the oxidation of the quaternary hydrogen atom, which would result in the imide ring opening to form a carboxylic acid. There have been a number of papers that suggest that the carbon-nitrogen imide bond is unstable and its breakage is the cause of the imide degradation, however evidence of this has only been provided for extremely high temperature treatments such as pyrolysis and there is no evidence that this same degradation mechanism occurs at lower temperatures [81, 82, 91].

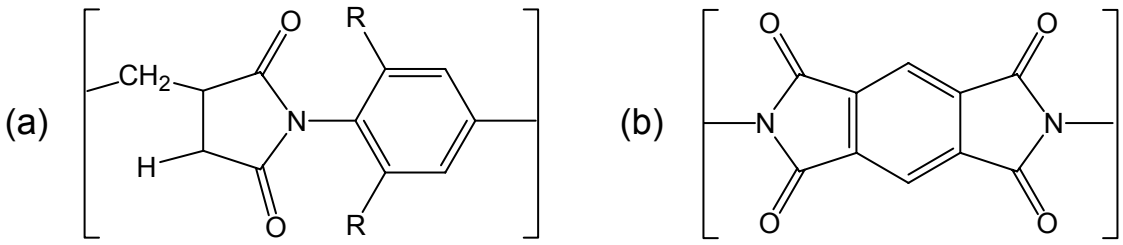

Figure 6.3: FTIR analysis of aged CBR 320/328 composites show peaks due to the saturated imide (a) disappear while peaks arising from the highly thermally stable unsaturated (b) imide structures remain after heat treatment.

Comparison of the final FTIR spectra recorded of the CBR 320/328 composites aged at both 204 and 250°C appear to be quite similar. When the final spectra of the Matrimid® 5292 composites are compared, significant differences may be observed. Although the peaks are in the same positions in both, there are marked differences in the relative intensities of these peaks. Peaks in the spectra from the accelerated aging test are

considerably broader and of greater intensity, indicating that the material is more highly degraded. This is also reflected in the greater loss of interlaminar fracture toughness.

6.6 Raman Spectroscopy

While FTIR spectroscopy yielded a great deal of information about the types of carbon-oxygen and carbon-nitrogen bonds present in the samples, Raman Spectroscopy is particularly sensitive to carbon-carbon double bonds. In addition to this, the Raman microscope technique allowed mapping across samples and enabled the examination of regions as small as 5 microns. The Raman Spectroscopy study performed on material aged at 250°C was limited due to a problem with a high degree of fluorescence arising from the materials aged at this temperature. Certain compounds (particularly those containing chromophores) are prone to high-energy transitions that cause fluorescence. If a compound exhibits a high degree of fluorescence, this saturates the accumulated Raman Spectrum, rendering it impossible to observe any of the peaks that usually arise from the sample. As a result of this, only the Matrimid® 5292 composites were studied and a spectrum could only be reliably obtained from samples aged for 1 week. The CBR 320/328 resin system was very prone to fluorescence, most likely because of its more complicated, highly aromatic structure. Chemical changes in the first week of aging were noted and in addition to this, the *xyz* stage of the Raman Microscope meant that transverse sections of samples could be scanned. This enabled the chemical changes as a function of sample thickness to be monitored.

An indication of the extent of the cure reaction can be gained from the relative intensities of the two peaks at 1608 and 1646 cm^{-1}. Both peaks can be assigned to carbon-carbon double bond stretching, the peak at 1608 cm^{-1} arising from a carbon-carbon double bond of an aromatic ring and the peak at 1646 cm^{-1} arises from the alkene group on Matrimid® 5292 B. As illustrated in reaction Scheme 2.1, it is the highly reactive alkene group that participates in the initial "ene" reaction during cure and continues to react even after the material has been cured using the appropriate cure cycle. Thus, the relative intensity of this peak compared with the aromatic peak (which does not change significantly after cure) can be used to estimate the degree of reaction.

In the study at 250°C, as the specimen was mapped from the surface of the sample to the core, the relative size of the peak at 1646 cm^{-1} increased towards the centre of the sample until at the core of the sample, the two peaks at 1608 and 1646 cm^{-1} were almost the same intensity. The logical conclusion to be drawn from this finding is that a higher degree of reaction of this alkene group takes place at the surface where there is the greatest oxidation. The degradation path at this temperature is from the surface of the material towards the core, with the degraded surface layer possibly playing a role in the protection of the core.

The above is reversed in the case of the 204°C study, where in both composite materials the intensity of the peak at 1646 cm^{-1} was found to decrease as the specimen was mapped towards the core. This indicates that the degree of reaction is greatest at the core of the sample. One possible explanation is that a reverse Diels-Alder reaction is occurring in this case [92], thus accounting for the increase in intensity of the C=C peak at the surface of the material. The implication is that a completely different aging mechanism takes place at the lower temperature and this helps to explain why the CBR 320/328 showed good retention of interlaminar fracture toughness at 250°C and very poor property retention at 204°C. At 250°C, the core of the material was protected by a highly crosslinked and degraded surface, whereas at 204°C, the core of the composite had a higher degree of crosslinking than the surface.

When the intensity of the peak at 1646 cm^{-1} was measured as a function of aging time, in the studies at both temperatures, it decreased, indicating that the degree of crosslinking increased with aging time. This was found to occur in the Matrimid® 5292 composite aged for 1 week at 250°C and in both composite systems when aged at 204°C for up to 15 weeks. This helps to explain the initial increase in $G_{IC\text{-prop}}$ observed in the interlaminar fracture toughness tests.

6.7 Dynamic Mechanical Thermal Analysis

Dramatic decreases in the Glass Transition Temperature (Tg) of composites aged at 250°C were observed in both composite materials. In the case of the Matrimid® 5292

composites, the Tg, as measured from the peak in the tan δ curve, decreased from an initial 365°C to 247°C after two weeks of aging. After 4 weeks of aging at this temperature, a peak in the tan δ curve could no longer be detected. The Tg of the CBR 320/328 composite decreased from an initial measurement of 302°C to 273°C after 2 weeks of aging to 230°C after 6 weeks of aging. An increase in Tg has also been observed in other studies of the aging of bismaleimides [56] with a concurrent deterioration of mechanical properties.

These changes were not emulated in the aging study at 204°C where the Tg of the Matrimid® 5292 composites was found to decrease only slightly; from 365 to 348°C after 15 weeks of aging. In the case of the CBR 320/328 composites, an initial increase was observed from 302 to 330°C after 5 weeks of aging after which time the Tg remained at around 330°C even after 30 weeks of aging. It appears that at the lower temperature, the matrix is undergoing further crosslinking, whereas at 250°C the matrix is oxidised, as evidenced by the relatively large weight loss of these composites at 250°C.

Chapter 7 - Conclusions & further work

The research presented in this thesis was conducted in order to assess the effect of isothermal aging on two high temperature composite materials. Aerospace composites are exposed to aggressive environments when in service and must withstand damage from heat, moisture and rapid temperature changes (they are protected from UV radiation as they are coated with paint). This study focused on the effect of heat as a means to establishing the effect of exposure to high temperatures resulting from friction heating during supersonic flight. Changes in mechanical properties were monitored, specifically the interlaminar fracture toughness as delamination of composites is a critical mode of failure in carbon fibre composites. Chemical changes in the matrix were also monitored to enhance the understanding of structure-property relationships, this being of assistance in predicting part lifetime. In addition to this, accelerated (elevated temperature) aging tests were evaluated to determine how accurately they reflect the aging mechanisms of composites exposed to lower temperatures for longer times.

The aging mechanisms of two aerospace composites were studied at two different temperatures. One material, CBR 320/328 was fabricated with a novel CSIRO resin and the other material Matrimid® 5292 was comprised of a commercial matrix for comparison. These materials were aged at 204 and 250°C and the results indicated that different aging mechanisms took effect at the different aging temperatures. At the higher temperature, the CBR 320/328 retained interlaminar fracture toughness better than the commercial material due to char protection of the composite core, however at the lower temperature, it was the Matrimid® 5292 composite that showed better property retention as a result of better fibre/matrix adhesion.

The resistance curves from double cantilever beam tests displayed similar trends for both materials and at both temperatures. $G_{IC\text{-prop}}$ initially increases with aging as a result of increased fibre bridging and an increase in the degree of crosslinking of the resin (as shown by Raman Spectroscopy). This initial increase was followed by a dramatic loss of toughness with longer periods of exposure. At 250°C, the final value

of $G_{IC\text{-prop}}$ measured (after 6 weeks) was found to be 30% of the original value in the case of the Matrimid® 5292 composites. After the same period of aging, $G_{IC\text{-prop}}$ for the CBR 320/328 composites was 100% of the unaged value, this decreased to 35% after 8 weeks of aging at this temperature. At 204°C and after 30 weeks of aging, $G_{IC\text{-prop}}$ for the CBR 320/328 composite had decreased to only 13% of the original measured value, whereas the Matrimid® 5292 composites had retained 64% of the unaged interlaminar fracture toughness. $G_{IC\text{-init}}$ (which can be closely correlated to matrix G_{IC}) was found to decrease consistently with the amount of time the material was aged at both temperatures.

Examination of fracture surfaces by SEM confirmed that pure Mode I failure had occurred. The CBR 320/328 fracture surfaces showed poor fibre-matrix adhesion as evidenced by bare and broken fibres. The fracture surfaces of the Matrimid® 5292 composites revealed better fibre-matrix adhesion, with an increasing degree of porosity with the amount of time the material was aged at 204°C. Despite the resulting "honeycomb" appearance of the composite under the microscope, samples retained interlaminar fracture toughness due to excellent fibre-matrix adhesion.

FTIR analysis of the composites showed that the surface of the materials degrades very rapidly, with the greatest amount of damage occurring in the first 4 days of aging at 250°C. Chemical changes at the core of the specimens occurred more gradually with aging at both temperatures, however these changes could be correlated with changes in mechanical properties of both composites. Evidence of oxidation of the methylene group bridging two aromatic rings present in the structures of both of the resin systems to a carbonyl group was found. In the CBR 320/328 composites in addition to this, the saturated imide was found to degrade whereas the unsaturated imide proved to be more stable. The strong correlation between chemical changes in the matrix and changes in the composite interlaminar fracture toughness highlight the potential for the use of chemical techniques in predicting mechanical property performance of carbon fibre composites.

The use of Raman spectroscopy revealed that the degradation path was different at each of the temperatures in this study. At 250°C, the intensity of the peak at 1646 cm^{-1},

assigned to the allylic C=C was found to be greatest at the surface, whilst at 204°C, it was found to be greatest at the core. At 250°C, it was concluded that the increase in intensity of the peak at 1646 cm^{-1} was the result of the material continuing to crosslink after cure. The reverse trend at the lower temperature was possibly attributed to a reverse Diels-Alder reaction.

DMTA of the untreated Matrimid® 5292 composite revealed that the recommended cure cycle did not result in a completely reacted material. The Tg of both composites was found to decrease with aging at 250°C until a peak could no longer be detected with extended exposure times. This was also found to occur at 204°C with the Matrimid® 5292 composites, however the Tg of the CBR 320/328 composites was found to increase slightly and then stabilise at this elevated value due to continued crosslinking.

In summary, the chemical changes observed were consistent with the changes in mechanical properties as measured by the composite interlaminar fracture toughness. The mechanisms by which aging occurred were found to be different at the two temperatures, which raises serious doubts about the reliability of results from accelerated aging programs.

Based on the above conclusions, there are numerous suggestions for future research directions. Large-scale production of the CBR 320/328 resin would allow for the expansion of mechanical property tests to include Mode II interlaminar fracture toughness as well as compression after impact tests. These additional tests may reveal different trends in the property retention of high temperature composite materials after aging. They will also enable the comprehensive characterization and prediction of mechanical property changes that may occur after an aircraft has experienced several thousand hours in service. In addition to this, evaluation of other novel CSIRO composite resin systems (e.g. the particularly stable CBR 330 resin) for comparative purposes would also be of interest.

Also of relevance, is the evaluation of the effect of isothermal aging at temperatures approaching the predicted 177°C surface temperature of an aircraft at Mach 2.4. The aging mechanism at this temperature may prove to be significantly different to the

mechanism observed at 204°C in the present study.

Based on the poor fibre/matrix adhesion exhibited by the CBR 320/328 composites in this study, it would be really interesting to see investigate the effect of the sizing of the carbon fibres. Using polyimide sized carbon fibres may increase the bonding between fibre and matrix and increase the strength of the interface. Increasing the interfacial strength would also increase the interlaminar fracture toughness of these materials.

Bibliography

1. Shin, E.E., C. Dunn, E. Fouch, R.J. Morgan, M. Wilenski, and L.T. Drzal, *Durability and Critical and Fundamental Aging Mechanisms of High Temperature Polymer Matrix Carbon Fiber Composites: Part Ii.* Proceedings of the ASME Materials Division, 1995. **69**(1): p. 191-200.

2. Wilson, D., *Polyimides as Resin Matricies for Advanced Composites*, in *Polyimides*, D. Wilson, H.D. Stenzenberger, and P.M. Hergenrother, Editors. 1990, Chapman and Hall: Glasgow, New York, Blackie. p. 187-226.

3. Dao, B., J.H. Hodgkin, and T.C. Morton, *The Utility of 2-Naphthol Derivatives as Diels-Alder Based Co-Reactants for Bismaleimides.* High Perform. Polym., 1997. **9**: p. 413-427.

4. *http://www.eurofighter.pso-online.com/eurofighter/structure_ie.html*.

5. Hergenrother, P.M. and M.E. Rogalski, *Composites for High Speed Civil Transports.* Polymer Preprints, 1992. **33**: p. 354-356.

6. Leach, D.C., *Continuous Fibre Reinforced Thermoplastic Matrix Composites*, in *Advanced Composites*, I.K. Partridge, Editor. 1989, Elsevier Science Publishers Ltd: London. p. 43-110.

7. Campbell, F.C., A.R. Mallow, and C.E. Browning, *Porosity in Carbon Fiber Composites an Overview of Causes.* Journal of Advanced Materials, 1995. **26**(4): p. 18-33.

8. Davies, P., *Delamination*, in *Advanced Composites*, I.K. Partridge, Editor. 1989, Elsevier: London. p. 303-329.

9. Dao, B., J. Hodgkin, and T.C. Morton, *Important Factors Controlling the Synthesis of Imides in Water.* High Perform. Polym., 1999. **11**: p. 205-18.

10. Stenzenberger, H.D., M. Herzog, P. König, W. Römer, and W. Breitigam. *Bismaleimide Resins, Past, Present, Future.* in *34th International SAMPE Symposium*. 1989.

11. Takekoshi, T., *Polyimides*, in *Advances in Polymer Science*, C.G. Overberger, Editor. 1990, Springer-Verlag, Berlin Heidelberg p. 1-25.

12. Dao, B., D.G. Hawthorn, J.H. Hodgkin, M.B. Jackson, and T.C. Morton, *Preparation and Characterization of Some Novel Bismaleimide Monomers and Polymers Based on Diaminobisimides.* High Perform. Polym., 1996. **8**: p. 243-263.

13. Stenzenberger, H.D., *Chemistry and Properties of Addition Polyimides*, in *Polyimides*, D. Wilson, H.D. Stenzenberger, and P.M. Hergenrother, Editors. 1990, Chapman and Hall: Glasgow, New York, Blackie. p. 79-128.

14. Morgan, R.J., E.E. Shin, B. Rosenberg, and A. Jurek, *Characterization of the Cure Reactions of Bismaleimide Composite Matrices.* Polymer, 1997. **38**(3): p. 639-646.

15. Mijovic, J. and S. Andjelic, *Study of the Mechanism and Rate of Bismaleimide Cure by Remote in-Situ Real Time Fiber Optic near-Infrared Spectroscopy.* Macromolecules, 1996. **29**(1): p. 239-246.

16. Hopewell, J.L., G.A. George, and D.J.T. Hill, *Quantitative Analysis of Bismaleimide-Diamine Thermosets Using near Infrared Spectroscopy.* Polymer, 2000. **41**: p. 8221-8229.

17. Hopewell, J.L., G.A. George, and D.J.T. Hill, *Analysis of the Kinetics and Mechanism of the Cure of a Bismaleimide-Diamine Thermoset.* Polymer, 2000. **41**: p. 8231-8239.

18. Lincoln, J.E., R.J. Morgan, and E.E. Shin, *Moisture Absorption-Network Structure Correlations in BMPM/DABPA Bismaleimide Composite Matricies.* Journal of Advanced Materials, 2000. **32**(4): p. 24-34.

19. Barton, J.M., I. Hamerton, J.R. Jones, and J.C. Stedman, *A Comparitive Study of the Relative Reactivity of Alkenyl Functionalized Toughening Modifiers for Bismaleimides.* Polymer Bulletin, 1991. **27**: p. 163-170.

20. Cunningham, I.D., A. Brownhill, I. Hamerton, and B.J. Howlin, *The Ene Reaction between Maleimides and Allyl-Substituted Aromatics.* Tetrahedron, 1997. **53**(39): p. 13473-13494.

21. Olesen, K.A., R. Falabella, and R.A. Buyny. *Mechanical Behavior of Three Generations of Bismaleimide Composite Prepregs.* 37th International SAMPE Symposium. 1992.

22. Fry, C.G. and A.C. Lind, *Curing of Bismaleimide Polymers: A Solid-State 13c-Nmr Study.* New Polymeric Materials, 1990. **2**(3): p. 235-254.

23. Hamerton, I., *High-Performance Thermoset-Thermoset Polymer Blends: A Review of the Chemistry of Cyanate Ester-Bismaleimide Blends.* High Perform. Polym., 1996. **8**: p. 83-95.

24. Barton, J.M., I. Hamerton, J.R. Jones, and J.C. Stedman, *Mechanical Properties of Tough, High Temperature Carbon Fibre Composites from Novel Functionalized Aryl Cyanate Ester Polymers.* Polymer, 1996. **37**(20): p. 4519-4528.

25. Hill, A.J., *Positron Annihilation Lifetime Spectroscopy to Probe Free-Volume Effects in High-Temperature Polymers and Composites.*, in *ACS Symposium Series, High-Temperature Properties and Applications of Polymeric Materials*. 1995: Washington, DC. p. 63-80.

26. Bigg, D.M., *A Review of Positron Annihilation Lifetime Spectroscopy as Applied to the Physical Aging of Polymers.* Polymer Engineering and Science, 1996. **36**(6): p. 737-43.

27. Struik, L.C.E., *Internal Stresses, Dimensional Instabilities and Molecular Orientations in Plastics.* 1990, John Wiley & Sons: Chichester. p. 76-78.

28. Fried, J.R., *Polymer Science and Technology*. 1995, New Jersey: Prentice Hall PTR. 135-136.

29. Kong, E.S.-W., *Physical Aging in Epoxy Matricies and Composites.* Advances in Polymer Science, 1986. **80**: p. 126-171.

30. Montserrat, S., *Physical Aging Studies in Epoxy Resins .1. Kinetics of the Enthalpy Relaxation Process in a Fully Cured Epoxy Resin.* Journal of Polymer Science Part B-Polymer Physics, 1994. **32**(3): p. 509-522.

31. D'Amore, A., G. Caprino, L. Nicolais, and G. Marino, *Long-Term Behaviour of PEI and PEI-Based Composites Subjected to Physical Aging.* Composites Science & Technology, 1999. **59**(13): p. 1993-2003.

32. Robertson, C.G., J.E. Monat, and G.L. Wilkes, *Physical Aging of an Amorphous Polyimide: Enthalpy Relaxation and Mechanical Property Changes.* Journal of Polymer Science Part B-Polymer Physics, 1999. **37**(15): p. 1931-1946.

33. Veazie, D.R. and T.S. Gates, *Compressive Creep of IM7/K3B Composite and the Effects of Physical Aging on Viscoelastic Behavior.* Experimental Mechanics, 1997. **37**(1): p. 62-68.

34. Bradshaw, R.D. and L.C. Brinson, *Mechanical Response of Linear Viscoelastic Composite Laminates Incorporating Non-Isothermal Physical Aging Effects.* Composites Science and Technology, 1999. **59**: p. 1411-1427.

35. Rodeffer, C.D., A.P. Maybach, and A.A. Ogale, *Influence of Thermal Aging on the Transverse Tensile Creep Response of a Carbon Fiber Thermoplastic Polyimide Composite.* Journal of Advanced Materials, 1996. **27**(2): p. 46-51.

36. Chan, L.C., H.N. Nae, and J.K. Gillham, *Time-Temperature-Transformation (TTT) Diagrams of High Tg Epoxy Systems: Competition between Cure and Thermal Degradation.* Journal of Applied Polymer Science, 1984. **29**: p. 3307-27.

37. Dine-Hart, R.A., D.B.V. Parker, and W.W. Wright, *Oxidative Degradation of a Polyimide Film.* Br. Polym. J., 1971. **3**: p. 222-234.

38. Stenzenberger, H.D., K.U. Heinen, and D.O. Hummel, *Thermal Degradation of Poly(Bismaleimides).* Journal of Polymer Science, Polymer Chemistry Edition, 1976. **14**: p. 2911-2925.

39. Morgan, R.J., E.E. Shin, J.E. Lincoln, J. Choi, and A. Lee. *The Structure Property Relations of Bismaleimide Composite Matrices and Durability of High Temperature Polymer Matrix Composites*. 28th SAMPE Technical Conference. 1996.

40. Morgan, R.J., E. Shin, C. Dunn, E. Fouch, B. Jurek, and A. Jurek. *The Durability of Composites for Potential High Speed Civil Transport Applications*. 39th International SAMPE Symposium. 1994.

41. Morgan, R.J., E.E. Shin, J. Lincoln, and J. Zhou, *Overview of Polymer Matrix Composites for Performance and Materials Development for Aero-Space Applications.* 45th International SAMPE Symposium, 2000: p. 345-351.

42. Meador, M.A.B., C.E. Lowell, P.J. Cavano, and P. Herrera-Fierro, *On the Oxidative Degradation of Nadic Endcapped Polyimides: 1. Effect of Thermo Cycling on Weight Loss and Crack Formation.* High Performance Polymers, 1996. **8**(3): p. 363-379.

43. Meador, M.A., J.C. Johnson, P.J. Cavano, and A.A. Frimer, *Oxidative Degradation of Nadic-End-Capped Polyimides. 2. Evidence for Reaction Occurring at High Temperatures.* Macromolecules, 1997. **30**: p. 3215-3223.

44. Meador, M.A.B., J.C. Johnson, A.A. Frimer, and P. Gilinsky-Sharon, *On the Oxidative Degradation of Nadic End-Capped Polyimides. 3. Synthesis and Characterization of Model Compounds for End-Cap Degradation Products.* Macromolecules, 1999. **32**(17): p. 5532-5538.

45. Hancox, N.L., *Thermal Effects on Polymer Matrix Composites: Part 1. Thermal Cycling.* Materials and Design, 1998. **19**: p. 85-91.

46. Hancox, N.L., *Thermal Effects on Polymer Matrix Composites: Part 2. Thermal Degradation.* Materials and Design, 1998. **19**: p. 93-97.

47. Liao, K., C.R. Schultheisz, D.L. Hunston, and L.C. Brinson, *Long-Term Durability of Fiber-Reinforced Polymer-Matrix Composite Materials for Infrastructure Applications: A Review.* Journal of Advanced Materials, 1998. **30**(4): p. 3-40.

48. Bowles, K.J., L. McCorkle, and L. Ingram, *Comparison of Graphite Fabric Reinforced PMR-15 and Avimid N Composites after Long-Term Isothermal Ageing at Various Temperatures.* Journal of Advanced Materials, 1998. **30**(1): p. 27-35.

49. Bowles, K., D. Jayne, and T.A. Leonhardt, *Isothermal Aging Effects on PMR-15.* SAMPE Quarterly, 1993(January): p. 2-9.

50. Bowles, K.J., *Adjusting the Measured Weight Loss of Aged Graphite Fabric/PMR-15 Composites.* Journal of Advanced Materials, 1998. **30**(3): p. 21-31.

51. Bowles, K.J. and J. Kamvouris, E., *Penetration of Carbon-Fabric-Reinforced Composites by Edge Cracks During Thermal Aging.* Journal of Advanced Materials, 1995. **26**(2): p. 2-11.

52. Bowles, K.J., D. Jayne, T.A. Leonhardt, and D. Bors, *Thermal Stability Relationships between Pmr-15 Resin and Its Composites.* Journal of Advanced Materials, 1994. **26**(1): p. 23-32.

53. Hinkley, J.A. and J.B. Nelson, *Lifetime Extrapolation of PMR-15 and LARC-160 Graphite Composites.* Journal of Advanced Materials, 1994(April): p. 45-48.

54. Marceau, C. and B. Hillaire, *Thermal Ageing of PMR-15 Polyimide Matrix.* Polymer., 1993. **34**(11): p. 2458-2459.

55. Jangchud, I., R.K. Eby, A.M. Serrano, and M.A. Meador, *Studies of Pan-Based Carbon Fiber Surfaces - Their Influence on Interfacial Bonding with PMR-15 Polyimide and Composite Thermo-Oxidative Stability.* Journal of Advanced Materials, 1996. **28**(1): p. 19-25.

56. Shin, E.E., R.J. Morgan, M. Wilenski, J. Zhou, J. Lincoln, and L.T. Drzal, *The Effects of Processing Conditions and Service Environmental Exposures on High Temperaure Polymer Matrix Carbon Fibre Composites.* 28th International SAMPE Technical Conference, 1996: p. 225-234.

57. Shin, E.E., R.J. Morgan, J.M. Zhou, J. Lincoln, R. Jurek, and D.B. Curliss, *Hygrothermal Durability and Thermal Aging Behavior Prediction of High-Temperature Polymer-Matrix Composites and Their Resins.* Journal of Thermoplastic Composite Materials, 2000. **13**(1): p. 40-57.

58. Li, L., *Thermal Aging Properties of Graphite Fibre Reinforced Peek and Graphite Fibre Reinforced BMI Composites.* Polm.-Plast. Technol. Eng., 1990. **25**(5&6): p. 549-562.

59. Hodgkin, J.H., R. Eibl, M.B. Jackson, and J.W. Loder, *Int. Patent Specification*. 1991. p. PCT/AU91/00454.

60. Hawthorne, D., J.H. Hodgkin, M.B. Jackson, J.W. Loder, and T.C. Morton, *Preparation and Characterisation of Some New Diaminobisimides.* High Perform. Polym., 1994. **6**: p. 287-301.

61. Ciba Specialty Chemicals, *Matrimid 5292 System.* Product Data, 1998.

62. Compston, P. and P.-Y.B. Jar, *Comparison of Interlaminar Fracture Toughness in Unidirectional and Woven Roving Marine Composites.* Applied Composite Materials, 1998. **5**: p. 189-206.

63. Russell, A.J., *Micromechanisms of Interlaminar Fracture and Failure.* Polymer Composites, 1987. **8**(5): p. 342-351.

64. Sela, N. and C. Ishai, *Interlaminar Fracture Toughness and Toughening of Laminated Composite Materials: A Review.* Composites, 1989. **20**(5): p. 423-35.

65. European Structural Integrity Society (ESIS), *Protocols for the Interlaminar Fracture Testing of Composites.* 1993: Delft, The Netherlands.

66. Partridge, I.K., *High Temperature Thermosetting Matrix Resins*, in *Advanced Composites*, I.K. Partridge, Editor. 1989, Elsevier Science Publishers Ltd: London. p. 14-23.

67. Compston, P. and P.-Y.B. Jar, *The Influence of Fibre Volume Fraction on the Mode I Interlaminar Fracture Toughness of a Glass-Fibre/Vinyl Ester Composite.* Applied Composite Materials, 1999. **6**: p. 353-368.

68. Koenig, J.L., *Spectroscopy of Polymers*. 1992, Washington DC: American Chemical Society. 115-135.

69. Turrell, G., *The Raman Effect*, in *Raman Microscopy, Developments and Applications*, G. Turrell and J. Corset, Editors. 1996, Academic Press: London. p. 1-23.

70. Hutapea, P. and F.G. Yuan., *The Effect of Thermal Aging on the Mode-I Interlaminar Fracture Behavior of a High-Temperature IM7/LARC-RP46 Composite.* Composites Science & Technology, 1999. **59**(8): p. 1271-1286.

71. Wang, W.X., Y. Takao, F.G. Yuan, B.D. Potter, and R.H. Pater, *The Interlaminar Mode I Fracture of Im7/Larc-Rp46 Composites at High Temperatures.* J. Composite Materials, 1998. **32**(16): p. 1508-1526.

72. Tsotsis, T.K. and S.M. Lee, *Long-Term Thermo-Oxidative Aging in Composite Materials - Failure Mechanisms.* Composites Science & Technology, 1998. **58**(3-4): p. 355-368.

73. Turi, E.A., *Thermal Characterization of Polymeric Materials*. 1981: New York Academic Press.

74. Ishida, H. and M.T. Huang, *Infrared Spectral Assignments for a Semicrystalline Thermoplastic Polyimide.* Spectrochimica Acta Part A-Molecular Spectroscopy, 1995. **51**(3): p. 319-331.

75. Jewell, R.A. and G.F. Sykes, *Thermooxidation of Methylene Bridging Groups in Polyimides.*, in *Chemistry and Properties of Crosslinked Polymers*, S.S. Labana, Editor. 1977, Academic Press: New York. p. 97-106.

76. Lin-Vien, D., N.B. Colthup, W.G. Fateley, and J.G. Grasseli, *The Handbook of Infrared and Raman Characteristic Frequencies of Organic Molecules*. 1991, New York: Academic Press.

77. Aust, J.F., M.K. Higgins, P. Groner, S.L. Morgan, and M.L. Myrick, *Fourier Transform Raman Spectroscopic Studies of a Polyimide Curing Reaction.* Analytica Chimica Acta, 1994. **293**: p. 119-128.

78. Hodgkin, J.H., M.B. Jackson, and T.C. Morton, *Thermal Stability Predictions of Polymeric Composites: Comparison of Medium - Term Weight Loss at 250°C with a Kinetic Mapping Procedure.* High Perform. Polym., 1994. **6**: p. 437-446.

79. Chifu, A.F. and J.H. Iroh, *Short Term Isothermal Aging of Epoxy Resin and Epoxy-Carbon Fiber Composites.* Polymer Composites, 1996. **17**(3): p. 408-13.

80. Turk, M.J., A.S. Ansari, W.B. Alston, G.S. Gahn, A.A. Frimer, and D.A. Scheiman, *Evaluation of the Thermal Oxidative Stability of Polyimides Via TGA Techniques.* Journal of Polymer Science Part A-Polymer Chemistry, 1999. **37**(21): p. 3943-3956.

81. Torrecillas, R., A. Baudry, J. Dufay, and B. Mortaigne, *Thermal Degradation of High Performance Polymers - Influence of Structure on Polyimide Thermostability.* Polymer Degradation and Stability, 1996. **54**: p. 267-274.

82. Torrecillas, R., N. Regnier, and B. Mortaigne, *Thermal Degradation of Bismaleimide and Bisnadimide Networks - Products of Thermal Degradation and Type of Crosslinking Points.* Polymer Degradation and Stability, 1996. **51**: p. 307-318.

83. Tsotsis, T.K., S. Keller, J. Bardis, and J.B. J., *Preliminary Evaluation of the Use of Elevated Pressure to Accelerate Thermo-Oxidative Aging in Composites.* Polymer Degradation & Stability, 1999. **64**(2): p. 207-212.

84. Morgan, R.J., R.J. Jurek, A. Yen, and T. Donnellan, *Toughening Procedures, Processing and Performance of Bismaleimide Carbon-Fibre Composites.* Polymer 1993, 34, 4835-842., 1993. **34**: p. 4835-842.

85. Tsotsis, T.K., *Long-Term Thermo-Oxidative Aging in Composite Materials - Experimental Methods.* Journal of Composite Materials, 1998. **32**(11): p. 1115-1135.

86. Tsotsis, T.K., *Thermo-Oxidative Aging of Composite Materials.* Journal of Composite Materials, 1995. **29**(3): p. 410-422.

87. Grenier-Loustalot, M.-F. and N. Aycaguer, *Monofunctional Maleimide or Acetylene Terminated Model Compounds-1. Molten State Homopolymerization Reactivity and Kinetics.* Eur. Polym. J., 1998. **34**(11): p. 1705-14.

88. Phelan, J.C. and C.S.P. Sung, *Cure Characterization in Bis(Maleimide)/ Diallylbisphenol A Resin by Fluorescence, FTIR, and UV-Reflection Spectroscopy.* Macromolecules, 1997. **30**: p. 6845-6851.

89. Hummel, D.O. and A. Solti, *Atlas of Polymer and Plastics Analysis. Volume 2. Plastics, Fibres, Rubbers, Resins; Starting and Auxiliary Materials, Degradation Products.* 1985, Munich: Vienna: Carl Hanser Verlag. 388-447.

90. Young, P.R. and A.C. Chang, *FTIR Characterization of Thermally Cycled PMR-15 Composites.* 33rd International SAMPE Symposium, 1988: p. 530-550.

91. Frimer, A.A., P.J. Cavano, and W.B. Alston, *New High-Temperature Polyimides Based on [5]Helicene Dianhydride.* High Perform. Polym., 1995. **7**: p. 93-104.

92. Hodgkin, J.H. Personal Communication, 2001.